TEMPERATURE-DEPENDENT GROWTH OF InP BY PLASMA-ENHANCED GSMBE

By

DANIEL BRUCE MITCHELL, B.Sc., M.Sc

A Thesis

Submitted to the School of Graduate Studies

in Partial Fulfilment of the Requirements

for the Degree

Doctor of Philosophy

McMaster University

(c) Copyright by Daniel Bruce Mitchell, September 1995

DOCTOR OF PHILOSOPHY (1995) MCMASTER UNIVERSITY
(Engineering Physics) Hamilton, Ontario

TITLE: Temperature-Dependent Growth of InP By Plasma-Enhanced GSMBE

AUTHOR: Daniel Bruce Mitchell, B.Sc. (University of Waterloo)

M.Sc. (McMaster University)

SUPERVISOR: Professor D.A. Thompson

NUMBER OF PAGES: viii, 121

Temperature-Dependent Growth of InP By Plasma-Enhanced GSMBE

ABSTRACT

This thesis reports on study of the effects of various plasmas on the growth of InP films by GSMBE. The samples were grown at temperatures ranging from 232 to 500°C. The plasmas were generated by electron cyclotron resonance, giving a broad distribution of ion energies in the 10-50 eV range. H, D, He and Ar plasmas were studied. Films were also grown at the same temperatures without plasma, as references.

The samples were characterized by: Nomarski phase contrast microscopy, Xray double crystal diffraction, Hall effect measurements, photoluminescence (PL), variable-energy positron annihilation, thermal desorption, nuclear reaction analysis and capacitance/voltage profiling. The Xray, Hall and PL measurements were repeated after the samples were annealed at 730°C for 10 seconds. In no case was the material produced of comparable quality to that grown under standard conditions (465°C, no plasma).

The films grown without plasma were n-type, reaching a carrier concentration of approximately $2\times10^{18}/cm^3$ at 300°C. This is in agreement with published results, which showed that the donor defect responsible is a P atom on an In site. This defect occurred in sufficiently high concentrations to mask the effects of the plasmas below 400°C.

H plasma increased the carrier concentration by approximately $7\times10^{16}/cm^3$. Some H atoms appear to bond to P atoms in the crystal, resulting in an excess In electron. The carrier concentration was not affected by annealing. Additional H atoms may be present as interstitials, causing a reduction in mobility and a broad PL peak near 1.05 eV. These effects were removed by annealing.

D plasma produced similar effects to H plasma, but the carrier concentration and mobility were lower. P interstitials, which act as deep acceptors, may be produced by recoiling surface P atoms into the bulk. Beryllium dopant, at a concentration of $2\times10^{18}/cm^3$, was passivated by this plasma. Silicon dopant was not strongly affected.

He plasma produced P interstitials and P vacancies, by recoil displacement from the surface and in the bulk. More P interstitials were produced, compensating up to $10^{17}/cm^3$ carriers. The interstitials were more mobile, diffusing out during the 500°C growth and during annealing.

The effects of the Ar plasma were small enough to be masked by the weak H plasma that results from H backstreaming.

Films grown at 400°C or less without plasma had textured surfaces. The plasmas usually smoothed the surfaces at these temperatures, resulting in defect densities lower even than occured at 465°C without plasma. Above 400°C, none of the plasmas significantly affected the surface defect densities.

Acknowledgements

I wish to thank my wife, Yvonne, and our families, for their support during this long work. My supervisor was Dr. Dave Thompson, with Dr. John Davies and Dr. Adrian Kitai completing the supervisory committee. Dr. Brad Robinson and Scott McMaster assisted with the MBE crystal growths. Dr. Peter Mascher and the University of Western Ontario Positron Annihilation Facility took care of the positron annihilation measurements. Dr. Song Kechang performed the CV measurements. Dr. Rick MacAuley-Newcombe did the NRA and the thermal desorption measurements.

TABLE OF CONTENTS

	page
1. Introduction	1
2. Experiments	9
3. Deposition of InP Epilayers at Different Temperatures	27
4. Hydrogen and Deuterium Plasma Assisted InP Growth	57
5. He Plasma Assisted InP Growth	86
6. Argon Plasma Assisted InP Growth	103
7. Conclusions	115
References	118

LIST OF FIGURES

	page
2.1: Schematic of the McMaster GSMBE system.	10
3.2a: Surface of a film grown at 500°C.	32
3.2b: Surface of a film grown at 400°C.	32
3.2c: Surface of a film grown at 300°C.	33
3.2d: Surface of a film grown at 300°C, with a flux of 2 sccm.	33
3.3a: Xray rocking curve of InP grown at 465 Celsius.	35
3.3b: Xray rocking curve of InP grown at 350 C, 5 sccm.	35
3.3c: Xray rocking curve of InP grown at 350 C, 2 sccm.	36
3.3d: Xray rocking curve of InP grown at 300 C, 5 sccm.	36
3.3e: Xray rocking curve of InP grown at 300 C, 2 sccm.	37
3.3f: Xray rocking curve of InP grown at 232 C, 4 sccm.	37
3.4: Positron annihilation profiles.	42
3.5a: Carrier concentration vs growth temperature.	46
3.5b: Hall mobility vs growth temperature.	46
3.5c: Carrier concentration vs growth temperature, after annealing.	48
3.5d: Hall mobility vs growth temperature, after annealing.	48
3.6a: PL results, 400-500°C.	50
3.6b: PL results, 300-400°C.	51
3.6c: PL results after annealing, 232-500°C.	53
4.5: Xray rocking curve, with RADS fit.	66
4.6: Positron annihilation profiles.	70
4.7a: Carrier concentration of InP grown with H-plasma.	71
4.7b: Mobility of InP grown with H-plasma.	71
4.7c: Carrier concentration of InP grown with D and H-plasmas.	75
4.7d: Mobility of InP grown with D and H-plasma.	75
4.8a: PL results from InP grown with H-plasma.	77
4.8b: PL results from InP grown with H-plasma, then annealed.	78
4.8c: PL results from InP grown with D.	80
4.8d: PL results from InP with D, then annealed.	82
4.9: Carrier concentration of Si-doped InP grown with D plasma.	83
4.10: Carrier concentration of Be-doped InP grown with D plasma.	83
5.5: Positron annihilation profiles.	93
5.6a: Carrier concentration of InP grown with He plasma.	95
5.6b: Mobility of InP grown with He plasma.	95
5.7a: PL spectrum of sample grown at 500C, with He plasma.	99
5.7b: PL results from InP grown with He, then annealed at 730C.	101

6.4: Positron annihilation profiles. 108
6.5a: Carrier concentration of InP grown with Ar plasma. 109
6.5b: Mobility of InP grown with Ar plasma. 109
6.6a: PL results from InP grown with Ar. 112
6.6b: PL results, after annealing, from InP grown with Ar. 113

I Introduction

Semiconductors are the key materials of the current information age. Their unique properties make possible the incredible array of integrated circuit devices now used by our society. Initially, group IV materials (germanium and silicon) were developed. Now, compound semiconductors are being emphasized in research and for niche applications. These are composed of III-V materials, such as gallium arsenide, and II-VI materials, such as zinc selenide, and have the added advantage of functioning as light emitters as well as allowing the fabrication of higher speed electronic devices. Gallium arsenide (GaAs) based materials have been the most studied, and are used for high speed and microwave devices as well as lasers operating at near infrared wavelengths. Another III-V material with considerable potential is indium phosphide (InP). In addition to its favourable electrical properties, its band gap can be tailored to allow light emission compatible with long distance optical fibre transmission by alloying with Ga and As. This should allow the production of practical optoelectronic and electronic devices on the same substrate, making it easier to take advantage of both the greater signal bandwidth of optical signals and the high speed of electronic devices. Furthermore, as optoelectronic devices develop, they can then replace the equivalent electronic devices in a gradual evolution to broad band information transfer.

In order to achieve these devices, with their inherent expanded capabilities, it is

necessary to establish refined techniques for growing high quality semiconductor material with precise structural geometries. The most precise growth techniques for semiconductors are the various forms of molecular beam epitaxy (MBE) and metal-organic chemical vapour deposition (MOCVD). The growth system used to grow the samples analyzed in this thesis was a variation of MBE called gas-source MBE (GSMBE). Every material grown by GSMBE has a particular ideal growth temperature range. If the growth temperature is extended beyond this ideal range, the material properties deteriorate. For example, the grown surface may become rough, the crystal may become polycrystalline, and the electrical and optical properties may deteriorate. The best growth temperature for InP by MBE is in the 450-500°C range. There is some variation from system to system, probably because temperature measurements are typically not very precise. For the McMaster system, the best results have been achieved at 465°C. This temperature gives smooth surfaces, with high electron mobility (~4700 cm^2/Vs) and low background carrier concentration (~$1x10^{15}/cm^3$). For GaAs, the ideal growth temperature range is 500-600°C. The various alloys made from Ga, As, In and P have still different preferred growth temperatures. To grow most device structures, though, it is necessary to grow layered heterostructures involving several different compositions. Changing from one temperature to another takes time, and can cause some deterioration in the materials grown at lower temperatures and degradation of the interfaces between the various layers comprising the heterostructure.

It has been postulated that, if a method could be found to reduce the growth temperatures so that all materials could be grown at the same temperature, improvements

in device performance would result. The quality of the film is actually only dependent on the temperature of the surface, while growth is occuring, so improvement might be achieved by adding energy to the growing surface to replace the lost thermal energy. One possible technique to accomplish this involves exposing the growing surface to a plasma. The resulting low-energy ion bombardment will transfer energy to the surface, without significantly affecting the bulk, provided that the ions don't penetrate far.

1.1 Low Temperature Effects

There has been a great deal of interest in the growth of InP at low temperature (ie in the 100-450°C range) in the last two years. This interest has been prompted by the discovery that GaAs grown at low temperature (<300°C) is semi-insulating. If semi-insulating InP could be produced in the same way, it would be a valuable material for use in devices. Several groups have studied the low temperature growth of InP [Dreszer *et al.* (1993a&b), Xie *et al.* (1992), Maracas *et al.* (1992, 1993), Garcia *et al.* (1992), Liang *et al.* (1992), Hautojarvi *et al.* (1993), Yu *et al.*(1992, 1994)]. The material produced is n-type, and the carrier concentration, n, increases as the growth temperature is reduced, reaching a maximum of about $3x10^{17}/cm^3$ near 300°C [Dreszer *et al.* (1993a&b), Maracas *et al.* (1992), Liang *et al.* (1992)]. The dependence of n on the growth temperature varies from paper to paper, though, with Maracas *et al.* (1992) reporting a sharp transition between 320°C and 280°C, while the others report a steady increase over a broad temperature range. Liang *et al.* (1992), only, report an experimentally significant drop in concentration if the growth temperature is further reduced down to 200°C.

InP grown at 200°C and lower has been shown to contain excess P [Xie *et al.* (1992), Garcia *et al.* (1992)]. This material is polycrystalline, but it is suggested that there is an excess even before the transition from single crystal material. Dreszer *et al.* (1993a&b) have found that the P_{In} antisite defect is the predominant electrically-active defect in single-crystal InP grown near 300°C. This defect, a P atom on an indium (In) site, acts as a double donor, explaining the n-type character of the InP grown at reduced temperature. The energy levels of the P_{In} were found to be E_C-0.23 eV and E_C+0.12 eV. An unexplained energy level was also found to exist at E_C-0.53 eV. Another group has proposed that the lower level of the P_{In} defect is actually at E_C-0.33 eV [Yu *et al.* (1992, 1994)]. Interactions with the Be dopant used by both groups make interpretation difficult. The upper energy level does not seem to be in dispute.

Positron lifetime analysis [Hautojarvi *et al.* (1993)] has shown that open-volume defects, in concentrations near $10^{18}/cm^3$, are present in material grown by GSMBE at 180°C. The defects are tentatively identified as In vacancies (V_{In}), which act as acceptors. In addition it was doped with beryllium, normally a p-type dopant, to a concentration of $5\times10^{17}/cm^3$. Despite the large concentrations of acceptors the sample is n-type, with a net carrier concentration of $5\times10^{16}/cm^3$. The material is thus highly compensated, perhaps close to 97% (from $(10^{18}+5\times10^{17})/(10^{18}+5\times10^{17}+5\times10^{16})$), so the quantitative results reported may not be true in general, but some In vacancies can be expected as the growth temperature is reduced.

Theoretical work by Seitsonen *et al.* (1994) predict that P_{In} and V_{In} should be the dominant defects in InP grown in a P-rich environment such as that in MBE growth.

While this is in agreement with the experimental results, the predicted energy levels for P_{In} are very low. The energy level for the doubly ionized P_{In} (donor) is given as E_C-1.31 eV and for singly ionized P_{In} (donor) is E_C-1.06 eV, far deeper than found by the experiments. It is also predicted that P_{In} acts as a double acceptor, at an energy of E_C-0.06 eV, which isn't seen in any of the experiments. I conclude from the large differences between the theoretical predictions and the actual measured values that the theoretical models will need to be greatly refined before they will be of use in interpreting my results.

In chapter 3, I present the results of a study of InP films grown at low temperature. Films have been grown at temperatures ranging from 232°C to 500°C. The large quantitative disagreements in the literature suggest the need for more data. Also, this data is necessary for comparison with samples grown at low temperature under low energy plasma bombardment, which is the main motivation for this thesis research.

1.2 Plasma Effects

Ion-assisted, low-temperature epitaxial growth has been shown in certain cases to produce material of better quality than that grown without ions at the same temperature. This has been demonstrated for silver (Ag) [Thomas *et al.* (1982)], gold (Au) [Harper *et al.* (1984)], germanium (Ge) [Thomas *et al.*(1982)], silicon (Si) [Narusawa *et al.* (1979), Zalm *et al.* (1982)], and GaAs [Hariu *et al.* (1981)]. Unfortunately, the electrical quality of the films is not reported. The improvements were detected using electron diffraction, which is sensitive only to structure. For example, GaAs grown without plasma at 350°C

was polycrystalline while that grown with plasma is single-crystal [Hariu *et al.* (1981)].

The objective was to provide energy to the surface of the growing crystal with the plasma, without affecting the underlying bulk material. Tsao *et al.* (1989) have done some theoretical modelling which suggests this is possible. If the energy is low enough, the impinging ions cannot penetrate into the bulk with enough energy to displace any of the lattice atoms. Thus, there exists an energy window in which there is still enough energy to break the bonds of the surface atoms, because they are less strongly bonded, without creating bulk defects. The window widens as the incident ion's mass increases.

Experiments suggest that the displacement energies for bulk InP atoms are 6.7eV for In and 8.7eV for P [Corbett *et al.* (1975)]. Theoretical modelling gives a value of 12.2eV for In and 16.5eV for P [Van Vechten (1980)]. The other materials modelled, including semiconductors, agreed with experiment to within 20%, so the large discrepancy between theory and experiment for InP is hard to understand. Whatever the reason, it will be assumed here that the minimum energy requirements are the experimental values, while recognising that the displacement energies could be much higher.

The effects of hydrogen and deuterium plasmas on the deposition of InP films are reported in chapter 4, with deuterium plasmas being used to clarify some aspects of the results using the hydrogen plasmas. Helium plasmas were used in growing the films described in chapter 5, and the results with Ar plasmas are described in chapter 6. Xenon plasmas were tried, but were found to be incompatible with the MBE system. Xenon freezes out on the liquid nitrogen cooled cryo-panel surfaces, resulting in problems in plasma control and a large gas loading on the vacuum pumps upon warm-up of the cryo-

panels.

1.3 Hydrogen Passivation

Hydrogen incorporated into semiconductors has been found to passivate many electrically active defects, in addition to dopants. Pearton *et al.* (1987) reviewed the effects on Si, Ge and GaAs. Donnelly *et al.* (1977) implanted InP with 400 keV protons and found that doped, p-type, material became highly resistive (>10^8 Ω-cm). The resistivity of n-type material also increased, but to only 10^3 Ω-cm. Cho *et al.* (1993) investigated the passivation of Zn acceptors by H diffusion. Pearton *et al.* (1992) passivated Zn, Cd and Mg dopants after growth, using an ECR hydrogen plasma. Sugino *et al.* (1991) apparently passivated some of the surface defect states of InP with hydrogen. Sidhu *et al.* found evidence that growing Si-doped InP by GSMBE (ie in a H-rich atmosphere) resulted in Si-H:P-H complexes. The presence of these complexes had very little effect on the electrical properties, presumably because the complex and the Si dopant both act as donors. Based on energy calculations, Baranowski *et al.* (1991) proposed that acceptors are passivated by H bonding to a nearest-neighbour P atom. The H provides the electron that the acceptor lacks.

In chapter 4, the effects of growing with D plasma on the properties of n- and p-doped InP are reported. A deuterium plasma was used because it is chemically identical to H, but has a different mass, so it can be distinguished from H by some measurement techniques. Deuterium atoms incorporated from the plasma can thus be distinguished from H atoms incorporated from the background.

1.4 Summary

In chapter 2, the experiments are described. In chapter 3, the properties of InP grown at low temperature are studied in detail. The experimental analysis is more detailed than any that has yet appeared in the literature. The results are comparable to those already reported, though there are some quantitative differences. These results are the standard against which the effects of the plasmas are studied. In chapters 4 through 6, plasma-assisted growth of InP is studied for the first time. Defect models are proposed for the observed effects of H, D, He and Ar plasmas. He plasma had the greatest effect, in that it passivated several samples by creating compensating phosphorus interstitials. Phosphorus vacancies were also created by the He plasma. H and D bond into the crystal, creating donors. For the first time, dopant passivation during deposition was observed, using a D plasma. (The studies in the literature have been on samples in which the H was incorporated after growth.) The effects of Ar plasma are small, they were hidden by the H plasma produced at the same time due to the large H background pressure in the growth system. Chapter 7 summarizes the conclusions.

2. Experiments

2.0 Abstract

The growth of the films, by gas source molecular beam epitaxy (GSMBE), is described in section 2.1. The plasma generation system is described in section 2.2. The following sections describe characterization of the samples by Nomarski microscopy, Xray diffraction, Hall effect and photoluminescence. Many samples were annealed in a rapid thermal annealer, described in section 2.7. In the course of the work, it became clear that additional measurements could be helpful in clarifying the results. Arrangements were made to have measurements made by positron annihilation, nuclear reaction analysis, thermal desorption and capacitance-voltage profiling. These techniques are described briefly in the final four sections of this chapter.

2.1 Growth

The samples were grown by gas source molecular beam epitaxy (GSMBE). Molecular beam epitaxy (MBE) was developed in the late 1960's and has been refined to allow precise control of the relative concentrations of the constituent elements of semiconductor compounds. Initially the sources of these elements were all heated crucibles, each filled with the appropriate element or a compound containing that element. By heating the crucible, the source element's vapour pressure can be increased to produce

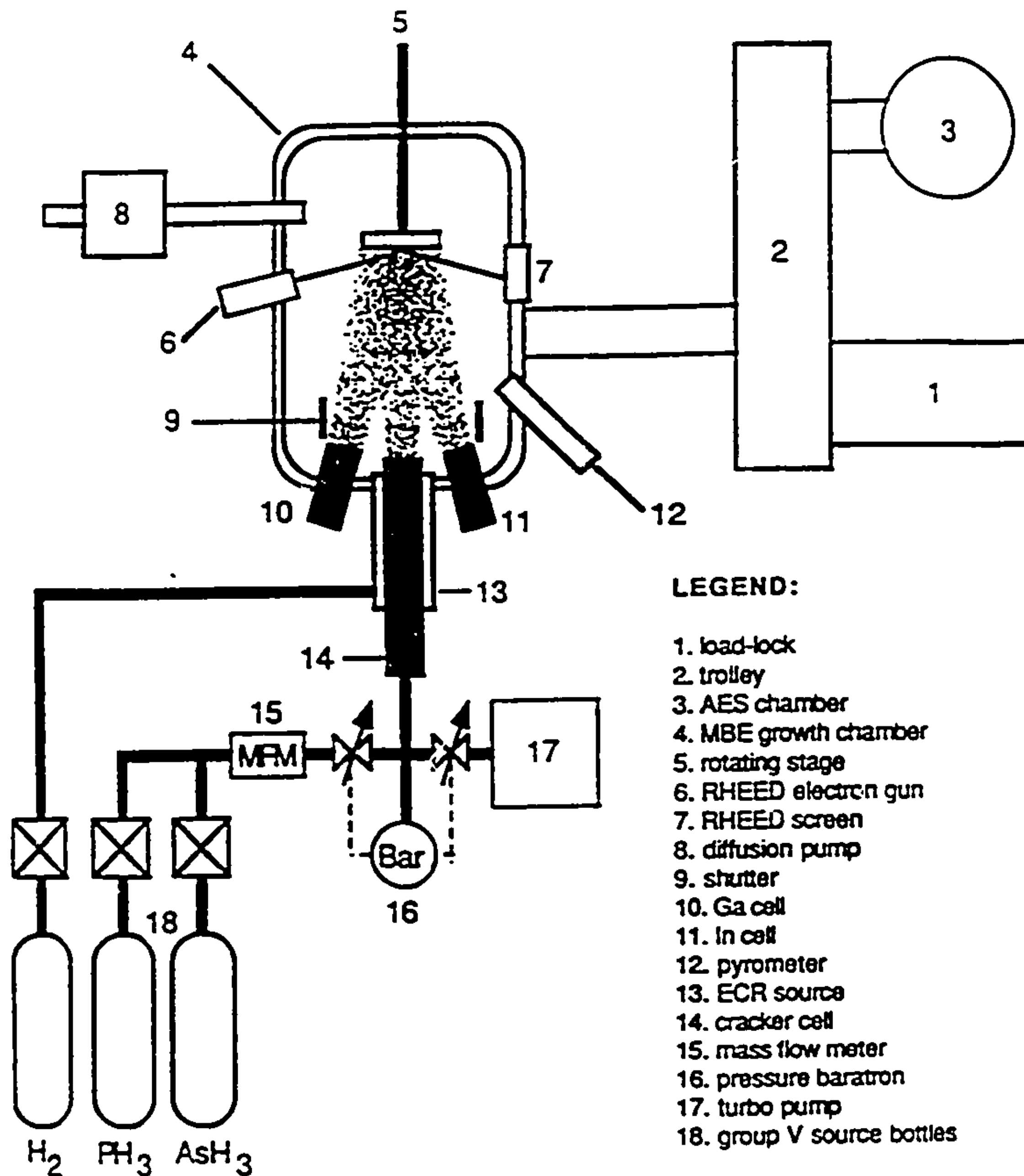

Figure 2.1: Schematic of the McMaster GSMBE system. Although seperate pressure control systems are used for H_2, PH_3 and AsH_3, a single system is shown here for simplicity. Reprinted from the M.Sc. thesis of Ray Lapierre, with permission.

a flux (beam) of atoms or molecules. Each crucible is located so that the output flux is directed toward the substrate growth surface, where a portion of the molecules condense to produce crystal growth. The flux is controlled through the temperature of the crucible, which determines the vapour pressure of the charge. One weakness of this approach arises from the relatively large group V flux that is required for stable crystal growth. The system must be shut down regularly to add group V material. Another is the inconsistency of the group V flux over time. For phosphorus, different allotropes form as the crucible is repeatedly heated and cooled, and each allotrope has a different vapour pressure. These two difficulties are avoided in a gas-source molecular beam epitaxy system, which uses arsine (AsH_3) and phosphine (PH_3) gases. These source gases are stored in pressurized bottles outside the system, so they can be replenished without breaking vacuum. The flow rate is controlled by setting the gas pressure. The gases enter the growth chamber through a cracker cell, which uses heat and a catalyst to dissociate them into As_2 or P_2. Operating the cell at 1000°C, 2 PH_3 molecules are converted to a P_2 molecule and 3 H_2 molecules. Arsine is cracked in the same manner. The group III flux is still provided by a heated crucible containing the pure material (In or Ga), as are the dopants, silicon (Si) and beryllium (Be). Thus, it is still necessary to open the system periodically to replenish the charge in these crucibles.

A schematic of the system is shown in figure 2.1. The In and Ga crucibles and the gas cracker are shown. The indium is 99.99999% pure, while the phosphine is 99.9995% pure. The electron cyclotron resonance plasma source is mounted normal to the substrate surface. Shutters are positioned to "turn" the vapour fluxes off and on by covering and

uncovering the sources. There are also shutters in front of the growth surface and at the mouth of the plasma source, which is described in detail in the next section .

The substrate temperature is monitored by an optical pyrometer and a thermocouple. The pyrometer is mounted on a viewport facing the sample. It is left shuttered for most of the growth, because the viewport gradually clouds over when exposed to the growth fluxes. The pyrometer is designed to be accurate above 450°C, though it comes online at 400°C. It was used periodically through the growths carried out above 400°C to verify that the temperature was stable. Below 400°C, only the thermocouple could be used to measure the growing film's temperature. The thermocouple is located in the cavity between the sample and heater, and is used by the temperature controller throughout each growth. The thermocouple is less accurate than the pyrometer at high temperatures, because of differences in thermal contact from sample to sample. It was therefore calibrated with the pyrometer before each growth. It had earlier been found to respond linearly to temperature in the 300 to 500°C range, by calibration against the melting temperatures of various materials mounted on a substrate surface. The samples grown at 232°C each had a small rectangular piece of tin clamped onto the surface, extending from one corner toward the centre. The material was grown at the temperature at which the tin melted. Differences from system-to-system in position of the thermocouple and geometry of the optics result in some variation in reported ideal growth temperatures. It is not unusual for temperatures quoted in the literature to differ from each other by 25°C.

The (100) InP substrates were 14mm x 14mm x 350μm, cleaved from "epi-ready"

2 inch diameter wafers produced by Sumitomo. Most samples were grown on semi-insulating (SI) substrates, though some were grown on n-type substrates in order that specific (capacitance-voltage) measurements could be made. Sumitomo guarantees that the SI wafers have a resistivity greater than $1.0x10^7$ ohm-cm, an etch pit density less than $5.0x10^4/cm^2$, and a mobility between 2200 and 2700 cm^2/Vs.

Immediately before loading, the substrate surfaces were cleaned by placing them in a UV-ozone system for ten minutes. The ozone is very reactive, removing impurities such as hydrocarbons from the surface and producing a protective oxide surface coating. The substrate was then placed in the loadlock and left under vacuum to degas for two or more hours. It was then further degassed in a second vacuum chamber at 400°C for twenty minutes. After cooling it was moved, still under vacuum, into the growth chamber. The substrate was then heated to 465°C, while a phosphorous overpressure was maintained to prevent surface damage due to preferential phosphorus evaporation, which typically occurs at temperatures above 360°C on an oxide-free surface. The surface oxide was then removed by exposure to a hydrogen plasma. Reflection high energy electron diffraction (RHEED) was used to verify that the oxide had been removed.

When practical, a thin buffer layer (up to 650 angstroms) was grown at 465°C. This provided the best possible surface for the sample film to be grown upon. The substrate was then ramped to the growth temperature and a thick layer (0.7 to 3 μm) was deposited under the conditions of interest. Sample thicknesses were chosen according to the expected carrier concentration, so that the Hall measurements would be accurate. The sample must be significantly thicker than the sum of the surface and interface depletion

widths, or the measured values are not meaningful. Depletion is discussed further in section 2.4. Since high carrier concentrations produce thinner depletion layers, samples that were expected to have high carrier concentrations were only grown to 0.7-1.1 μm. The thickest samples, when the carrier concentration was expected to be less than $1 \times 10^{16}/cm^3$, were grown to about 3 μm.

Samples were grown at temperatures from 232°C to 500°C. They were grown with hydrogen, helium, deuterium, and argon plasmas, and without plasma to provide reference values. The growth rate was between 0.7 and 0.8 μm/hr. This rate was determined by the In flux, as the growths were all done in an excess flux of phosphorus.

The samples were cleaved into pieces after growth for analysis by various techniques listed later in this chapter. The edge regions of the grown samples were discarded, to avoid any possible anomalous properties near the mounting clips or substrate edges, where temperature gradients might exist.

The film thicknesses were measured after growth by an Alpha-step 200 system, produced by Tencor Instruments. The Alpha-step measures the heights of surface irregularities by dragging a stylus across the surface while recording vertical movements. The clips, which hold the substrate in place during growth, shadow two corners of the sample so that no growth occurs under them. The films' thicknesses were measured by running the stylus over the step between the growth and nogrowth regions. Measurements were made at four different points on each sample. Standard deviations were in the 1-3% range.

2.2 Plasma Generation System

A Microscience ECR-900 Series Plasma Ion Source is mounted at the centre of the front flange of the chamber, normal to the surface of the sample being grown. The plasma is generated in a small chamber by electron cyclotron resonance. A microwave source at 2.45 GHz is used to excite the electrons, with a corresponding magnetic field intensity for resonance of 875 Gauss. The induced circular motion of the electrons produces an opposing magnetic field, causing them to move toward the sample. This distribution of electrons results in an electric field which propels the positively ionised gas atoms to the sample.

The input gas line is connected to a "T" and valved so that two gas bottles can be connected at once, making it easy to switch between the two gases. Hydrogen is always connected, because it is used to remove the surface oxide before growth. When the sample was to be bombarded with deuterium, helium or argon, a pressurized bottle of that gas was connected to the other line of the "T". To prevent contamination of the growth system, the lines were flushed and vacuum pumped before being opened to the plasma chamber. The plasma source was then operated for several minutes, further flushing impurities, prior to use during sample growth.

Several papers have been published [O.A. Popov (1988, 1989a&b, 1990a&b)] describing the performance of the Microscience system. Various other groups have also produced and studied ECR plasma sources [Ono *et al.* (1986), Matsuo *et al.* (1983)]. The plasma was found to be uniform to within a few percent over a radius of 8 cm, so we can consider it to be uniform across our 1.4 cm sample. The plasmas produced have ion

energies in the tens of electron volts, with the peak flux occuring at an energy of about 25eV. The ion energy distribution is very broad, with significant fluxes for energies in the range from about 10 to 50 eV.

A Langmuir probe can be moved into the plasma stream, near the position of the sample. Ideally, probes of this type can measure the ion current and average ion energy. Unfortunately the presence of magnetic fields, such as that produced by the plasma generation system, seriously limit the usefulness of Langmuir probes [Chen (1965)]. The ion energy could not be determined. The ion current was in the 0.5-5 $\mu A/cm^2$ range at a bias of -100 V, depending on the atom species. Hydrogen and deuterium plasmas typically had ion currents around 4 μA, helium about 3 μA, and argon about 1 μA, with variations of a μA fairly common. Small changes in the plasma parameters could be accomplished by varying the magnetic fields in the ECR source, but at the expense of stability. Only the most stable condition was used, corresponding to a minimum in the reflected microwave energy. A stage that can be biased through a broad range of voltages has recently been installed, so this line of inquiry can be pursued in future work.

A Spex optical emission spectrometer was used to monitor the plasma whenever a new species was used. The detector was located in two different positions. One position was at a window perpendicular to the plasma flow. The other was at the output end of the optical pyrometer, with the pyrometer focused on the position of the sample. In both positions it was used to confirm that the intended plasma species was being formed, ie that the optical lines detected corresponded to the appropriate atom.

2.3 Nomarski Phase Contrast Microscope

For device applications it is important that the surface of the grown film be smooth and defect-free. Defect regions usually have a negative effect on the electrical and optical properties of the semiconductor, reducing the carrier mobility and possibly quenching photon emission. Rough surfaces result in variations in layer thickness, which can significantly alter the performance of devices with thin active layers.

The Nomarski phase contrast microscope is a standard measurement tool for studying surface defects. Illumination was provided by a mercury lamp. The light beam passes through a green filter and a polarizing filter, before it is split. By illuminating the sample from two sources, phase interference is induced at topological irregularities. Differences in height show up as differences in brightness, making surface defects more visible than with a standard optical microscope.

The equipment used was a Zeiss Differential Interference-Contrast Microscope capable of magnification of up to 1000X for photographs (800X through the viewer). Thus, defects of 1 micrometre dimension can easily be observed. The microscope has a field of view of about 3.6×10^{-4} cm^2, so a single defect per field of view corresponds to 2778/cm^2. Any defect densities close to this level, or less than this, are determined by averaging over several fields of view, and can only be considered as rough estimates. The densities are mainly useful as a tool for comparing surface quality between samples.

2.4 Xray Double Crystal Diffraction

This technique was used to measure the strain in the grown films. It is commonly

used to determine the lattice constant of grown alloy layers. Changes in lattice constant can also be induced by large concentrations of defects (if they are of different volume than the portion of crystal they replace), so this technique was used to look for changes in lattice constant due to the presence of these defects. If strain is present in the grown layer, the layer shows up as a diffraction peak that is shifted in position relative to the peak of the strain-free substrate. The change in lattice constant is related to the peak shift by the equation

$$\frac{\Delta a}{a} = \Delta\theta \frac{1-\nu}{1+\nu} \cot\theta_B$$

where a is the lattice constant of the InP substrate, 5.86930 angstoms, Δa is the change in lattice constant, $\Delta\theta$ is the spacing of the peaks, ν is Poisson's ratio for InP, 0.36, and θ_B is the Bragg angle for InP.

The double crystal Xray diffractometer used was a Bede Scientific Instruments Ltd model QC1. Its copper source emits Xrays with a wavelength of 1.542 angstoms. The corresponding Bragg angle is 31.68°.

None of the samples grown were thick enough to totally mask the signal from the substrate, though its peak clearly becomes smaller when the thickness of the grown layers excedes 1.7 μm. If the grown layer is unstrained, the two peaks superimpose into one larger, symmetric peak. For good quality InP crystals, the full width at half maximum (fwhm) of the peak is about 13 arcseconds (the peak widths are measured in tilt of the sample). Measured fwhm's can vary by several arcseconds over a grown film, possibly due to strain-induced curvature of the sample.

The direction and magnitude of the strain can be estimated by modelling using the RADS (Rocking curve Analysis by Dynamic Simulation) program, also produced by Bede Scientific. The program is not capable of simulating strain due to defects, but only that produced due to lattice mismatch in various alloys. By fitting materials with larger or smaller lattice constant, the direction of the strain is determined. This is only possible when there is enough strain to produce two separate peaks, or a very distinct shoulder on the main peak. The manufacturer predicts, based on comparison with experiments, that the modelled intensities should be accurate to within 5%.

2.5 Hall Effect

The electrical properties of the samples were measured by the Hall effect. Hall carrier concentration and mobility are standard measures of material quality. For InP, a mobility of 4700 $cm^2/V/s$ with a carrier concentration in the low $10^{15}/cm^3$ range is considered to indicate excellent crystal with few defects or unwanted impurities. The mobility is of primary significance, because while defects and impurities can compensate carriers, leading to low carrier concentrations, the effects of compensation will be apparent as a reduction in the mobility.

The van der Pauw measurement technique was used [van der Pauw (1958)]. A square sample, approximately 5mm on a side, was cleaved from each grown sample. Tin contacts were melted onto the corners, and tested for ohmic conductivity. The magnetic field used was 0.2 Tesla. Most of the measurements were done at room temperature, but it is possible to controllably cool the samples, in vacuum, to as low as 10 K. Several

samples were studied over the full temperature range (10-300 K).

The primary limit on the sensitivity of the measurements is the depletion thickness. This consists of two components, the substrate/film interface depletion and the film surface depletion. Interface depletion results from conduction band electrons in the grown layer becoming trapped at unfilled deep energy states due to the iron dopant atoms in the substrate. These atoms act as deep acceptors and are used to make the substrate highly resistive (semi-insulating). The interface depletion width in the film is given by [Omar *et al.* (1975), Chandra *et al.* (1979), Lepkowski *et al.* (1987)]:

$$w_i = \frac{N_T}{n_o + N_T}\sqrt{\frac{2\epsilon}{q n_o}}\sqrt{\varphi_T - \frac{kT}{q}\ln\frac{N_c}{n_o}}$$

N_T, the concentration of traps (in this case Fe atoms) in the substrate is approximately $10^{15}/cm^3$, ϕ_T (0.65 volts) is the depth of the traps relative to the conduction band, n_o is the density of carriers in the undepleted region, ε is the permitivity of InP, q the charge of an electron, k is Boltzmann's constant, T is the temperature and N_c is the effective density of states in the conduction band. Similarly, the depletion layer at the surface is caused by defects at the surface which trap electrons. The width of the surface depletion region is given by:

$$w_s = \sqrt{\frac{2\epsilon}{q n_o}}\sqrt{\varphi_s - \frac{kT}{q}\ln\frac{N_c}{n_o}}$$

where ϕ_S (0.4 volts) is the depth below the conduction band of the dominant surface traps in InP [Spicer *et al.* (1980)]. The sum of these two equations is the total estimated

depletion of the grown film. Note that n_o is not directly measured. An apparent carrier concentration, n_{eff}, is first found using the total measured film thickness (neglecting depletion). The depletion thickness is then estimated, assuming $n_o = n_{eff}$. Since the measurement current does not flow in the depleted regions, the film thickness is reduced by the total estimated depletion thickness. A more accurate carrier concentration n_{eff} is next calculated, using the revised film thickness. This process is iteratively repeated until the carrier concentration and depletion thicknesses are self-consistant, yielding n_o.

There is a variation in measured carrier concentration by as much as a factor of 3 from sample-to-sample grown under nominally the same conditions. This is not because of inaccuracies in the Hall system but because of variations in the growth system itself. The most common growths in the McMaster GSMBE system, of undoped InP at 465°C, typically varied in carrier concentration from $1\text{-}3\times10^{15}/cm^3$. The mobilities of grown samples vary less, about 20%, depending how long the growth system had been operating since its last maintenance involving exposure to air.

2.6 Photoluminescence

This technique can identify luminescent defects in a sample. The wavelength emitted by some common defects and impurities is known, so if that wavelength is detected, that species is probably present. Quantitative results are generally not possible, as the signal is not linearly dependent on defect concentration even when there are no interactions with other defects.

The samples were cooled to approximately 11K, reproducible to within 2K. An argon ion laser was used at a wavelength of 488 nm (blue) to excite luminescence in the samples. The laser power was always set to 25 mW, the middle of the rated power range of 5 to 45 mW, in order to produce as stable and reproducible a signal as possible. An InGaAs detector was used to detect the emitted light. A monochrometer was used to scan the wavelength of the luminescence signal in steps of 0.5 nm near the band edge, where the peaks are narrower. To detect deeper levels the scans were carried out in steps of 5 to 10 nm. The resolution is limited by the step size and noise for these measurements, and must be estimated separately for each sample, from the graphed results.

2.7 Annealing

Some defects can be inactivated, or even removed, by annealing. Light interstitial atoms often diffuse out, so long as they are not strongly bonded. Changes in the properties of a sample due to annealing yield hints as to the nature of the defects in the grown film, so most of the samples were annealed and examined for changes.

The rapid thermal annealer used was a Mini-Pulse 610, produced by AG Associates. After growth, a piece of each sample was heated to 730°C for 10 seconds. The temperature was reproducible to within 7°C. The samples went from 100°C to 730°C in about 8 seconds. The ramp-down was slower, dropping about 300°C in the first 10 seconds and more slowly after that. 730°C was chosen as the highest temperature that didn't produce visible degradation of the surfaces of the first group of samples. Surface damage due to phosphorus evaporation was minimized by placing an InP substrate in

contact with the sample surface. However, some surface damage will always occur, and represents the primary source of uncertainty in analyzing the effects of the annealing.

The annealed samples were studied by Xray DCD, Hall and PL.

2.8 Variable-Energy Positron Annihilation

Samples were sent to be analyzed by this technique in order to check for the presence of vacancy-type defects. Positrons are directed into the sample, where they annihilate with electrons, emitting 511 keV gamma radiation. The γ-emission line will be broadened due to the motion of the annihilating particles, with core electrons causing a greater energy change than valence electrons, because of their greater momentum. The ratio of the central portion of the peak signal to that occuring in the wings represents a measure of the relative numbers of positron annihilations at valence electrons to the number at core electrons. This ratio is called the S-parameter. Positrons preferentially annihilate in regions of empty volume (away from the positive atomic nuclei), where the electrons are of low energy, so an increase of the S-parameter indicates an increase in the concentration of open volume defects, all other variables being equal. Only neutral and negatively charged vacancies are detected, because positive charge repels the positrons. Thus, ionized donor vacancies cannot be detected. The sensitivity limit to open-volume defects is about $10^{17}/cm^3$, depending on the positron capture cross-section of the defect.

The incident energy of the positrons controls the depth into the bulk at which the annihilation occurs, so the S-parameter can be measured vs penetration depth (or positron energy). The positron energy was varied from 0 to 32 keV, giving a maximum mean

penetration of roughly 1.2 μm. This depth control is not precise, because the rate of energy loss is not accurately known and the energy loss process is statistical. For example, as the positron energy is increased, the component of signal from the surface is reduced, but not eliminated. When the results are analyzed, this smearing of the signal must be considered.

A selection of samples were analysed at the Positron Beam Laboratory at the University of Western Ontario. The results of their modeling are qualitative, because the diffusion constant of positrons in InP is not yet known. The diffusion constant for GaAs was therefore used, which is expected to result in an error of less than an order of magnitude. No other source of error is of comparable magnitude.

2.9 Thermal Desorption

In order to determine whether deuterium or helium atoms were present, and at what concentrations, thermal desorption measurements were made. Samples grown with a helium plasma were heated to destruction in a vacuum chamber with a mass spectrometer and the desorbed mass 4 molecules detected and integrated. A large hydrogen background is present in the analysis system, so the desorption of hydrogen from the samples could not be directly determined. Consequently, a deuterium plasma was used and the "hydrogen" incorporation determined by monitoring the desorption of mass 3 (H-D) and mass 4 (D_2). The signals were integrated over the full temperature range to give a total yield. Dividing by the volume of film gives the concentration of that mass. In the system used, concentrations down to $10^{16}/cm^3$-$10^{17}/cm^3$ are normally visible,

depending on the thickness of the film and the size of the sample analysed. Measurements could be in error by approximately a factor of two at these levels. For concentrations in the $10^{18}/cm^3$-$10^{19}/cm^3$ range, errors should be less than 50%. D or He bubbles might trap in InP at high temperatures in much the same manner that He traps in some metals. To reduce the probability of this source of error, the samples were heated well past the point of destruction. The thickness of material vapourized could not be measured, but rough surfaces resulting from the process suggest that most or all of the films were removed. The system was recalibrated every time a sample was desorbed, using a known flux from a calibrated leak.

2.10 Nuclear Reaction Analysis

This technique was used as an alternative method to measure D concentrations in the samples. It is based on the nuclear reaction

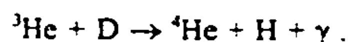

$$^3He + D \rightarrow {}^4He + H + \gamma\ .$$

In this case, a beam of $^3He^+$ ions was directed into the sample. The reaction produces alpha particles and protons which are identified and counted with a detector located nearby. The output signal is proportional to the D concentration in the sample. In all cases, the energy of the incident ^3He atoms was 825 keV.

The system can be optimised, using a large-area detector, to detect D concentrations as low as $10^{16}/cm^3$, with uncertainties of about a factor of two. At higher concentrations, the primary cause of error is beam-induced desorption of D during the measurement itself. The number desorbed depends on the initial concentration of the D

atoms, and on the number of $^3He^+$ ions incident on the target film. The uncertainties will therefore be specified for each sample when the results are discussed.

2.11 Capacitance/Voltage (CV) Profiling

This is a technique for measuring the carrier concentration, but not the mobility, of a sample. Rather than obtaining just the average, a profile of the carrier concentration with depth into the sample is produced. The best measurements are made when the substrate is highly doped, because good electrical contact can then be made to the back of the sample. An electrolyte solution, which acts as both an electrical contact and an etchant, is placed in contact with the film surface, producing a Schottky diode. By measuring the capacitance vs the applied voltage, the carrier concentration is determined. As the film is etched, the carrier concentration is measured as a function of depth.

The system used was a PN4300 Semiconductor Profile Plotter produced by Bio-Rad Laboratories, Ltd. Ammonium titride was used to etch both of the samples studied. The n-type sample was illuminated to induce etching during the measurement. The greatest source of error is due to non-uniform etching.

In chapter 4, this technique was used to determine whether a D plasma passivated Si or Be dopants in InP.

3. Deposition of InP Epilayers at Different Temperatures

3.0 Abstract

Films were grown at temperatures from 232°C to 500°C, under varying phosphorus fluxes. The primary defect produced at low temperatures is the phosphorus antisite, in agreement with reports in the literature. The properties of the film showed no dependence on the degree of excess of the phosphorus growth flux. The samples were characterised through a variety of techniques, for comparison with the films grown under plasma bombardment.

3.1 Growth Conditions

Samples were grown at temperatures from 232°C to 500°C. The growths are summarized in Table 3.1. Film thicknesses were measured with the alpha-step system. The ~ symbols in the chart mean that the alpha-step was not used on that sample, but the growth rate was calibrated from other samples. One sample (452) was grown using a phosphine flux of 5 sccm (standard cubic centimetres per minute) and a growth temperature of 465°C. This had been found in the past to produce the best quality (highest mobility) material. For all other samples, except 869, a thin buffer layer was grown using these conditions before adjusting to the required growth temperature and phosphine flux. For sample 869, the growth temperature was set to the melting point of a small piece of

tin attached to the substrate and the buffer layer of InP was omitted since it could have affected the melting temperature.

Table 3.1: Summary of GSMBE Growths At Various Temperatures Without Plasma

Growth #	Tg (Celsius)	Thickness (μm)	PH_3 Flux (sccm)	Buffer (μm)
640	500	1.09	5.5	0.04
452	465	2.96	5	2.96 or 0
593	465	0.26	4	.002
595	465	0.26	3	.002
597	465	~0.26	2.5	.002
598	465	~0.26	2	.002
608	465	?	1.5	.002
543	400	1.97	5	.06
563	400	1.79	5	.06
553	350	1.89	5	.06
609	350	2.45	2	.06
625	300	1.01	5	.06
693	300	0.67	2	.06
869	232	~1.9	4	0

In one series of experiments, the phosphine flux was reduced down to as little as 1.5 sccm in order to observe the effects of a lower phosphine overpressure. These growths

were generally only 20 minutes long, so that more samples could be grown. As a consequence the accuracy of some measurements is reduced. For the lowest phosphine flux, 1.5 sccm, growth was stopped after 8 minutes because the sample surface had visibly degraded. This sample has a question mark in the thickness column, and was not characterized further. The results indicate that the minimum phosphine flux required to maintain growth with a smooth surface morphology is thus between 1.5 and 2 sccm. Calculations show that this is consistent with the maintenance of growth in a phosphorus overpressure. Consider that the net phosphorus flux at the substrate surface is the incident flux (supplied from the PH_3) minus the evaporation flux. Only the P_2 flux need be considered, since P_4 has a lower production rate, lower sticking coeficient and lower vapour pressure by an order of magnitude [Stanley *et. al.*, (1985)] and can be reasonably ignored. The P_2 evaporation flux is given by:

$$f = \frac{p}{\sqrt{2\pi mkT}}$$

where p is the vapour pressure, m is the mass of P_2, k is Boltzmann's constant, and T is the temperature of the surface. Unfortunately, some discrepancies appear in the published vapour pressure values. Considering growth at 465°C, vapour pressures of 1.3×10^{-6} atm [Farrow, (1974)] or 1.93×10^{-5} atm [Panish *et. al.*, (1970)] are given for P_2 over InP. Note that these results differ by more than an order of magnitude. Farrow's work is more recent, and he argues that there is a systematic error in the work of Panish *et. al.* On the

other hand, Farrow only made measurements above 545°C, making it necessary to extrapolate to 465°C, while Panish *et. al.* measured down to approximately 460°C. Calculations have been made here using both values, yielding a P_2 evaporation flux of either $1.6 \times 10^{12}/cm^2/sec$ or $2.4 \times 10^{13}/cm^2/sec$. The incident In flux can be determined from the growth rate to be $2.7 \times 10^{14}/cm^2/sec$. This ignores any In evaporation loss, which is negligible (less than 1%) at 465°C and lower temperatures. Thus, the phosphine flow needed to give a 1:1 (P:In) net flux ratio is 1.74 sccm or 1.61 sccm. For a growth temperature of 465°C, the net flux ratio at 2 sccm is about 1.1, while at 5 sccm it is about 2.9.

Growth at 500°C was carried out in a phosphine flux of about 5.5 sccm, to ensure sufficient P_2 for good quality growth at the higher growth temperatures. Evaporation fluxes at 500°C were determined to be $1.5 \times 10^{13}/cm^2/sec$ [Farrow, (1974)] or $1.6 \times 10^{14}/cm^2/sec$ [Panish *et. al.*, (1970)], i.e. equivalent to about a PH_3 flow of 0.14 sccm or 0.93 sccm. The sample surface was monitored by RHEED, and stayed good throughout the growth process, indicating an adequate P_2 flux.

Growths at lower temperatures were carried out with fluxes of 2 and 5 sccm and the sample quality compared.

3.2 Nomarski Microscope Results

After growth, samples were viewed under a Nomarski Phase Contrast Microscope and the surface defect densities estimated. Samples 869, 553 and 609 could not be included, due to damage to the microscope. The surface defect density of a sample grown

using the best conditions (5 sccm P_2, T=465°C) was about $5.6x10^5/cm^2$. This is similar to the only defect density reported in the literature for MBE grown InP, $10^5/cm^2$ [Rakennus *et. al.*, (1992)], which is very large compared to densities of 100 to $500/cm^2$ reported in the literature for GaAs [Schlom *et. al.*, (1989), Kondo *et. al.*, (1989), Chand *et. al.*, (1990)]. Growths done under nominally the same conditions at different times have produced similar electrical quality but lower surface defect densities. A major factor determining surface quality appears to be the number of growths carried out after the MBE system had been opened to air (for maintenance or repair). The result shown here is for a growth carried out shortly after a system overhaul, when surface defects are common. The primary defect looks similar to the oval defects that have been observed on GaAs grown by MBE. Impurities have been shown to be the cause of some oval defects in GaAs [Fujiwara *et al.*(1987), Bachrach *et. al.*, (1981), Chai *et. al.*, (1985)]; it appears that a similar process occurs for InP.

The surfaces of the samples grown at 465°C with reduced phosphine flux were also viewed. These growths were carried out "back-to-back", so the time since the last MBE system overhaul was not a significant factor. A trend to greater surface defect densities at reduced P_2 fluxes was observed, culminating in the extreme degradation of sample 608 for a flux of 1.5 sccm.

The sample grown at 500°C is shown in figure 3.2a. It had a surface defect density of about $4.2x10^4/cm^2$, which is better than the growth at 465°C, probably because more time had passed since the system was opened. Oval defects were also the most common surface defect on this film.

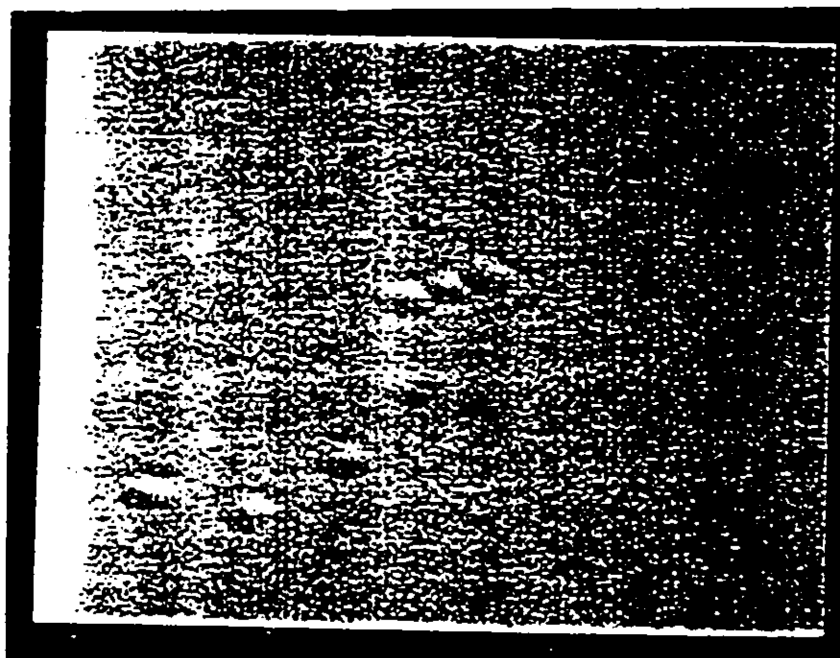

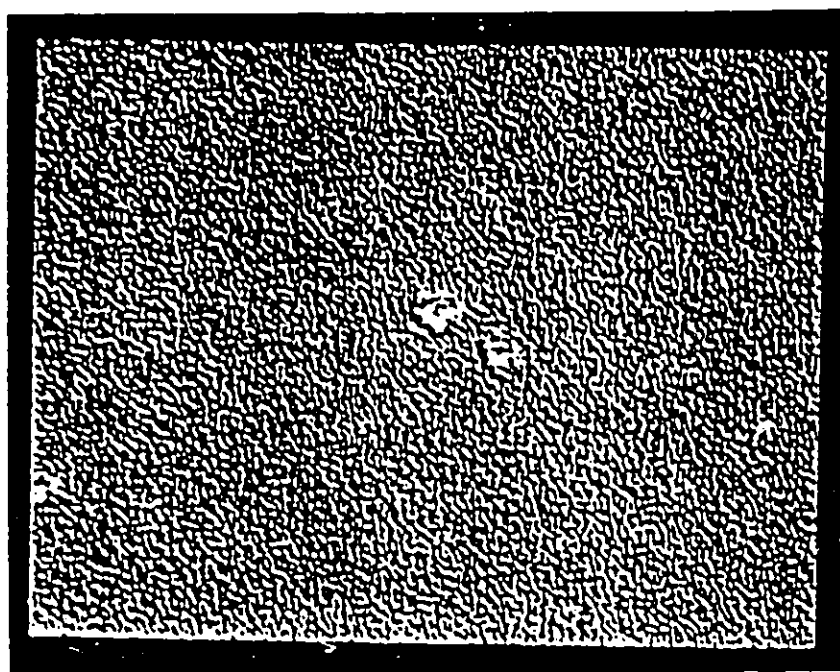

Figure 3.2a (top): Surface of a film grown at 500°C. 1000x magnification.
Figure 3.2b (bottom): Surface of a film grown at 400°C. 1000x magnification.

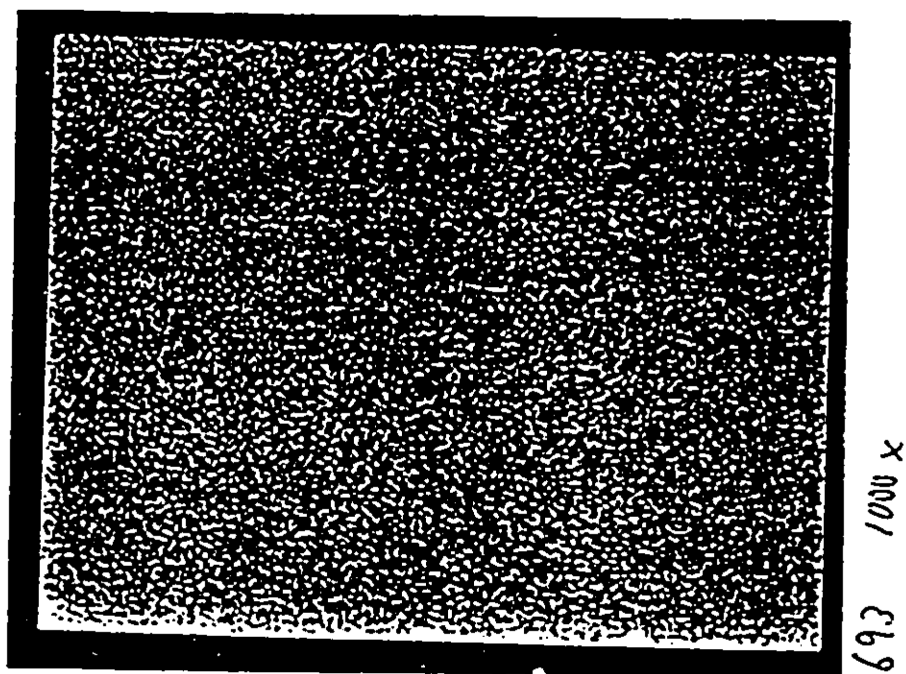

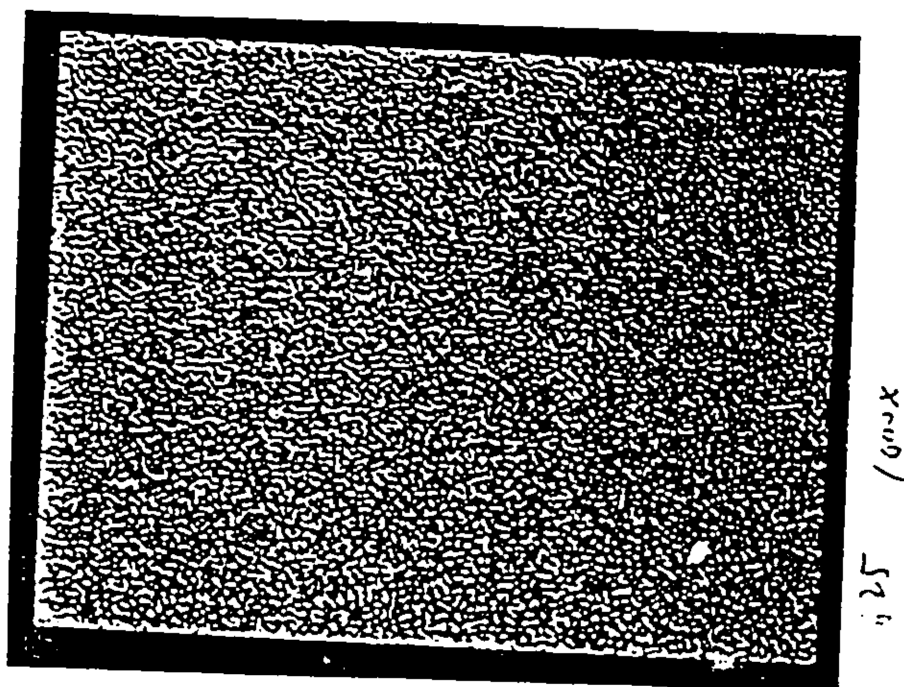

Figure 3.2c (top): Surface of a film grown at 300°C. 1000x magnification.
Figure 3.2d (bottom): Surface of a film grown at 300°C, with a flux of 2 sccm. 1000x magnification.

All of the growths at 400°C or less exhibited a textured surface, with small rougher regions. These small regions appeared somewhat like a superposition of an oval defect on the textured surface. The surface was textured both for the standard 5 sccm phosphine flux and when the flux was reduced to 2 sccm. The effect is clearly related to the lower growth temperature. Figures 3.2b and 3.2c show the surfaces for growths at 400°C and 300°C with 5 sccm of PH_3, and 3.2d shows a growth at 300°C with a phosphine flux reduced to 2 sccm. The surface morphologies look quite similar. It appears that there is a transition to three-dimensional growth between 400°C and 465°C.

3.3 Xray Double Crystal Diffraction

The results of the Xray measurements are shown in Table 3.3. A high quality crystalline InP sample will have a full width at half maximum (FWHM) of about 13 seconds of arc. The samples with FWHM of 11 to 14 seconds are thus of good quality. An example is shown in figure 3.3a.

Broadening of the peak indicates reduced crystal quality, which occurs for all growths below 400°C. Figures 3.3b, c, d and e show the results for the growths at 350 and 300°C. One growth at 300°C (3.3d) is clearly asymmetric, showing that there is strain in the grown layer. The other growths have only widened from the ideal by 3 seconds, not enough for asymmetry to show. Note that while the growth at 300°C with reduced phosphine flux (3.3e) is narrower than at standard flux (3.3d), part or all of the difference is because the film in 3.3e is much thinner, and its Xray signal is correspondingly weaker. The sum of the film and substrate peaks thus consists primarily of the substrate peak,

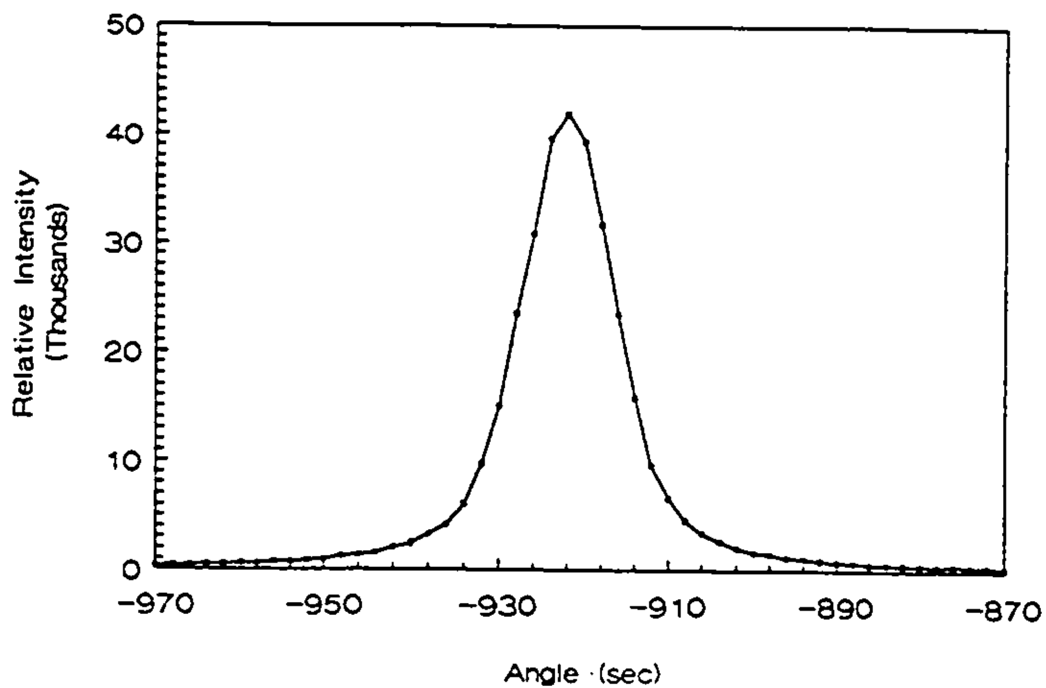

Figure 3.3a: Xray rocking curve of InP grown at 465 Celsius.

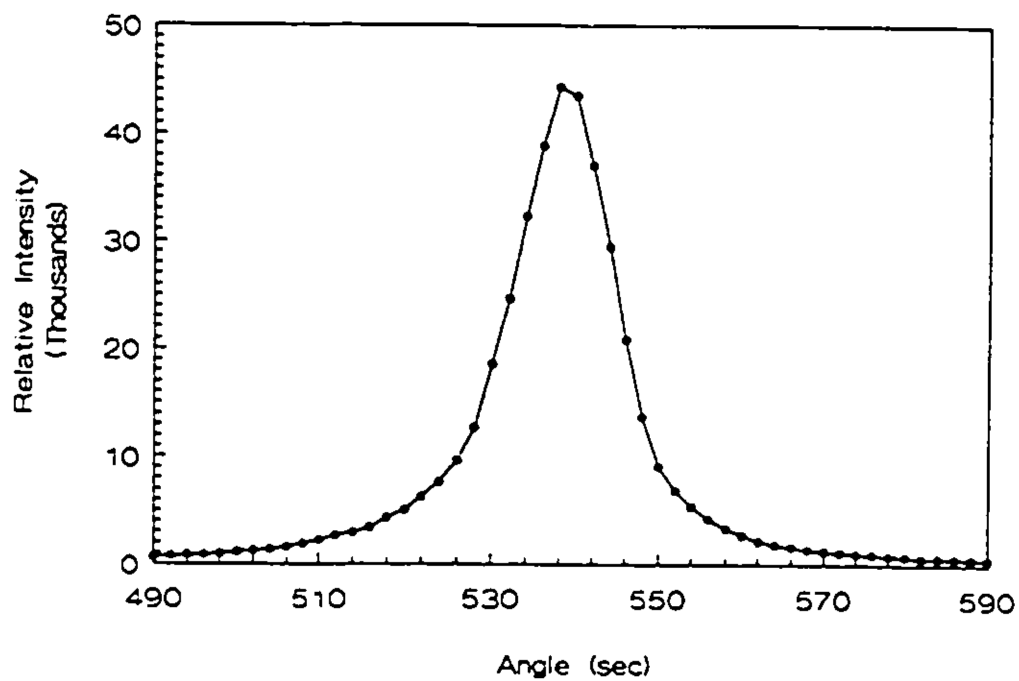

Figure 3.3b: Xray rocking curve of InP grown at 350 C, 5 sccm.

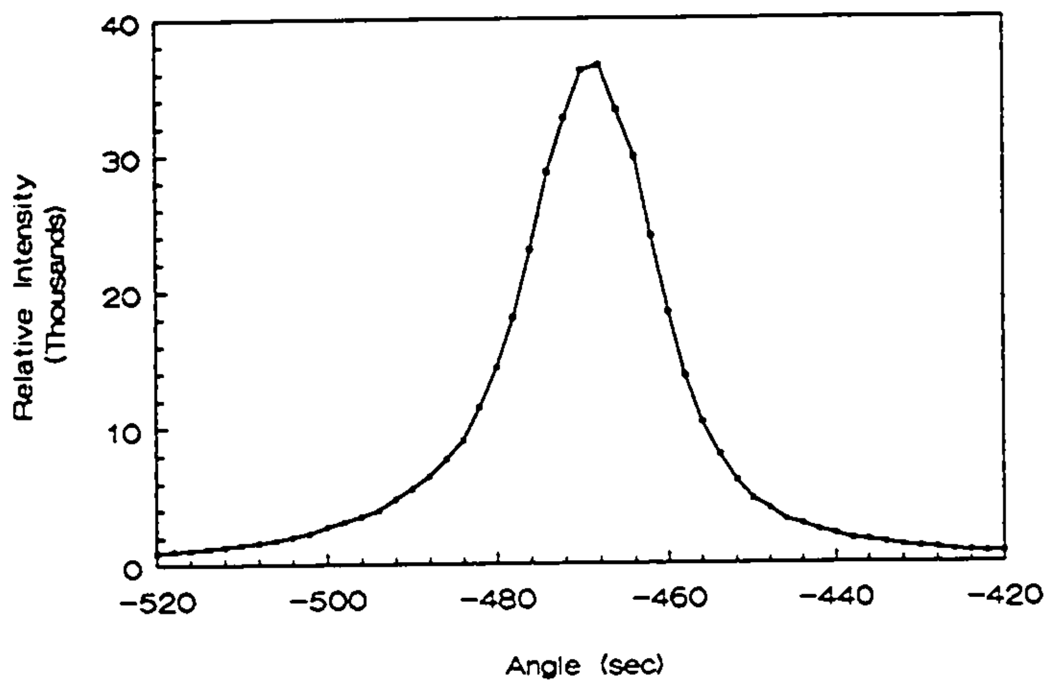

Figure 3.3c: Xray rocking curve of InP grown at 350 C, 2 sccm.

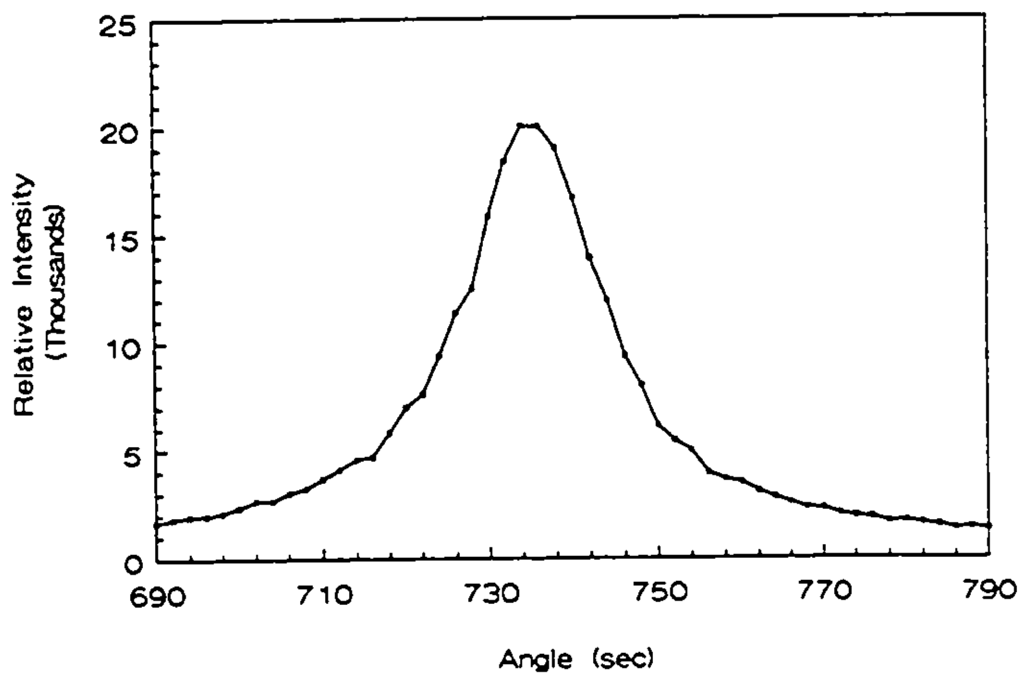

Figure 3.3d: Xray rocking curve of InP grown at 300 C, 5 sccm.

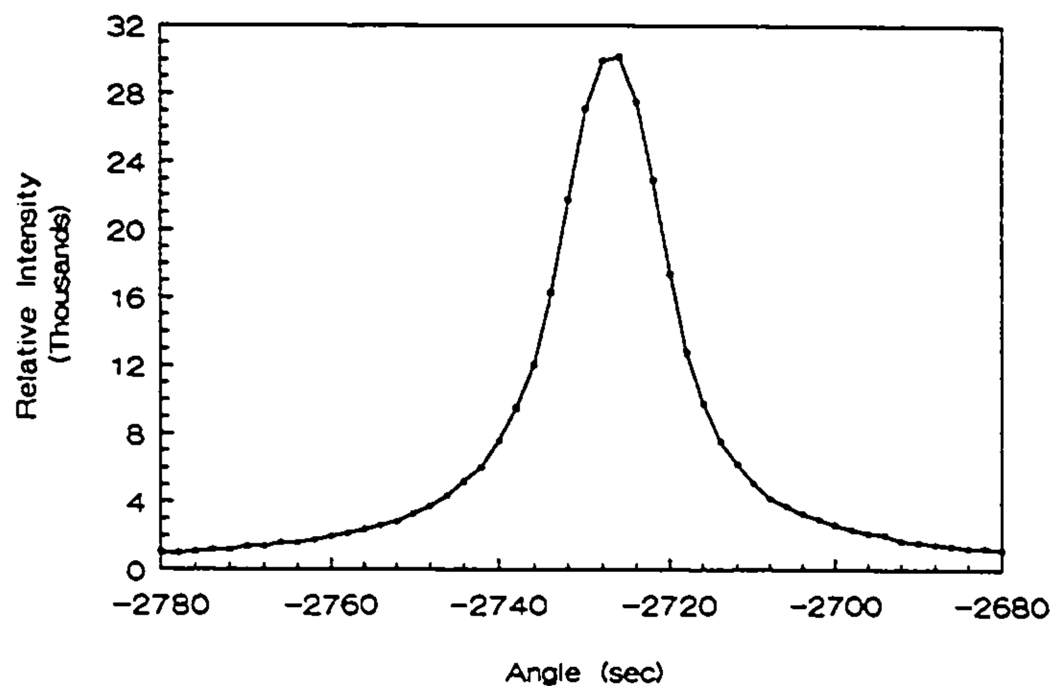

Figure 3.3e: Xray rocking curve of InP grown at 300 C, 2 sccm.

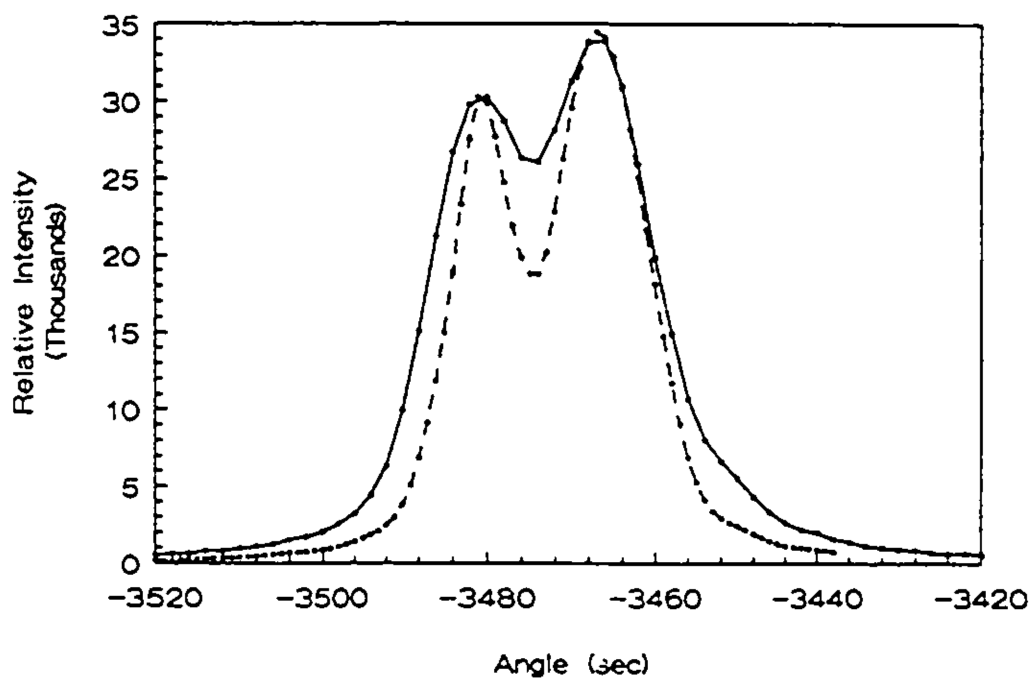

Figure 3.3f: Xray rocking curve of InP grown at 232 C, 4 sccm.

which is only about 13 sec wide. It may be that the reduced phosphorus flux reduces the concentration of P_{In}, so there is less strain in the grown film, but this wasn't seen at higher temperatures.

Table 3.3: Summary of Xray double crystal diffraction results. At 232°C, the signal had broadened into two distinct peaks.

Growth Temperature (°C)	PH_3 Flux (sccm)	Peak Width (FWHM) in seconds of arc
500	5.5	12
465	5	13
465	2.5	13
465	2	14
400	5	11
400	5	13
350	5	16
350	2	16
300	5	21
300	2	16
232	4	2 peaks

The sample grown at 232°C actually has two separate peaks, indicating that the epitaxial layer is strained (figure 3.3f). The dashed curve in the figure is the RADS fit. The peak separation of 14 seconds corresponds to a strain of .005%. The peak on the left is due to the substrate, the peak on the right is due to the grown film (for samples of thickness >1.7μm, the peak from the film is larger). Fitting by RADS shows that the film

has a smaller lattice constant than the s- bstrate, that is, that the film is under tension. This implies that the defect(s) producing the strain are vacancies, P-antisites (P atoms are smaller than In atoms, so when a P atom occupies an In site, tensile strain results) or complexes that include either or both. Evidence for the existence of both vacancies and interstitials has been reported from studies of growths at reduced temperatures [Dreszer *et al.* (1993a&b), Hautojarvi *et al.* (1993), Liang *et al.* (1992)]. In this work the film was grown in a large excess flux (~140%) of P_2, so P-vacancies are not likely to be present in significant concentrations. Thus, In-vacancies and/or P-antisites are probably the defects responsible for the strain observed, possibly as part of complexes. The broadening seen in the 300 to 400°C growths is probably due to the same defects, occurring in smaller quantities at higher growth temperatures. The fit in figure 3.3f has narrower peaks than the experimental curves because the fit assumes uniform strain and a flat sample. The strain in the film will vary with distance from the defects producing the strain, broadening the signal compared to an isotropically strained film. The strain will tend to produce curvature of the sample, which will also broaden the peak.

One sample grown at each temperature with the higher phosphorus flux was annealed at 730°C for 10 seconds. The growths at 500°C and 400°C were unchanged, the 465°C growth widened by two seconds (so it's still in the good range, and within scatter of the original sample), and the growths at 350°C and 300°C narrowed by two arcsec. The lowest temperature growth, 232°C, had a single peak with a FWHM of 13 arcsec after annealing. Recall that before annealing the grown layer had so much strain that two separate peaks were visible. It is not clear why this sample should be less strained after

annealing than the growth at 350°C, perhaps it is just scatter in the data. The small narrowing at 350°C and 300°C may be indicative of a trend which is most obvious in the results at 232°C. The mechanism by which the strain is reduced is not clear. The defects could be fully removed by the annealing, but this would require movement of the large In-atoms to the defect sites, and so seems unlikely, but no other mechanism is apparent.

The measured strain in the sample grown at 232°C can be used to estimate the concentration of defects in the sample. Consider the effect of removing a small percentage of the atoms present in a crystal (creating vacancies). The remaining atoms will move slightly inward to partially fill the voids left behind. This will reduce the volume of the crystal by a small fraction. The number of lattice sites will be unchanged, although some of the lattice sites will be unoccupied. A reduction in volume without a change in the number of lattice sites is equivalent to a reduction of the lattice constant. The magnitude of the reduction will depend on the number of vacancies, and on the reduction in volume per vacancy. The relative change can be written:

$$\frac{\Delta V}{V}=C_v\frac{\Delta v}{\theta}$$

where V is the volume of the film, ΔV is its change in volume, C_V is the concentration of vacancies, Δv is the change in volume per vacancy and θ is the volume per lattice site. Using the relationship

$$\frac{\Delta V}{V}=\left(\frac{a+\Delta a}{a}\right)^3-1\approx 3\frac{\Delta a}{a}$$

where a is the lattice constant, the concentration of vacancies is given by

$$C_v = 3\frac{\Delta a}{a}\frac{\theta}{\Delta v}$$

For metals, $\Delta v/\theta$ has been found to be approximately 0.2 [Thompson (1969)]. Using this value, since $\Delta v/\theta$ isn't known for InP, gives a vacancy concentration of 0.075 atomic percent, or $3.0 \times 10^{19}/cm^3$, for "average-sized" vacancies. Assuming that they are all In vacancies gives a small correction. The radius of the In atom is 1.44Å and the P-atom's radius is 1.10Å [Suchet (1965)]. Thus the In:P volume ratio is 2.24:1. Taking this into account gives a correction factor of 0.722, yielding a concentration of $2.2 \times 10^{19}/cm^3$ of In vacancies. The same approach can be followed for P-antisites. The concentration is then $4.0 \times 10^{19}/cm^3$ of P-antisites. Either In-vacancies or P-antisites, or a mix of the two, could be responsible for the strain observed.

Note that defects which produce compressive strain, such as interstitials, may also be present. These would compensate for some tensile strain in the film. The concentration of In-vacancies and/or P-anitsites could then be even higher.

The concentrations cannot reasonably be estimated for the growths at higher temperatures, since the positions of the peaks cannot be resolved, but they are clearly much smaller.

3.4 Variable-Energy Positron Annihilation

The samples grown at 500°C and 300°C were analyzed by Variable-Energy Positron Annihilation. The results are shown in figure 3.4. Results from the growth at 500°C indicate that the concentration of defects to which positrons are sensitive is below

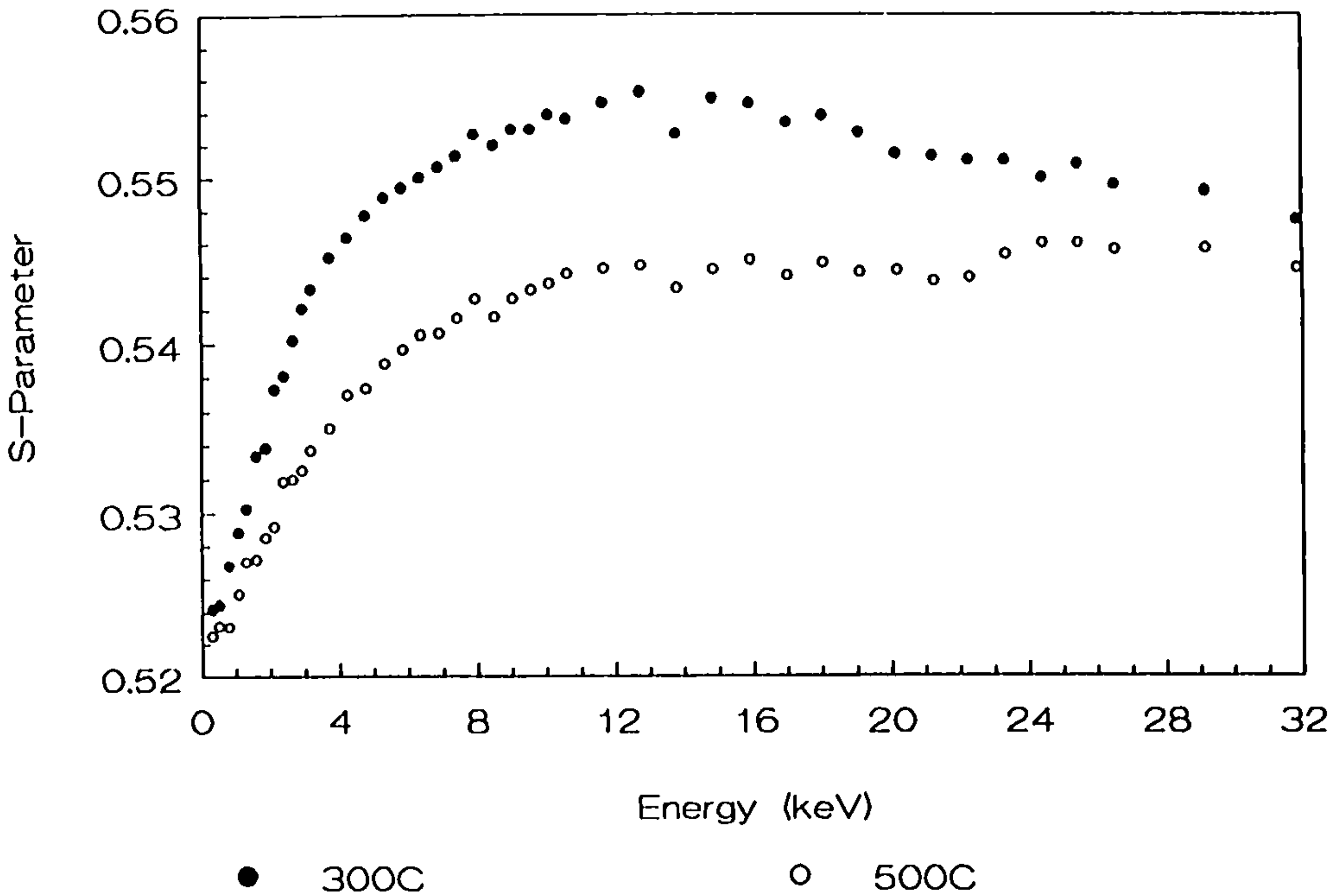

Figure 3.4: Positron annihilation profiles.

the detectable level (ie $< \sim 10^{17}/cm^3$). Positron traps are clearly present in the sample grown at 300°C. The single-point dip at 13.8 keV is a systematic error due to a scale shift, not a significant datum.

As mentioned in Chapter 2, the characteristics of InP are not known well enough to allow precise analysis of the results, so the values for GaAs were used in the modelling. This led to an estimate for the defect concentration in the T_g=300°C sample of about $4x10^{18}/cm^3$. This concentration is predicted to be accurate to within an order of magnitude, which puts the estimated concentrations of In vacancies and/or P antisies from the Xray data just within range.

The defects detected by positrons must be either neutral or negatively charged (acceptors). Hall effect measurements given in the next section show that the film is heavily n-type, so any acceptors should be negatively charged. Possible acceptors are [Liang *et al.* (1992)]: In-vacancies, P-interstitials, In-antisites (In on a P site) and complex defects. This high electron carrier concentration puts the Fermi level in the conduction band, which means that most donors will be inactive, and therefore neutral. P-vacancies, In-interstitials, P-antisites and possibly some donor complexes would be uncharged. Finally, complexes that aren't electrically active (not donors or acceptors) will be neutral. The film was grown under P-rich conditions, so P-vacancies, In-interstitials and In-antisites are unlikely to be present in significant concentrations. To be detectable by positrons, besides a non-positive charge state, a defect needs to have a significant open volume in which the positron can be trapped. P-interstitials are therefore not detected here. The possibilities that remain are: In-vacancies, P-antisites and complexes. The In-

vacancies and P-antisites are consistent with the Xray results.

3.5 Hall Effect

The Hall mobility and carrier concentration were measured at room temperature. Table 3.5 summarises the results. For the sample grown at 465°C with 2 sccm phosphine flux only approximate values are given because the film was only 0.26 μm thick and hence fully depleted for carrier concentrations $<8\times10^{15}/cm^3$. There is little or no difference between the material comprising this sample and that grown at standard flux. Large differences would have been visible, but any differences in this case are small enough to be hidden by the surface and interface depletion effects. The growths at 300°C and 350°C with 2 sccm of phosphine are also in good agreement with those at the standard 5 sccm. The electrical properties are clearly not significantly affected by the degree of excess of the P_2 flux.

The factor of 3 difference in n for the growths at 400°C is probably not significant. The samples were grown two weeks apart, and variations of that size occurred under standard conditions (465°C, 5 sccm). Below 450°C, the temperature is difficult to control precisely, because the pyrometer doesn't operate accurately, so the difference in carrier concentration may also arise from a small difference in growth temperature.

Table 3.5: Electrical properties of InP films at room temperature. The growth at 465°C with 2 sccm was totally depleted, so only limiting values are known.

Growth Temperature (°C)	Phosphine Flux (sccm)	n (/cm^3)	Mobility (cm^2/Vs)
500	5.5	1.0×10^{15}	4300
465	5	1.1×10^{15}	4880
465	2	$<8\times10^{15}$	>3100
400	5	3.2×10^{16}	3500
400	5	9.5×10^{16}	3230
350	5	8.1×10^{17}	2010
350	2	6.0×10^{17}	2190
300	5	2.0×10^{18}	650
300	2	1.5×10^{18}	500
232	4	2.7×10^{18}	1190

A graph of carrier concentration vs growth temperature is presented in figure 3.5a. The maximum of 2.7×10^{18}/cm^3 agrees roughly with most recent results [Dreszer *et al.*(1993a&b), Liang *et al.* (1992), Maracas *et al.* (1992)]. A maximum of about 4×10^{18}/cm^3 has been predicted [Dreszer *et al.*(1993a&b)], due to pinning of the Fermi level by the P-antisite defect. As shown in the previous sections, the Xray and positron results are consistent with large concentrations of In-vacancies, P-antisites and/or clusters including some vacant volume. In-vacancies behave as acceptors, so they cannot be the dominant defect here. Some form of cluster cannot be disproven, but P-antisites are clearly the simplest explanation. They have been seen under similar growth conditions already, and the electrical properties are in reasonable agreement with the measured

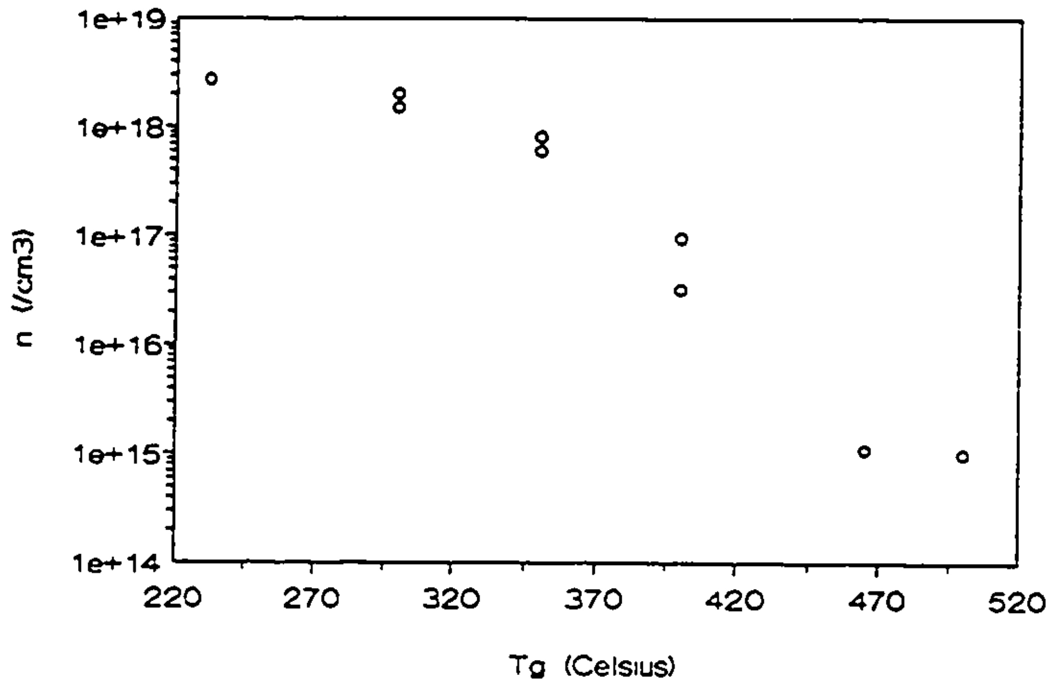

Figure 3.5a: Carrier concentration vs growth temperature.

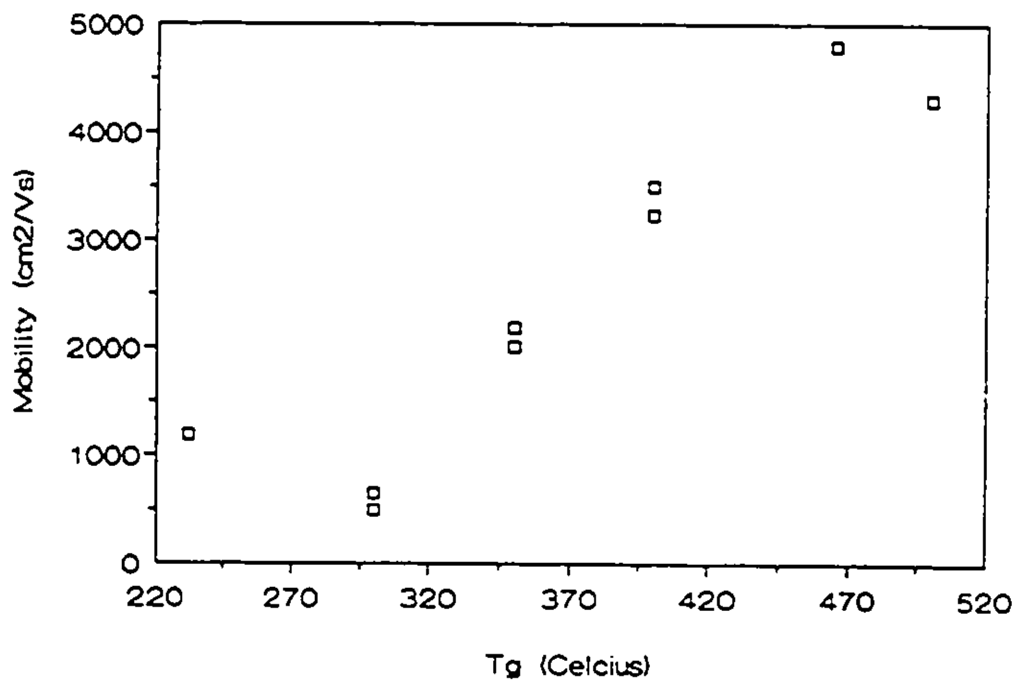

Figure 3.5b: Hall mobility vs growth temperature.

properties of P-antisites.

The mobilities are plotted in figure 3.5b. The only surprising result is at 232°C, where the mobility increased compared to the growths at higher temperature. This may mean that significant conduction is occuring in a defect band, in addition to the conduction band. The very large concentration of donor defects makes it possible. Such conduction is called hopping conduction. It occurs when the defects are close enough together for electrons to move (hop) from defect site to defect site.

Temperature dependent (10-295K) Hall measurements were also made on the sample grown at 300°C. The material was too heavily doped to exhibit any temperature dependence. The mobility varied by only about 10% over the full range, while the carrier concentration varied less. Meaningful analysis is not possible with such small changes.

Figures 3.5c and 3.5d show the effects of annealing on the carrier concentration and mobility, respectively. The carrier concentration for the annealed sample grown at 500°C is not shown, because the sample was fully depleted. For the samples grown at 400°C and higher both the carrier concentrations and mobilities were reduced slightly. Normally, a drop in carrier concentration is indicative of an improvement in film quality, but the mobility has also decreased. It may be that a compensating defect was produced by the annealing. More probably, some electrically active defects were annealed out while surface dissociation also occured. This damage to the surface would reduce the measured mobilities, though the effect would be small for the thicker samples.

The samples grown below 400°C all have much better electrical properties after annealing. The concentration of donor defects dropped by about an order of magnitude,

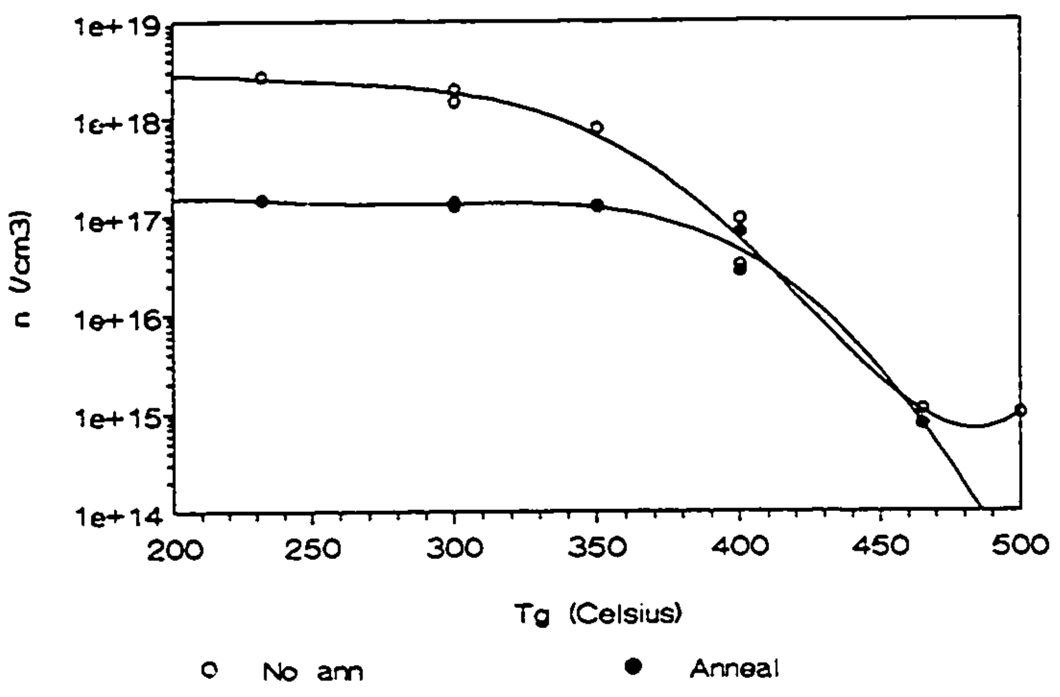

Figure 3.5c: Carrier concentration vs growth temperature, after annealing.

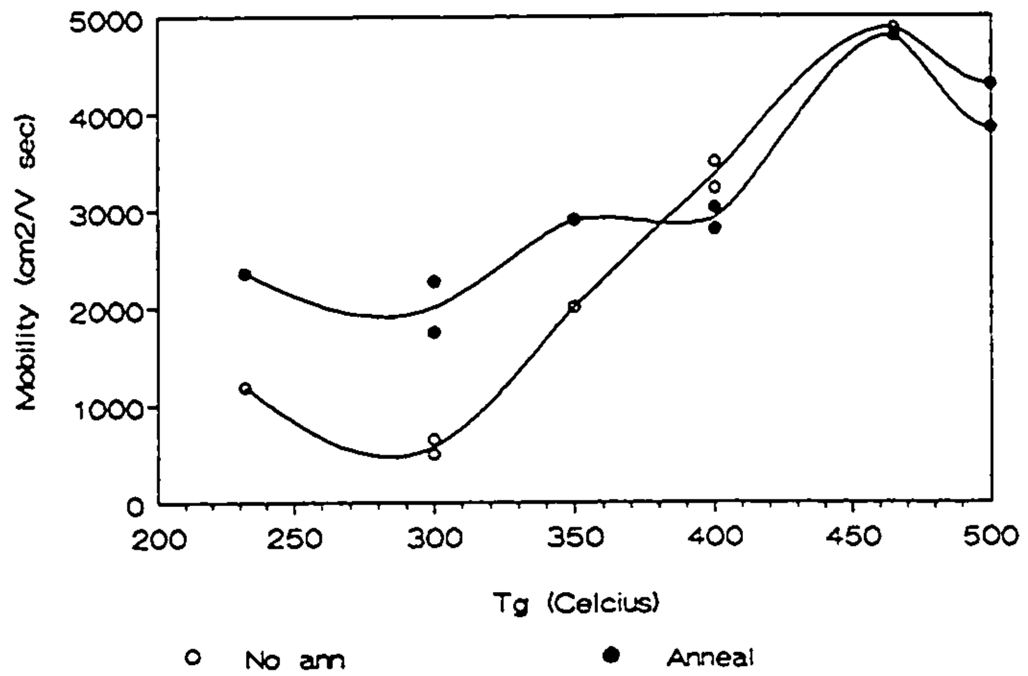

Figure 3.5d: Hall mobility vs growth temperature, after annealing.

while the mobilities are much higher. Thus it appears that most of the phosphorus antisites were removed or inactivated by annealing.

3.6 Photoluminescence

The PL spectra are shown in figures 3.6a and 3.6b. Growth temperatures from 500°C down to 400°C are included in 3.6a, and from 400°C to 300°C in 3.6b. To make comparison between the figures easier, one growth at 400°C was included in both figures. The growths at 500°C and 465°C all have two peaks present in the PL spectrum, the band edge (1.417eV) and a donor-acceptor peak [Yu *et. al.* (1992)] at about 1.385 eV. There may also be a very weak peak at about 1.34 eV, which is positioned as a LO phonon replica of the peak at 1.385 eV. Both of the growths at 400°C also have a peak at just over 1.35 eV, possibly due to the phosphorus antisite [Yu *et al.* (1994)]. (There is disagreement on the energy of the lower level of the phosphorus antisite [Yu *et al.* (1994), Dreszer *et al.* (1993a&b)] as described in section 1.1.) The 350°C growths are similar to those at 400°C, but the peaks are wider, so they overlap more. The growths at 232°C with 5 sccm and 300°C with 2 sccm of phosphine flux showed no luminescence. The band edge peak of the growth at 300°C with 5 sccm of phosphine was barely detectable.

The weaker signal for the lowest-temperature growths confirms the lower quality of these films. There was no apparent correlation between phosphine flux and optical intensity. The growths at 465°C and 350°C with 2 sccm have a stronger signal (but no change in peak placement), while the growth at 300°C is weaker (undetectable). No

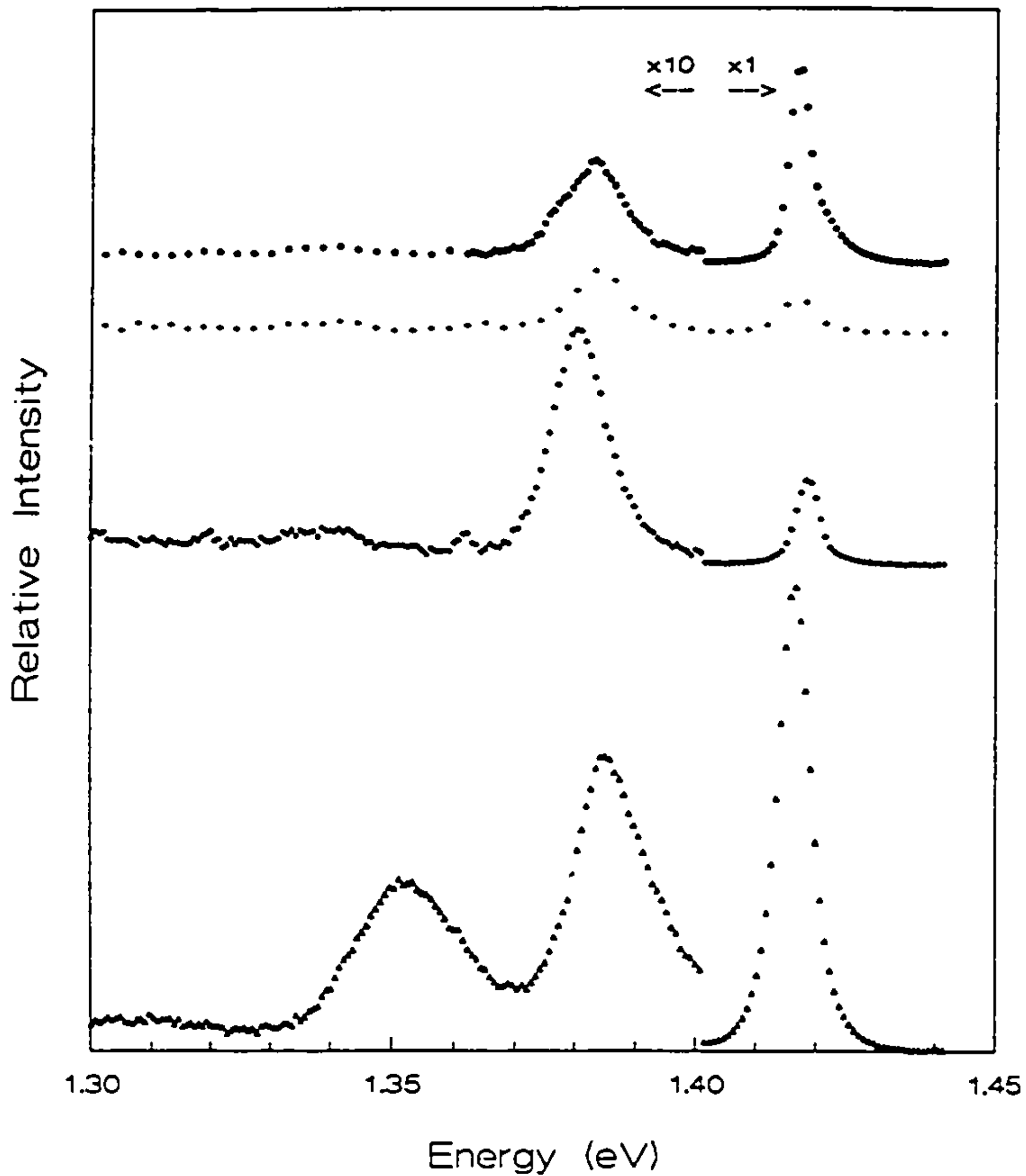

Figure 3.6a: PL results from InP grown at 1) 500C, 5 sccm (top) 2) 465C, 5 sccm 3) 465C, 2 sccm 4) 400C, 5 sccm (bottom, also at top of b).

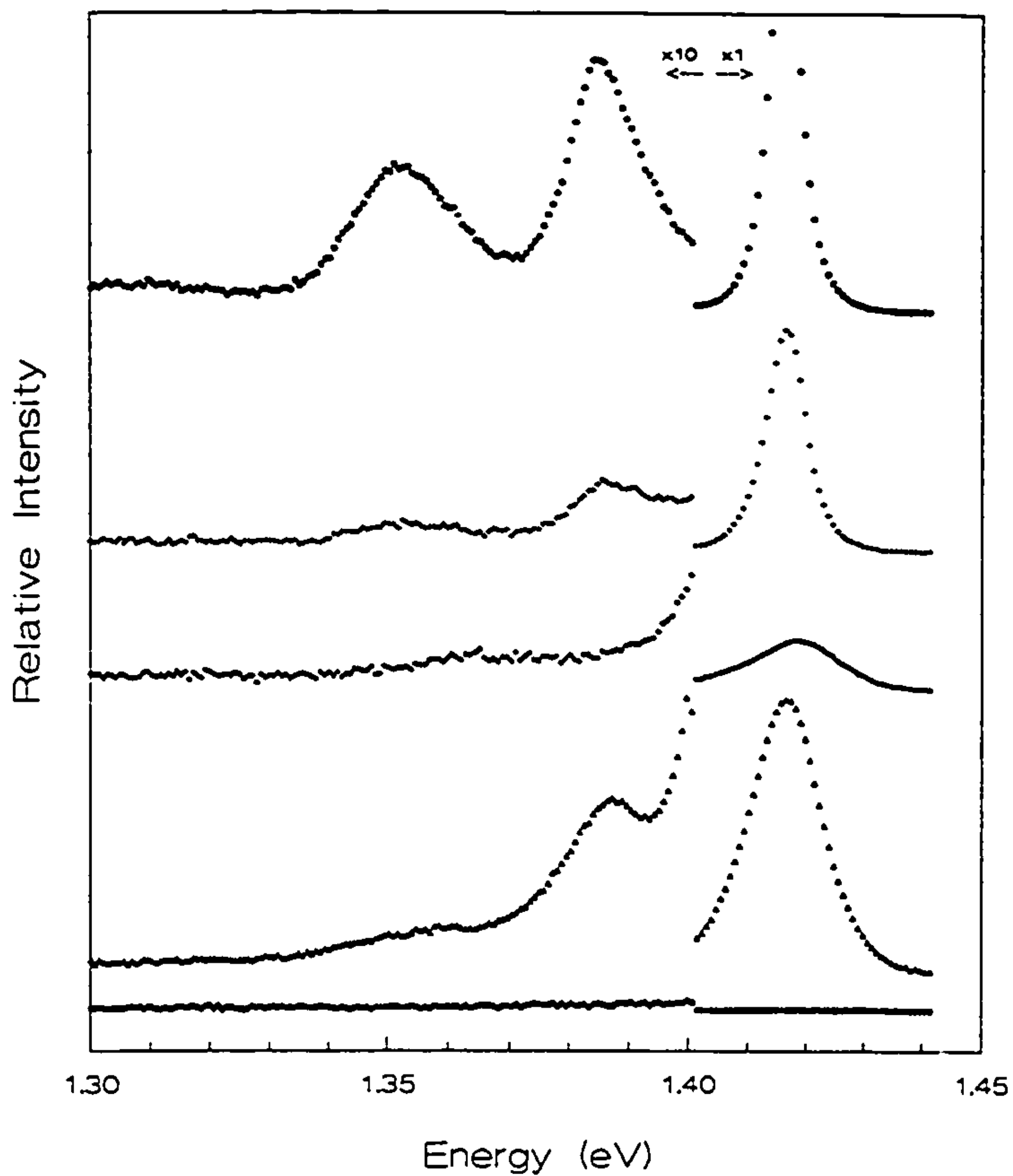

Figure 3.6b: PL results from InP grown at 1) 400C, 5 sccm (top) 2) 400C, 5 sccm 3) 350C, 5 sccm 4) 350C, 2 sccm 5) 300C, 5 sccm (bottom).

sample had any luminescent peaks below 1.3 eV, not even near 1.17 eV, reported to be the first level of the phosphorus antisite [Dreszer *et al.* (1993a&b)]. This level was found by pressure dependent Hall measurements, not PL. It seems more likely that the lower level of P_{In} is at about 1.35eV, as suggested by Yu *et. al.* (1994). There was a weak correlation between relative peak height and carrier concentration. In growths at 465°C or higher, which had concentrations near $1x10^{15}/cm^3$, the 1.35eV peak was much weaker than in the growths with higher P_{In} concentrations.

Not all of the annealed samples could be studied by photoluminescence, but those that were are shown in figure 3.6c and confirm the general trend of the Hall measurements. The signals from films grown at temperatures below 400° were improved, while the higher temperature growths became less luminescent. The two lowest temperature growths (232 and 300°C) that gave no signal as grown exhibit measurable luminescence after anneal. At the highest growth temperature, 500°C, the signal after anneal is very weak. However, significant surface damage was created by the anneal, producing a very rough surface. This is probably the cause of the reduction in PL intensity. For the growths at 400°C the PL intensity decreased. The only exception to the pattern seen in the Hall results is one growth at 350°C, for which the PL signal became weaker while the electrical properties were improved, perhaps because of annealing damage (again visible with a microscope, but to a lesser degree than the 500°C growth). There were still no deep luminescent peaks in samples grown at any temperature. Annealing seems to sometimes create surface damage, as well as annealing out bulk damage. This surface damage is unpredictable depending on the reproducibility of the

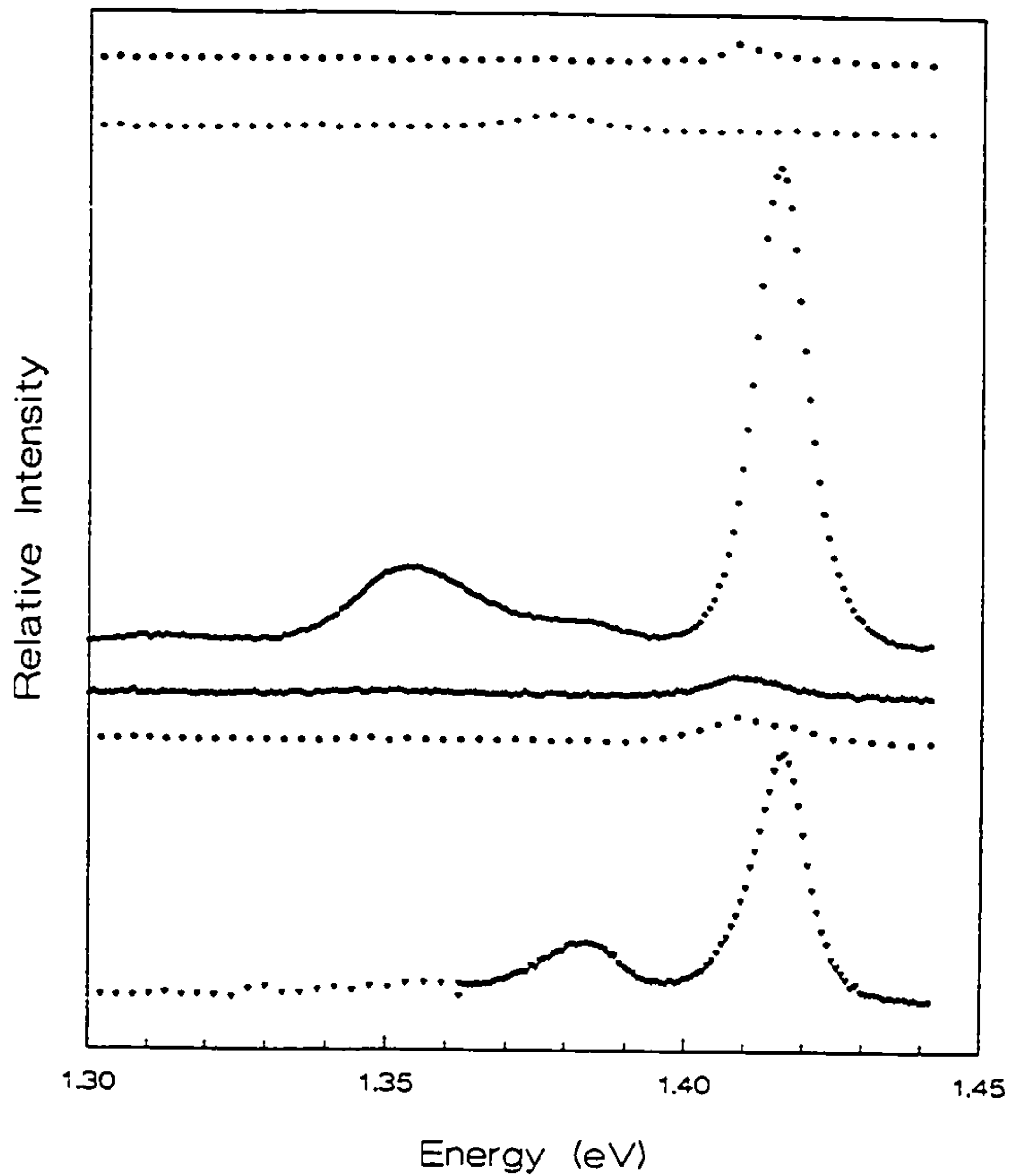

Figure 3.6c: PL results from annealed InP grown at 1) 500C, 5 sccm (top) 2) 400C, 5 sccm 3) 400C, 5 sccm 4) 350C, 5 sccm 5) 300C, 2 sccm 6) 232C, 5 sccm.

anneal conditions, in particular the capping process as discussed in section 2.7. In cases where there was a significant concentration of bulk defects, the sample was clearly improved by annealing. If the film was already of good quality, the largest effect was the surface damage, which showed as a reduction in luminescence.

3.7 Discussion and Conclusions

These results agree quite well with the general trends reported in the literature. All films are n-type, with carrier concentrations reaching the 10^{18}/cm^3 range at a growth temperature of 300°C. If the temperature is reduced far enough, strained material is produced. The PL peaks seen at 1.35 and 1.38eV have also been reported. Positron annihilation studies detect open-volume defects present at concentrations of ~4x10^{18}/cm^3 in the samples grown at low temperatures. Annealing reduces the strain and improves the electrical and optical properties of the samples grown at low temperatures.

The results reported here disagree with several of the specific details reported elsewhere, though. Maracas *et al.*'s (1992) finding of low carrier concentration until growth temperatures of less than 320°C is not observed. Rather the temperature dependence found is qualitatively similar to that of Dreszer *et al.* (1993a&b) and Liang *et al.* (1992), though there is a quantitative difference from each of theirs, perhaps due to differences in temperature calibration. Liang *et al.* (1992) reports that the carrier concentration decreases after peaking near 300°C. The results reported here, as in Dreszer *et al.* (1993a&b), have no such turnover. Finally, the dependence of the mobility on Tg is different from that reported by Dreszer *et al.* (1993a&b), who are the only group to

report on this. They find a slight decrease from ~2500 to ~2000 cm^2/Vs as the temperature is reduced to 300°C, at which point it drops sharply to ~400 cm^2/Vs and gradually declines from there. The results reported here show a steady decline from ~4800 cm^2/Vs to ~600 cm^2/Vs as Tg is reduced to 300°C, and an increase to 1190 cm^2/Vs at Tg of 232°C. The results of Dreszer *et al.* (1993a&b) indicate that their best quality material only exhibits a mobility of ~2500 cm^2/Vs, which is clearly not as good as the present work where the best mobility exceeded 4800 cm^2/Vs, suggesting the presence of additional defects or impurities in the previous work.

In conclusion, as the growth temperature of InP deposition by GSMBE is lowered, phosphorus antisite defects (donors) steadily increase in concentration. The concentrations appear to be essentially independent of the excess phosphorus flux. The carrier concentration cannot exceed ~$4x10^{18}cm^3$, because of the Fermi level pinning reported by Dreszer *et al.* (1993a&b). The P_{In} defects are probably responsible for the PL line seen at about 1.35eV. The mobility drops with Tg to 300°C, and then levels off or even increases. The increasing concentration of P_{In} is visible as a widening of the FWHM of the Xray rocking curve as Tg of the samples is reduced. This occurs because a P-atom occupies less than half the volume of an In-atom. The unoccupied space may also present a large cross-section for positron annihilation. Thus, the apparently contradictory results in the literature - large concentrations of vacancies reported by some groups but antisites reported by others - are reconciled. The P-antisite is associated with an open volume which can trap positrons as a vacancy does. In-vacancies are probably also present, but not necessarily in significant concentrations. In addition, the surfaces of the lowest

temperature growths are much rougher than those grown near 465°C. Annealing at 730°C can cause some surface damage but also removes or inactivates most of the defects, which shows as improvement in the Xray, Hall effect and PL properties.

4. Hydrogen and Deuterium Plasma Assisted InP Growth

4.0 Abstract

The hydrogen and deuterium plasmas were found to create donors in the growing material at concentrations near $10^{17}/cm^3$, apparently by forming a P-H bond in place of one P-In bond, freeing one In electron. A large concentration of the plasma atoms were also present in a weakly bonded state which didn't affect the carrier concentration but was apparent in other measurements. These atoms were largely removed by annealing at 730°C. The plasmas also prevented the surface roughening which normally occurred during growths below 400°C. The deuterium plasma, only, created enough phosphorus interstitials to noticably compensate the donors created.

4.1a Growth Conditions (Hydrogen)

InP layers were grown over the same temperature range as the growths described in chapter 3 (232°C to 500°C), but the sample surface was exposed to an ECR-generated hydrogen plasma throughout the growth. The hydrogen gas used to produce the plasma was 99.9995% pure. Sample thicknesses were chosen based on the expected carrier concentration, in order to minimize depletion effects and thus obtain reliable Hall effect data . The H-plasma was expected to cause chemical etching of P from the film surface,

through the formation of PH_3, which could result in an In-rich surface. This could lead to the formation of In droplets. To overcome such an effect, the phosphine flux was increased to the maximum the vacuum pumps could handle, about 7 sccm. Although the exact rate of P loss was not known, the quality of the grown films suggested that the 40% increase (5 sccm to 7sccm) of the incident P_2 flux was adequate to maintain the stoichiometry of the film.

The incident H ions require only about 4 eV to penetrate the surface of the growing film, calculated using the Moliere approximation to the Thomas-Fermi interatomic potential [Feldman and Mayer (1986)]. This is well below the average ion energy, 25 eV. The average distance travelled in the crystal by 25 eV H ions can be estimated using a computer to numerically integrate the range from LSS theory [Feldman and Mayer (1986)]. The electronic stopping (rate of energy loss to interactions with the electrons in the crystal) was calculated assuming a square-root dependence on the ion's energy [Winterbon (1975)]. The nuclear stopping (rate of energy loss to the nuclei) was calculated using the universal stopping curve [Ziegler (1977)] In both calculations, Ge was used in place of InP, because it closely approximates the averages of both the mass and atomic number of P and In. The program was checked against several published collections of ion ranges [Winterbon (1975), Anderson and Ziegler (1977) and Ziegler (1977)] and found to give reasonable agreement, though its predicted ranges at lower energies averaged somewhat larger than the published values. It was found that 25 eV H ions (ε=0.0075) travel an average of approximately 110 angstroms. This should be enough to penetrate well into the bulk and out of the region where growth processes have

an effect.

The hydrogen plasma is not likely to produce any atomic displacements in the grown film via collisions. In order to do so, the impinging H atoms must possess sufficient kinetic energy to either displace atoms in the bulk or recoil atoms from the surface into the bulk. The displacement energy of In has been measured to be 6.7 eV [Corbett *et. al.* (1975)]. Theoretical modelling puts the energy far higher, at 12.2 eV [Van Vechten (1980)]. The experimentally measured displacement energy for P is 8.7 eV [Corbett *et. al.* (1975)], while the theoretical value is 16.5 eV [Van Vechten (1980)]. It is thus reasonable to take 6.7 and 8.7 eV as minimum energy requirements. The energy, E_2, transfered in a head-on elastic collision is given by:

$$E_2 = \frac{4 m_1 m_2}{(m_1 + m_2)^2} E_0$$

where m_1 is the mass of the incident atom (in this case H), m_2 is the mass of the struck atom and E_0 is the kinetic energy of the incident atom. To displace a P-atom in a head-on elastic collision, a H-atom requires an energy of 72 eV, and creation of an In displacement would require even more energy. This is considerably higher than the energy of most of the plasma particles (recall that the mean energy is about 25 eV). Bulk displacements clearly should not be produced in measurable quantities by the plasma. In the case of atoms on the surface, the picture is less clear. Ideally, these atoms have two bonds instead of four, so the energy required to displace them might be half the bulk displacement energies. In reality, the surface P-atoms bond to each other (dimerize) with bonds of unknown strength, so the displacement energy is probably somewhat more than

this. Taking half as a reasonable minimum, P-interstitials could then be created by head-on collisions with H-atoms with more than 36 eV of energy. This energy is above the average, but certainly present in the high energy tail of the plasma particle energy distribution. Displacement of an In atom requires much more energy, because it is much more massive. Thus, the only defect that is energetically possible to create is a P-interstitial, from a P atom recoiled from the surface into the bulk, and even then only for a relatively rare near head-on elastic collision at above-average energies. In such a collision process, the resulting surface phosphorus vacancy would probably be quickly filled from the excess P_2 flux, leaving behind only the P-interstitial which is commonly believed to act as a deep acceptor [Liang *et. al.* (1992)].

Some change in film quality could be caused by chemical bonding between hydrogen and the film constituents. Also, impurities introduced into the plasma stream, such as boron and nitrogen from the lining of the ECR chamber, could be present in the grown films, but these are typically isoelectronic and therefore should have little effect on the electronic properties.

4.1b Growth Conditions (Deuterium)

Deuterium plasma assisted InP layers were grown from 300°C to 500°C. Sample thicknesses were again chosen to minimize depletion effects. The deuterium was 99.5% pure. As with the H plasma, the phosphine flux was increased to 7 sccm. No indium droplets were observed on any of the grown surfaces.

The reason for the use of deuterium plasma was to provide more information

about the incorporation of "H"-species into the epitaxial layers. As an isotope of hydrogen, deuterium should produce similar chemical effects. The difference in mass between D and H makes it possible to detect D atoms in the grown films, using thermal desorption and nuclear reaction analysis.

The threshold energy for D atoms to penetrate the surface is 4 eV, just as for H in the previous section. The average distance travelled by 25 eV D ions (ε=0.0074) is also about 110 angstroms, using the same calculation method as for H ions in the previous section.

The larger mass of the deuterium atoms means that more energy is transferred to the atoms of the crystal in collision processes. In a head-on elastic collision, 38 eV is enough to displace a phosphorus atom in the bulk. If the atom is on the surface, at least 19 eV is required to recoil it into the bulk, producing a phosphorus interstitial. Focussing collisions (in which the first P interstitial collides with a nearby P atom, displacing it and replacing it, and the second does the same with a third, etc) may cause the final interstitial to be located well-separated from the corresponding vacancy or surface site, enhancing defect stability. The <110> and <100> directions are the most likely directions for the collision chain to lie along. The separation of the atoms is larger in InP than in the materials where focussing has clearly been seen [Carter and Grant (1976)], so this effect may be uncommon or of limited range, but it should occur in some cases. For indium atoms, even if they are located on the surface, the deuterium atom would need at least 50 eV to drive the atom into the bulk. Thus, it is reasonable to expect the deuterium plasma to produce more phosphorus interstitials than the H plasma, but no other

displacement defects should be produced in significant quantities. As with the hydrogen plasma, deuterium could bond into the crystal itself, or introduce new impurities.

4.2a Nomarski Microscope Results (Hydrogen)

Table 4.2 gives the measured surface defect densities. Textured surfaces were uniformly patterned. The surface features had lateral dimensions on the order of 1 µm. The growth at 500°C with H plasma is similar to the growth without plasma. At lower temperatures the plasma produces a marked improvement in the surface quality, compared to the no-plasma growths. From 400°C to 300°C, the defect densities are more than an order of magnitude lower than the values mentioned in the literature [Rakennus *et. al.* (1992)].

The plasmas generally seem to prevent the formation of surface roughness, though discrete surface defects are still present. There were no signs of even precursors to texture. The surface quality is also affected by the recent history of the MBE system, but that isn't responsible for the change from texture. The films at 300°C (without plasma and with H plasma) were grown back-to-back, and the growths at 350 and 400°C were only spaced by several days, so changes in system quality would be minor. The growths at 465°C were on widely spaced dates, so the change in the defect density might be due in part to an overall improvement in growth system quality. However, this doesn't affect the conclusion that clear improvement in surface quality is effected by the H plasma, particularly for growths between 300 and 400 °C. Similar results were seen with He and Ar plasmas (Ch. 5 and 6), so the effects are not due to a chemical reaction. The effects

correlate with the ion current as is discussed later.

Table 4.2: Surface defect density (/cm^2), determined by viewing with a Nomarski microscope.

Tg (°C)	No plasma	H plasma	D plasma
500	42000	33000	42000
465	560000	39000	42000
400	Texture	6000	50000
350	Texture	4000	3000
300	Texture	6000	3000

4.2b Nomarski Microscope Results (Deuterium)

Table 4.2 gives the measured surface defect densities, as well as the results of the growths with H plasma and without plasma for comparison. The growths at 500°C are all fairly similar. The defect densities of the growths with hydrogen and deuterium plasma at 465°C are similar to each other, but differ from the growth without plasma, probably because it was grown relatively soon after the MBE system had been up to air. The growths at 300°C and 350°C are much smoother than the growths without plasma, just as with hydrogen plasma.

The only significant difference between the two plasmas occurs for the growth at 400°C, where the sample grown with the deuterium plasma has almost ten times as many defects. From the growths without plasma, there is clearly a change in the growth mode between 465°C and 400°C. Also, the temperature control from 400°C down is less

accurate than at higher growth temperatures. The growth with the hydrogen plasma appears to have occurred on the low-temperature side of the growth transition, while the growth with the deuterium plasma occurred on the high-temperature side. Thus, the growth at 400°C with hydrogen plasma is similar to the growths at lower temperatures, while the growth with deuterium plasma is more similar to the growths at higher temperatures.

4.3 Thermal Desorption

Two samples grown with D-plasma at 300°C and one at 350°C were heated to destruction, and the evolved deuterium measured. The desorption from the first sample grown at 300°C indicated that deuterium was present at a density of $1 \times 10^{19}/cm^3$. The second growth at 300°C was cut into four pieces, which were measured over the course of a week to check for room temperature diffusion of the deuterium. The results, in order, were: $7 \times 10^{18}/cm^3$, $4.4 \times 10^{18}/cm^3$, $6.6 \times 10^{18}/cm^3$ and $7 \times 10^{18}/cm^3$. No trend is apparent, so the time between growth and measurement shouldn't be significant. The scatter in the results corresponds to a standard deviation of 20%. The differences in concentration between this sample and the first sample correspond to a larger deviation, perhaps because there is also some variation in temperature from sample-to-sample. The deuterium concentration in samples grown at 300°C can be estimated to be $\sim 8 \times 10^{18}/cm^3$, with a large uncertainty.

Two pieces from the growth at 350°C were studied. Neither showed a measurable level of deuterium, so the concentration was less than $10^{17}/cm^3$. It appears that deuterium is trapped in the material at low growth temperatures, but that the concentration is very

temperature dependent. Films grown at higher growth temperatures contain very little deuterium.

Hydrogen concentrations couldn't be studied by this technique, but they are assumed to be quite similar to those found for deuterium, given the chemical equivalence of the atoms.

4.4 Nuclear Reaction Analysis

One sample grown with D plasma at 300°C and one grown at 465°C were analyzed. The sample grown at 300°C was the second one studied by thermal desorption, above. It was found to have a deuterium concentration of $1\times10^{19}/cm^3$, with an unceratainty range of +30% / -10%. This is in agreement with the desorption results. The sample grown at 465°C had a deuterium concentration of $2.5\times10^{16}/cm^3$, with a factor of two error range.

4.5a Xray Characterization (Hydrogen)

The samples grown with hydrogen plasma bombardment trend to greater strain as the growth temperature is lowered, but the strain is compressive, the opposite of that seen in the growths without plasma. Table 4.5 lists the measured FWHM of the growths. The 500°C growth and one of the 400°C growths are not included, because a small quantity of argon was apparently incorporated into these samples and skewed the measurement. The growths from 465°C to 350°C were of good quality, and then the 300°C growth produced a strained layer (fig 4.5). Finally, the growth at 232°C had a broad peak, but

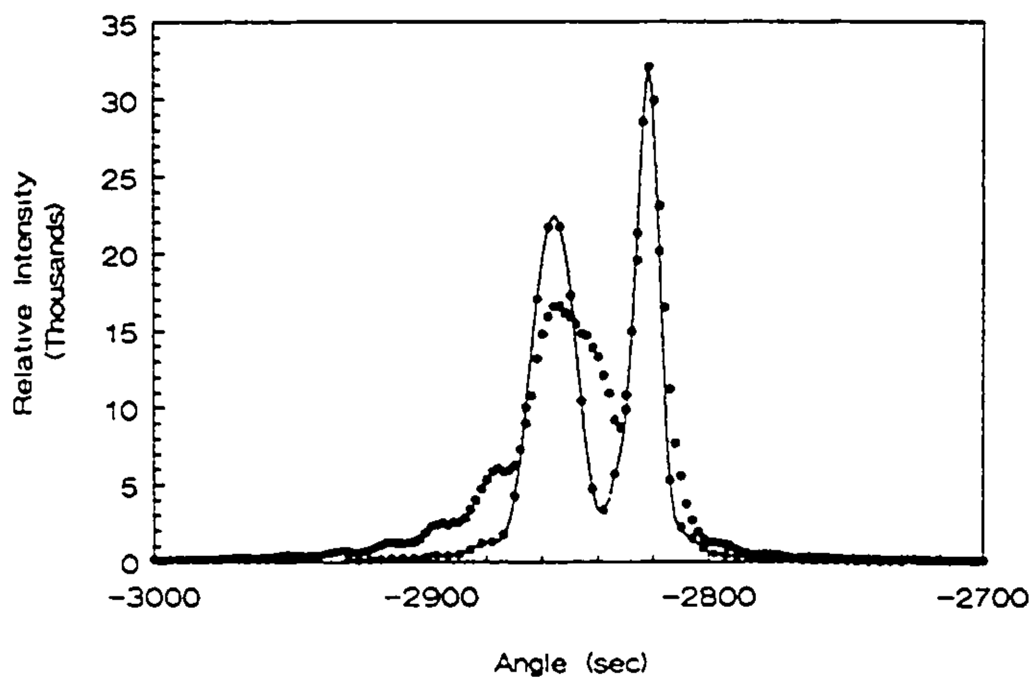

Figure 4.5: Xray rocking curve of InP grown at 300 C with H plasma, with RADS fit (empty circles).

exhibited less strain than the growth without plasma.

Table 4.5: Results from study by Xray double crystal diffraction. Full width at half maximum of the peaks, in seconds of arc.

Tg (°C)	No plasma	H plasma	H plasma, annealed	D plasma	D plasma, annealed
500	12			13	12
465	13	13,12	13,14	13	15
400	11,13	12	14	12	14
350	16	13	19	17	16
300	21	2 peaks	13	12	17
232	2 peaks	24	14		

Figure 4.5 was modelled using RADS, because it was the only film with enough strain to be modelled with confidence. This sample, grown at 300°C, has a larger lattice constant than the substrate, such as would be seen if a large concentration of interstitials were present. From the results of the thermal desorption and nuclear reaction analysis measurements, it is known that a high concentration of hydrogen is present. Though phosphorus interstitials could be produced as well, they are unlikely to be produced by the hydrogen plasma in significant quantities, since the material would then be heavily compensated (chaper 5), but in fact it is n-type (next section). Thus, the strain must result from hydrogen interstitials introduced by the plasma.

The effects of annealing were most apparent on the films grown at the lowest temperatures (table 4.5). The samples grown with H at 400°C or more changed by less

than the normal scatter in the data. The sample grown at 350°C widened by six arcseconds. Before annealing, the Xray peak was narrower than was found for growth without plasma, because the H interstitials present compensated for the strain introduced by the phosphorus antisites. Annealing apparently removed many of the hydrogen atoms, so that the sample had more net strain than was present before. The samples from 300°C and 232°C both showed much less strain after annealing, as enough H interstitials were removed by annealing to leave little net strain.

4.5b Xray Characterization (Deuterium)

The growths with D plasma all have narrow Xray peaks, except for the growth at 350°C. This growth has a wider peak, though the growth at 300°C is very good. Table 4.5 lists the measured FWHM of the growths. None of the peaks are wide enough to show whether the strain in the film is tensile or compressive. There is less net strain for the 300°C growth than for the 350°C growth, probably because there are far more deuterium atoms present in the lower-temperature growth (thermal desorption results, section 4.3). The deuterium interstitials are present in the 300°C film at a concentration that balances out the strain from the phosphorus antisites, so that there is no measurable net strain.

Annealing didn't have a significant effect on the widths of the Xray peaks, except for the growth at 300°C. Annealing appears to have preferentially removed one of the defects, resulting in a greater net strain. From the results with hydrogen plasma at 300°C, a greater proportion of the deuterium interstitials were probably removed. There was very little strain in the other samples, and annealing doesn't appear to add or subtract a

significant number of strain-related defects.

4.6 Positron Annihilation Results

The open volume defect profiles obtained by variable energy positron annihilation measurements carried out on the growths with H plasma are very similar to the results for the growths without plasma (figure 4.6). The H plasma doesn't produce additional detectable "open-volume" defects. This is in agreement with the Xray results, which show a strain opposite that produced by "open-volume" defects. As mentioned in chapter 3, the growths at 500°C have a concentration of less than $1\times10^{17}/cm^3$ of "open-volume" defects. The growths at 300°C have a concentration of the order of $4\times10^{18}/cm^3$.

4.7a Hall Effect (Hydrogen)

For growths at 465°C and 500°C, the H plasma increased the carrier concentration to $\sim10^{17}/cm^3$, compared to $\sim10^{15}/cm^3$ for growths without plasma (fig 4.7a). Below ~400°C the carrier concentration vs growth temperature agrees well with the no-plasma data, saturating at $\sim3\times10^{18}/cm^3$ near 300°C. Annealing reduced the carrier concentrations of the lowest temperature growths by about a factor of 30 (fig 4.7a), just as was found for the growths without plasma. At the same time, the Hall mobilities increased. Phosphorus antisites, as discussed in chapter 3, are apparently produced regardless of the presence of the plasma. Donors are almost certainly being produced by the plasma at lower growth temperatures in concentrations similar to those seen at the higher temperatures, but the phosphorus antisites produced at the lower growth temperatures dominate the carrier

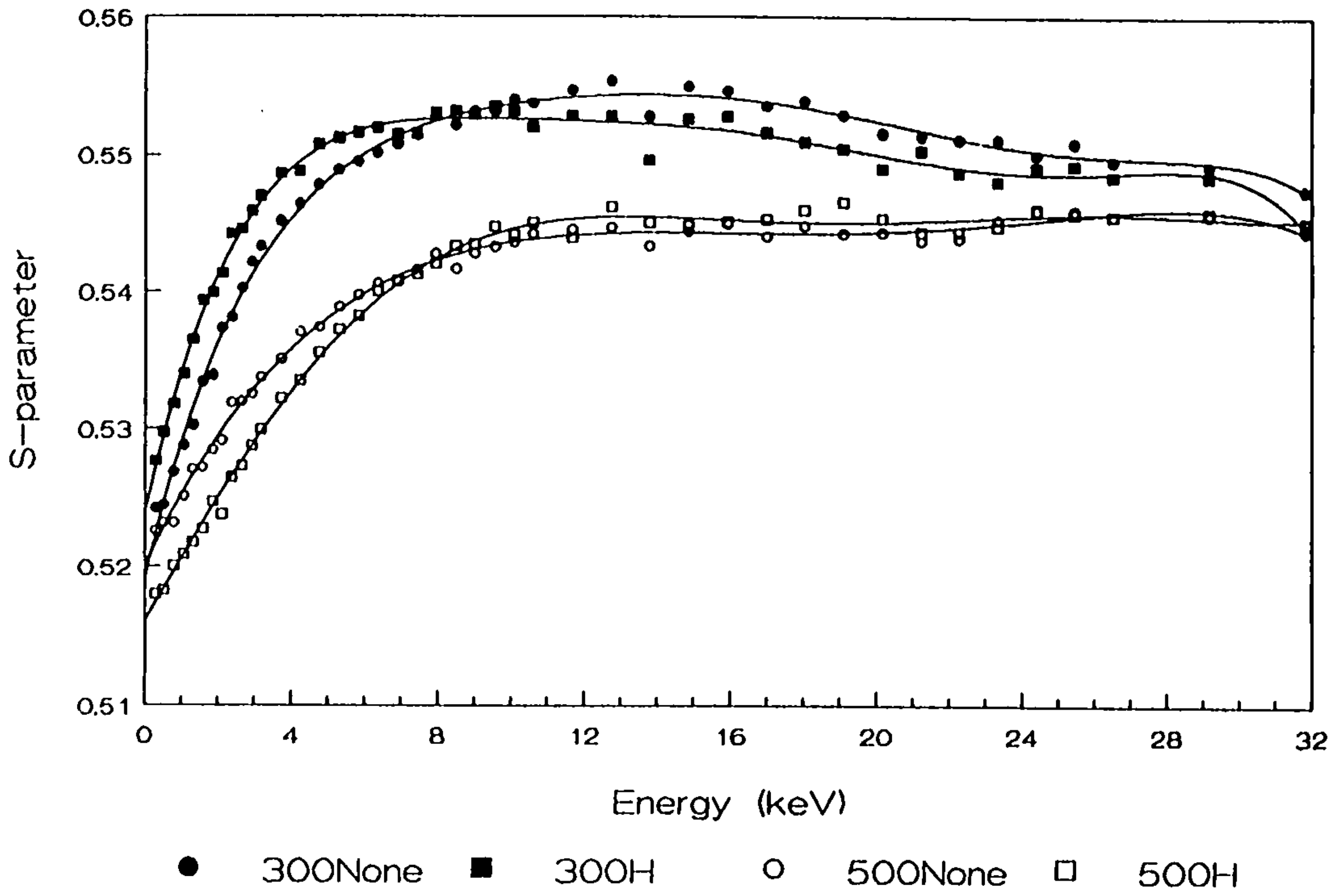

Figure 4.6: Positron annihilation profiles.

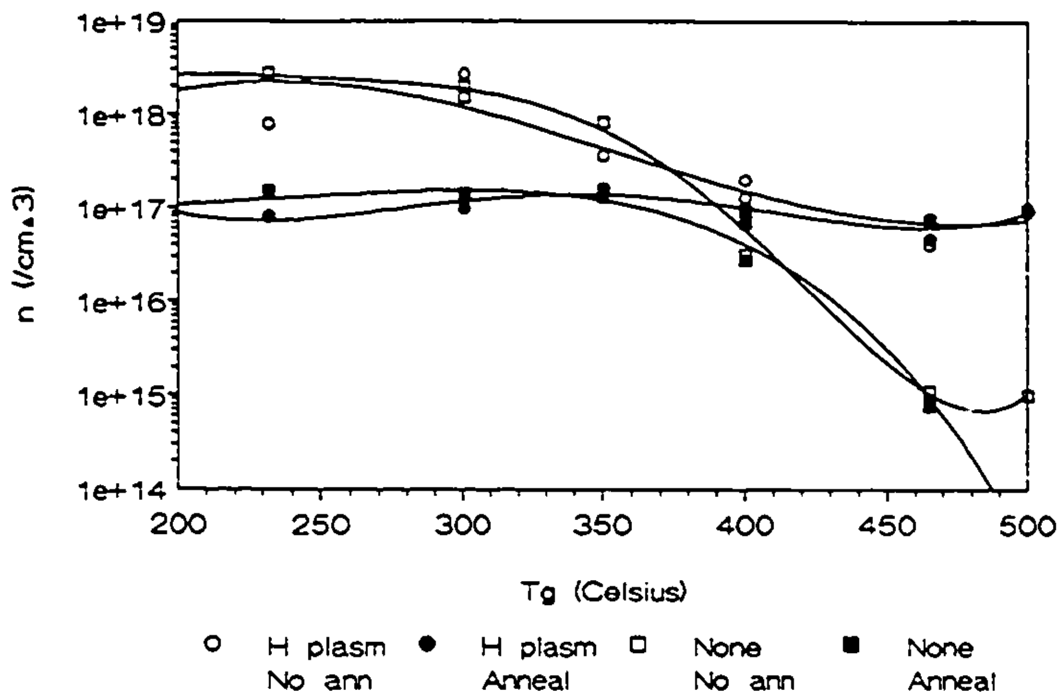

Figure 4.7a: Carrier concentration of InP grown with H-plasma.

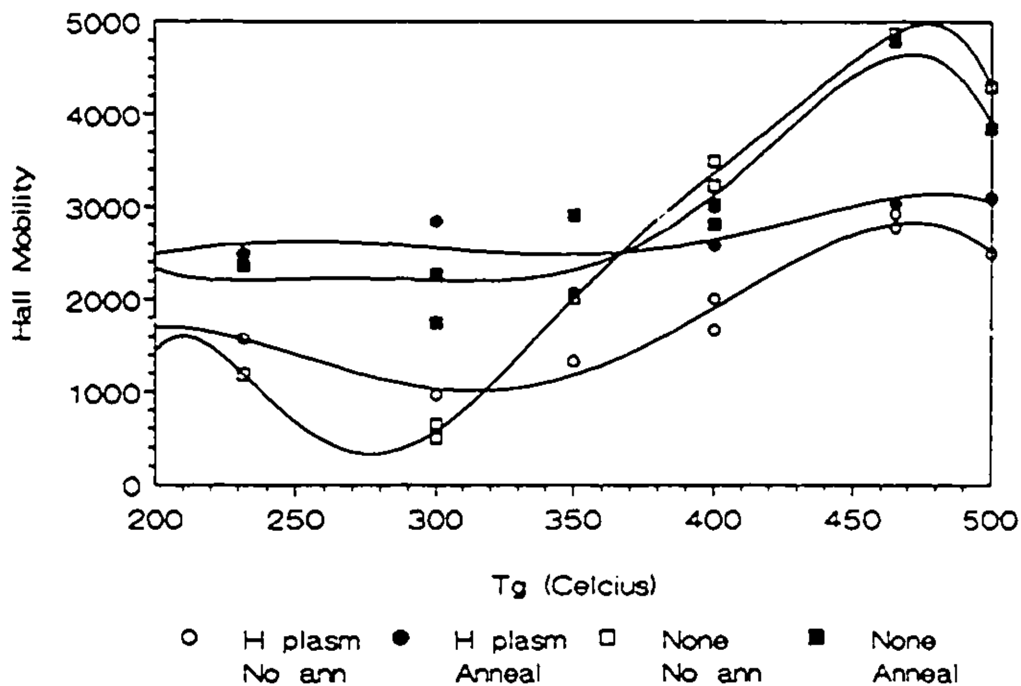

Figure 4.7b: Mobility of InP grown with H-plasma.

concentration.

In addition to increasing the carrier concentration, the plasma also reduced the mobility of the material grown at 465°C and 500°C. This is to be expected, because the mobility must drop as the concentration of active dopants increases, due to scattering effects. However, the change was too large to be explained entirely by the change in carrier concentration. The measured mobilities vs carrier concentrations of these samples correspond to compensation ratios of 22-45% [Walukiewicz *et. al.* (1980)], with an average of 34% compensation. Additional scattering centres appear to be produced, besides those that acted as donors.

The Hall mobilities increased on annealing. For the growths at 465 and 500°C, where the defects were primarily due to the plasma exposure, the carrier concentration was not changed significantly by annealing, but the mobility increased for all three samples. The mobilities after annealing correspond to a compensation ratio of 18% [Walukiewicz *et. al.* (1980)]. The improvement in mobility without a change in carrier concentration suggests that neutral scattering centres are created by the plasma, which reduce the mobility without affecting the carrier concentration. These are removed by annealing, while the donor defects are not affected.

At growth temperatures of 400°C or less, the dominant effect is the creation of phosphorus antisites. The effects of the plasma are clear only in the growths at 465°C and 500°C, by comparing with the growths without plasma. It is clear that the plasma creates donors, which are not significantly removed by annealing at 730°C. Additionally, defects may be created which reduce the mobility, but don't affect the carrier concentration, and

are removed by annealing at 730°C.

It was shown in section 4.1a that hydrogen plasma could only produce defects by impurity incorporation or chemical reaction. If impurities were present in any part of the system but the plasma source, they would have shown up in the growths without plasma, so these parts of the system are clean. If the plasma source is introducing impurities, they should be apparent in all of the growths with plasma, but they aren't (see chapters 5 and 6). Thus, the donors are due to chemical reaction between the hydrogen in the plasma and the InP crystal being grown. If some hydrogen atoms present bond to phosphorus atoms, each freeing one indium electron that is normally tied up in a bond to P, the site will act as a donor. P-H bonds have been detected in GSMBE grown InP by far-infrared absorption spectroscopy [Sidhu *et. al.* (1995)]. They have also been seen in proton-implanted InP [Fischer *et. al.* (1994)]. It may be that this bond would survive even after annealing at 730°C. Hydrogen bonded to phosphorus in the bulk InP film can explain all of the observed properties of the donor defect, so it is reasonable to suggest that it is the defect responsible.

If there are additional scattering centres present, which reduce the mobility without affecting the carrier concentration, they are harder to identify. There could be approximately equal numbers of active donors and acceptors, but it is very unlikely that two different defects would anneal at the same rate in all three samples. Inactive donors (ie the donor level is set by Fermi pinning instead of donor concentration) and compensating acceptors (again with Fermi pinning) are not present, because there is too much variation in carrier concentration to be consistent with Fermi pinning, particularly

when the deuterium results are included. From the NRA, thermal desorption and Xray measurements, it is known that there are large concentrations of electrically inactive hydrogen interstitials present which are removed by annealing. At higher growth temperatures. NRA showed that there are still small concentrations of deuterium, and presumably hydrogen, atoms present in the crystal. The electrically inactive scattering centres could be hydrogen interstitials, perhaps in the form of H_2, which would disrupt the lattice and reduce the mobility.

4.7b Hall Effect (Deuterium)

The results of the Hall-effect studies of deuterium plasma effects are shown in figures 4.7c and 4.7d, and are similar to the results of the growths with hydrogen plasmas. The carrier concentrations and mobilities are both somewhat lower in the growths near 500°C, though, corresponding to compensation ratios of approximately 66% [Walukiewicz *et. al.* (1980)]. This is the region where the effects of the plasmas dominate the effects of growth temperature, and so the result is particularly significant. The differences are consistent with the presence of additional acceptors. As mentioned in section 4.1b, the greater mass of the deuterium atoms means that more phosphorus interstitials (acceptors) will be produced than by the hydrogen plasma. It may be that the differences are due to these defects. Annealing increased both carrier concentrations slightly, while the mobility increased more significantly, corresponding to compensation ratios of about 30%. This also suggests that the donor is strongly bonded, while a compensating acceptor is removed by the annealing.

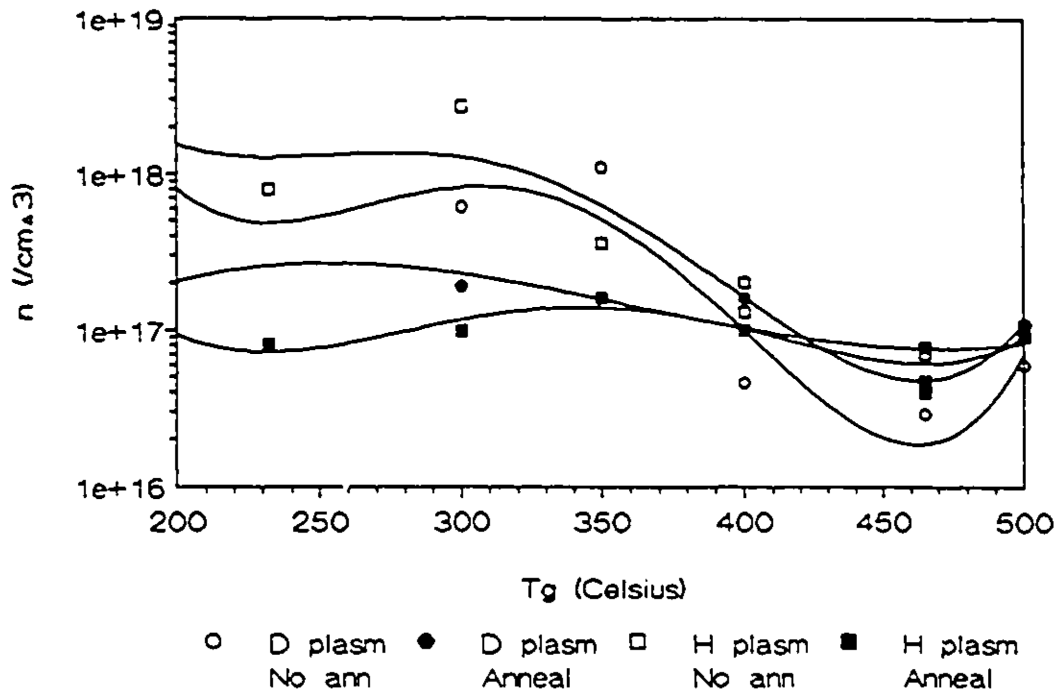

Figure 4.7c: Carrier concentrations of InP grown with D and H plasmas.

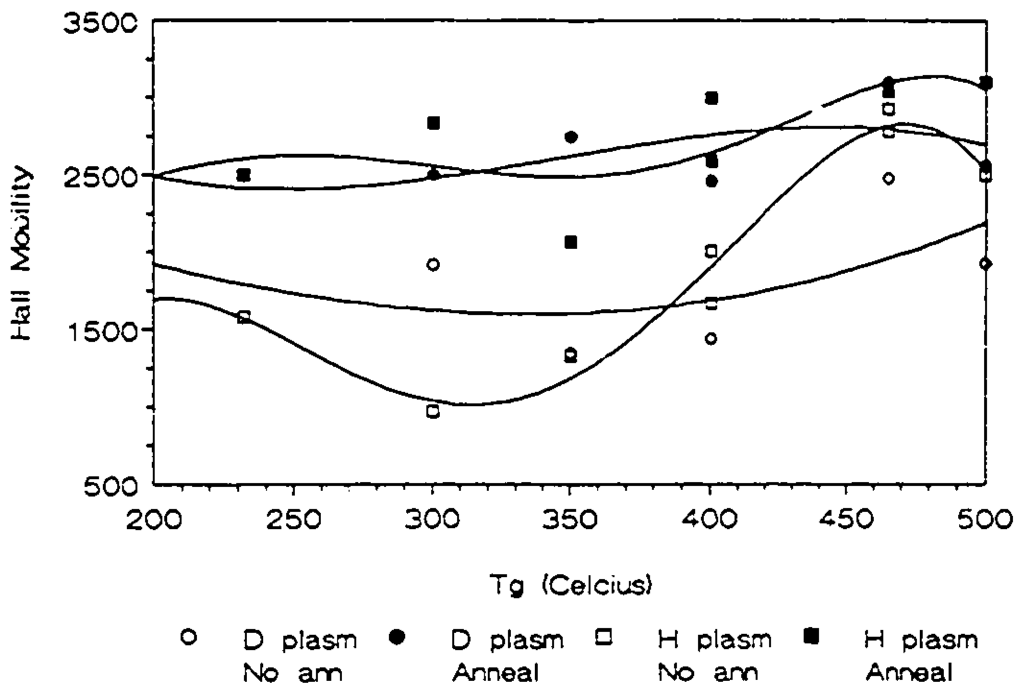

Figure 4.7d: Mobility of InP grown with D and H plasmas.

The results of the growths from 400°C down, both before and after annealing, agree well with the growths without plasma, so the creation of phosphorus antisites is again the dominant effect.

4.8a Photoluminescence (Hydrogen)

The main new PL peak present, compared to the growths without plasma, is a very broad peak near 1 eV (fig. 4.8a). It becomes stronger, and its maximum shifts to lower energy, as the growth temperature is reduced. The band edge peak (1.417 eV) is only visible for the sample grown at 465°C, presumably because so much recombination is now happening at the ~1eV level. The peaks seen at approximately 1.38eV and 1.34eV were also seen without the plasma (pp 48-50), so they are not due to defects created by the plasma, though luminescence due to a defect may now be present at the same energy. There is some structure from ~1.3 to 1.35 eV produced by the 465°C sample, only. It is also produced by the sample grown with D plasma at 465°C. Since it doesn't correspond to any change in other properties of the samples, and is only seen under ideal growth conditions, it is difficult to study. It won't be considered further.

The photoluminescence spectra of the samples show improvement after annealing. The peak near 1 eV is eliminated, and the band edge peak is now visible. The growths at 465°C and 500°C show a new peak near 1.17 eV. None of the other measurements showed any evidence for the creation of new bulk defects on annealing. It is already known that annealing does some damage to the sample surface, this peak is probably due to that damage.

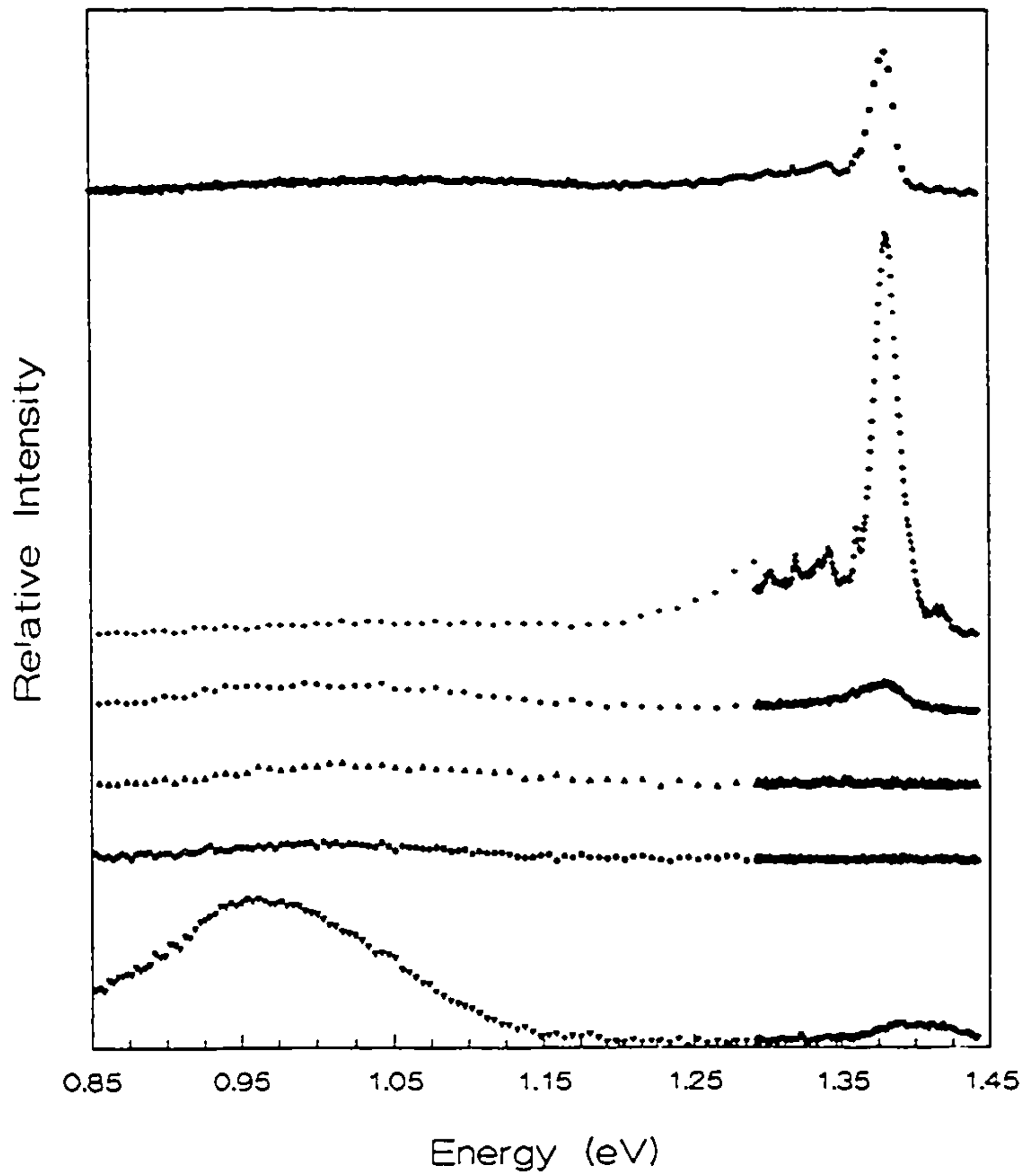

Figure 4.8a: PL results from InP grown with H-plasma at:

1) 500C (top) 2) 465C 3) 400C 4) 350C 5)300C 6)232C.

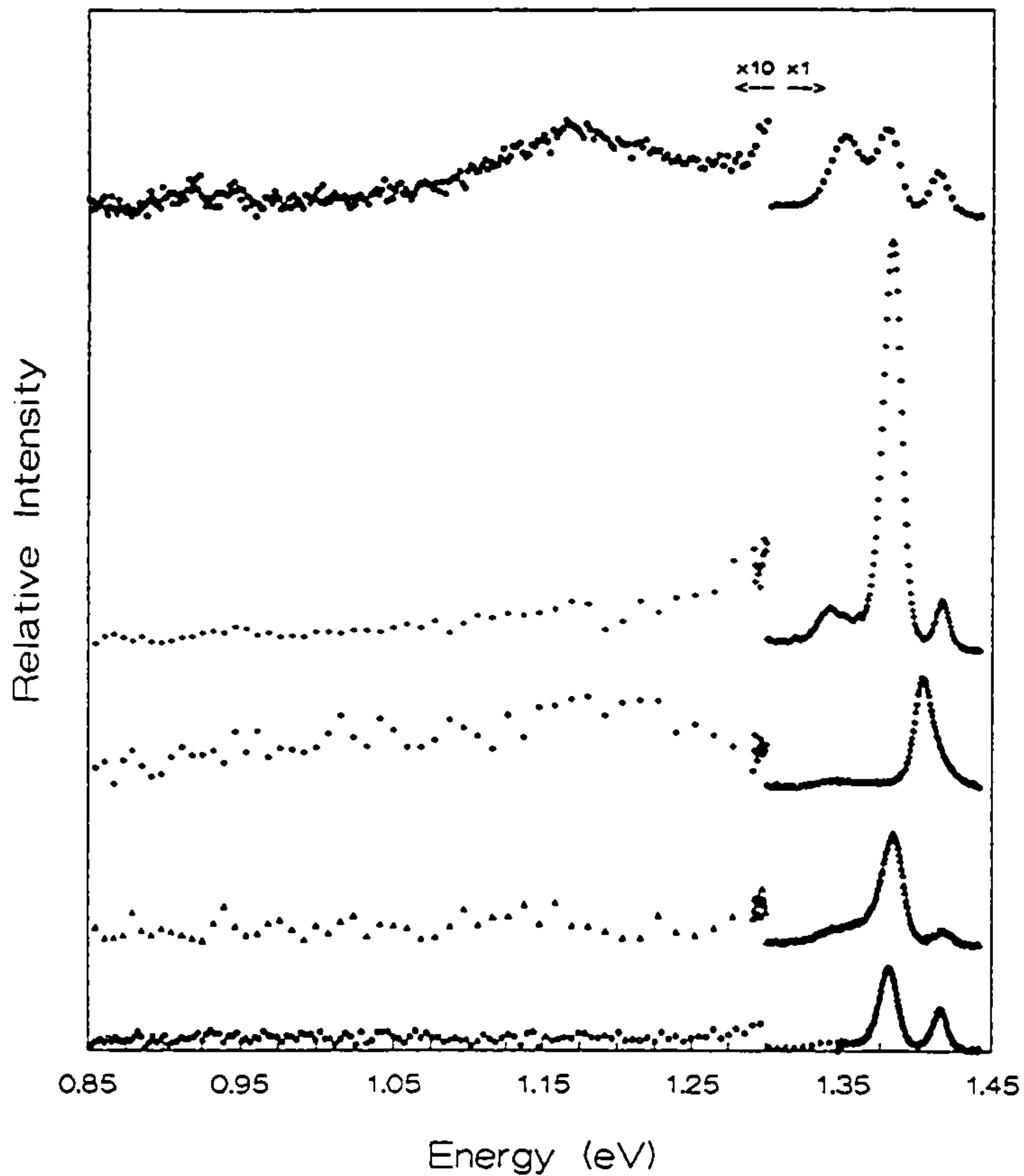

Figure 4.8b: PL results from InP grown with H-plasma, then annealed.

1) 500C 2) 465C 3) 465C 4) 350C 5) 232C.

The total disappearance of the 1 eV peak without change in the carrier concentration shows that the peak is not due to the donor defect created by the plasma, because the Hall effect measurements showed that defect was not annealed out. It will be shown in later sections that this peak is visible for growths with all of the plasmas, not just hydrogen. It was not seen for any of the growths without plasma, so it relates to the plasma source. A large H background is present for all of the growths, from the cracking of the phosphine. Some will diffuse into the plasma source, and be emitted as a weak H plasma, even when a different source gas is used. As seen earlier, some hydrogen incorporates into the film, particularly at low temperatures. The Hall effect results have already provided some evidence for the presence of hydrogen in a second form (non-donor), which is removed by annealing. It appears that this hydrogen, incorporated from the plasma, is responsible for the 1 eV luminescence peak. The peak is exceptionally broad, probably because the luminescence energy level depends on the proximity of phosphorus antisites. It has been shown that nearby defects can affect hydrogen bonds [Fischer *et. al.* (1994)]. The PL peak's maximum shifts downward for lower growth temperatures, when there are more antisites, suggesting that H near an antisite results in a lower PL level than in good crystal.

4.8b Photoluminescence (Deuterium)

The samples grown under D plasma have some similarities to those grown under H. There is practically no band edge signal and there is a broad peak around 1 eV whose peak reduces in energy as the growth temperature is reduced. The peak at 1.38 eV is

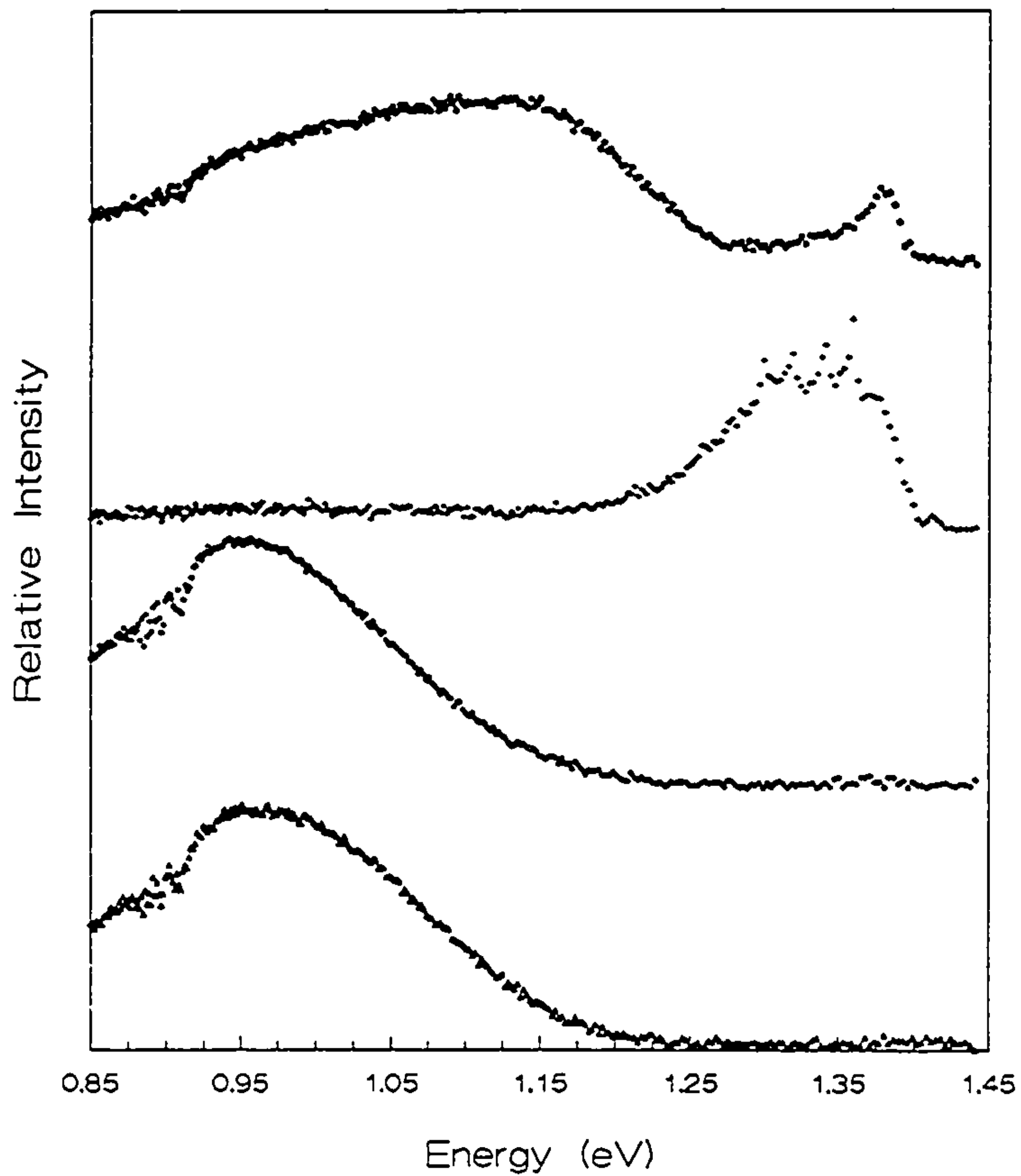

Figure 4.8c: PL results from InP grown with D at 1) 500C (top) 2) 465C 3) 350C 4) 300C.

relatively smaller than for H plasma. For the growth at 465°C, a group of peaks seems to exist between 1.3 and 1.38 eV (fig 4.8c), as discussed in the previous section. The sample grown at 400°C, only, didn't produce a detectable signal.

The photoluminescence spectra of these samples also show improvement after annealing, as shown in figure 4.8d. Two sets of data were magnified tenfold, to make their structure more visible. The peak near 1 eV was no longer present in any of the results. The pattern of peaks is similar to that seen for the annealed samples grown with hydrogen plasma, showing again that the hydrogen and deuterium plasmas were very similar in effect.

4.9 Silicon Passivation

Hydrogen incorporated into InP has been found to passivate dopants in some situations, as discussed in section 1.3. A film was grown with deuterium plasma at 465°C doped with silicon, which acts as a donor in InP. The sample was grown on an n-type wafer so that contacts were easier to make. This made it possible to study the carrier concentration vs depth using a CV profiler. A layer of silicon-doped, D-plasma-assisted InP was grown between two layers doped with silicon at the same concentration. The plasma-assisted layer was approximately 0.75 μm thick, while the growths on either side were approximately 0.25 μm thick. The carrier concentration on either side of the plasma-assisted growth region provides a calibration that make the effects of the plasma clear. The silicon doping was maintained at a constant level of $4 \times 10^{17}/cm^3$ throughout the growth. Not surprisingly, the carrier concentration is affected by the plasma (fig 4.9), but

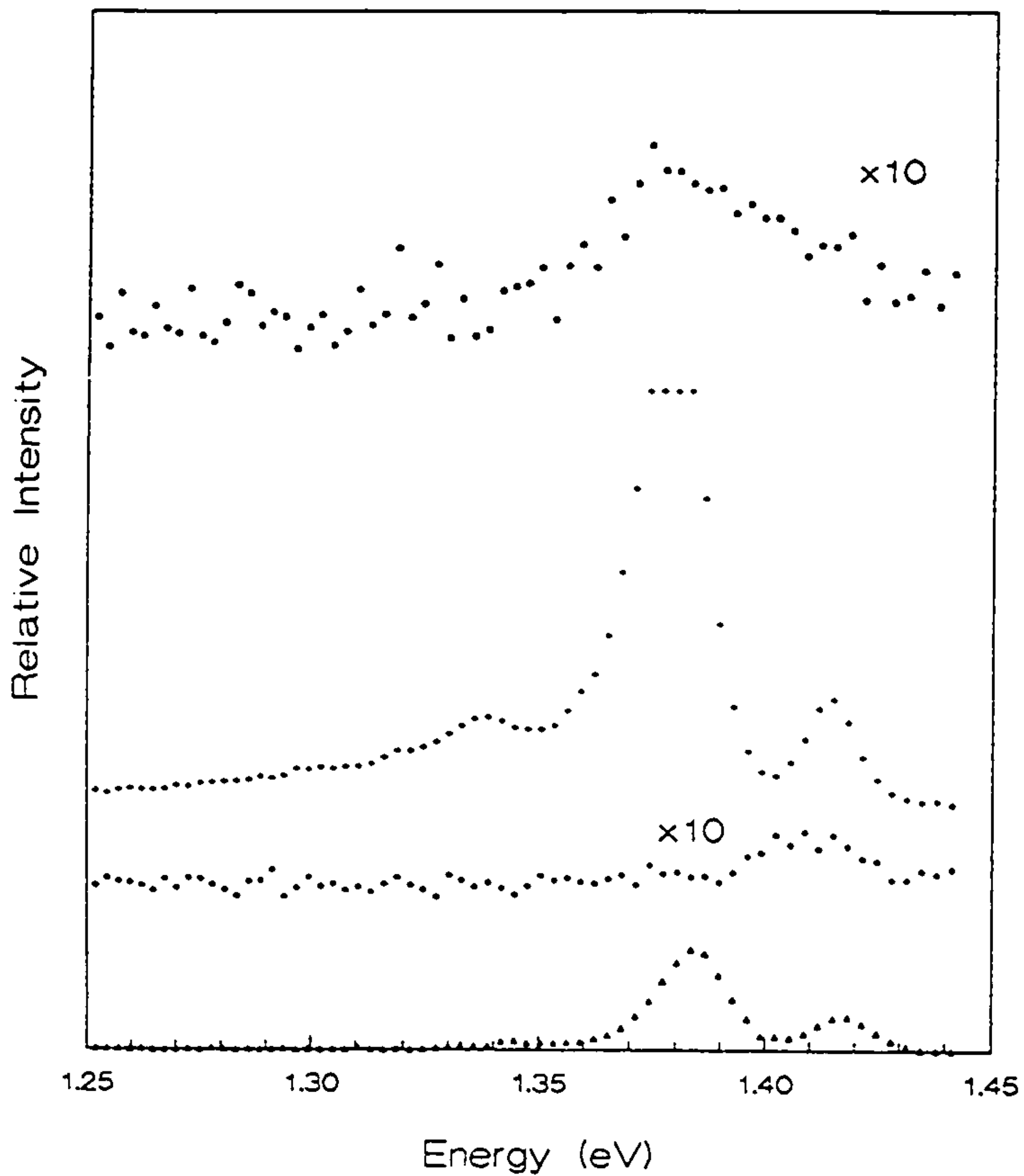

Figure 4.8d: PL results from InP grown with D, then annealed 1) 500C 2) 465C 3) 350C 4) 300C.

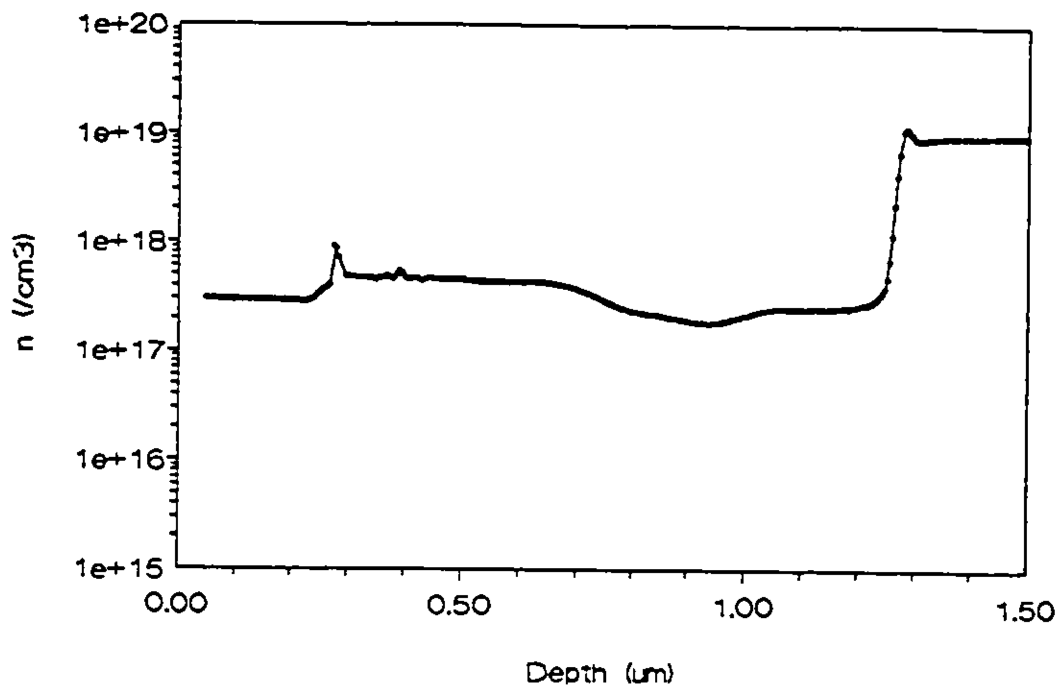

Figure 4.9: Carrier concentration of Si-doped InP grown with D plasma.

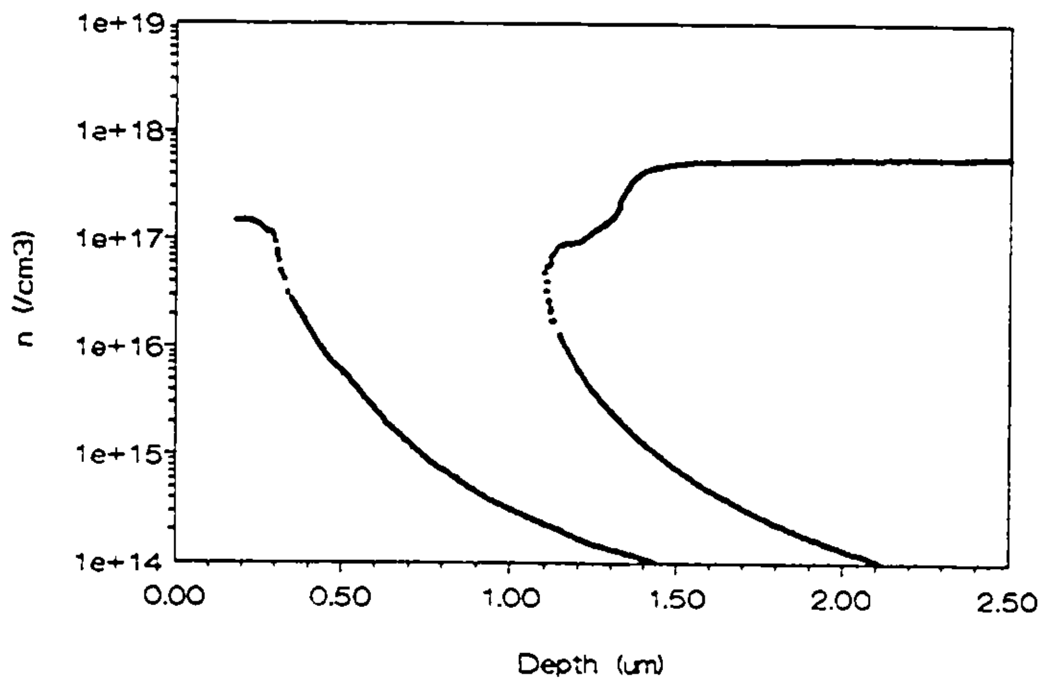

Figure 4.10: Carrier concentration of Be-doped InP grown with D plasma.

the silicon is clearly not passivated.

4.10 Beryllium Passivation

Beryllium is an acceptor in InP. A sandwich structure like that described above was grown, but p-type on a p-type substrate. The doping level was set to $\sim 1.5 \times 10^{17}/cm^3$. In this case the plasma-assisted layer was passivated below the detection limit of the CV profiler ($\sim 1 \times 10^{14}/cm^3$). The result is shown in figure 4.10. The unrealistic curve for the section grown with the plasma is because the carrier concentration was too small for the system to measure.

Another sample was grown, this time a uniform layer with the Be cell set to its maximum temperature, estimated to give a concentration of $\sim 5 \times 10^{18}/cm^3$. The deuterium concentration in this sample was found by desorption and nuclear reaction analysis to be $2 \times 10^{18}/cm^3$ +/-50% and $3.5 \times 10^{18}/cm^3$ +/-25%, respectively. These concentrations are close to the estimated Be concentration. Also, the concentration in a sample grown without Be but with deuterium plasma at the same temperature contained deuterium at a concentration of $2.5 \times 10^{16}/cm^3$. Thus, the deuterium atoms are bonding at beryllium sites. Beryllium is passivated by the D atoms themselves, rather than a defect created by the deuterium plasma. This agrees with the results with other materials, as described in chapter 1. In this case, however, the dopant was passivated in situ, during the growth.

4.11 Conclusions

The hydrogen and deuterium plasmas smoothed the surface of the films grown at

low temperature. Without plasma, the films were very rough. Films grown with the plasma had surface defect densities more than an order of magnitude lower than the value reported in the literature as good.

The electrical and optical properties of the films grown with H and D plasmas are similar to each other, as expected. The Hall effect and photoluminescence measurements on the samples grown at 465°C and 500°C show that there must be two different defects, both hydrogen interstitials, produced by the hydrogen plasma. The first is a donor, produced when a hydrogen (or deuterium) atom bonds to a phosphorus atom, which is very stable and hard to anneal out. It is not luminescent, or its level is close to 1.34 eV or 1.38 eV, so that it cannot be distinguished from these peaks, which occur anyway. The second form of hydrogen interstitials is not a dopant, but is luminescent at approximately 1 eV. It is not strongly bound into the crystal, so annealing removes it almost entirely, as seen by both the Hall effect and photoluminescence measurements. When it is present, it has a small effect on electron mobility in the films. The donors created by the plasma are insignificant in growths at 400°C or less, compared to the large concentrations of phosphorus antisites that occur at these growth temperatures.

There is some difference in the electrical properties of the films grown with D plasma and H plasma, probably due either to normal scatter in the data or to the creation of phosphorus interstitials (acceptors) by the heavier ions in the D plasma.

Deuterium plasma was used to show that it is possible to passivate beryllium dopant atoms during film growth. Hydrogen plasma should do the same. Silicon dopant wasn't affected by the plasma.

5. Growth of InP With He Plasma

5.0 Abstract

The He plasma was found to create phosphorus interstitials and phosphorus vacancies, the interstitials being more common. The interstitials are deep acceptors, so the material produced was often highly compensated. Annealing and high growth temperatures both caused the interstitials to diffuse out, leaving enough vacancies to make the material n-type. The surfaces of the films grown at low temperatures were again smoothed by the plasma.

5.1 Growth Conditions

InP layers were grown from 300°C to 500°C, and the sample surface was exposed to an ECR helium plasma throughout the growth. The helium gas used was 99.9999% pure. As mentioned in chapter 2, the measured ion current of the helium plasma tended to be somewhat lower than the current of the hydrogen plasma. Sample thicknesses were chosen based on the expected carrier concentration, in order to minimize depletion effects at the film-substrate interface and at the surface, so that reliable Hall-effect data could be obtained. Depletion effects could not be avoided in some of the samples, due to their very low carrier concentrations.

For helium ions, the threshold energy required to penetrate the surface is 7 eV, again using a Thomas-Fermi interatomic potential [Feldman and Mayer (1986)]. The average distance travelled (as opposed to the depth of penetration) by a 25 eV He ion (ε=0.0035), is about 48 Angstroms, using LSS theory as described in section 4.1.

The effect of the collisions between the plasma atoms and the crystal atoms can be predicted using simple elastic theory, as was done for the plasmas in the previous chapters. Consider first the In atoms. Due to the large excess of phosphorus in which the crystals are grown, the surface can be considered to be phosphorus terminated, so only indium bulk displacements should be possible. Recall that the displacement energy for In atoms located in the crystal bulk is probably not less than 6.7 eV. The energy transfered in a head-on elastic collision is given by:

$$E_2 = \frac{4 m_1 m_2}{(m_1 + m_2)^2} E_0$$

An elastic collision between He and In can impart a maximum of 13% of the He atom's energy to the In. Thus, the minimum He energy required to displace an In atom is 51.5 eV. The plasma ions have measured energies in the 10-50 eV range, so only an insignificant portion of the atoms in the plasma will have more than 51.5 eV. Another mechanism that could displace an In atom is a He - P - In chain collision. In this case, if all of the collisions are head-on and elastic, the In atom will receive 27% of the He atom's initial energy. However, the atoms do not line up in the direction of travel of the ions (normal to the crystal surface). The P atom must be struck so that it travels at an angle of 54.7° from the initial He path. The energy transferred in this case, assuming

elastic collisions, is given by:

$$E_2 = \frac{4m_1m_2\cos^2\theta}{(m_1+m_2)}E_0$$

Thus the phosphorus atom will receive a maximum of 13.5% of the He atom's energy. The head-on collision between the P and In will then transfer up to 67%. This gives a net energy transfer from He to In of 9%. The minimum He energy required is thus 74 eV, well beyond the energy typical of the plasma atoms. In summary, it is not likely that a significant number of In atoms will be displaced by the plasma.

Phosphorus atoms have considerably less mass than indium atoms, so much more energy is transferred from the plasma particles. Assuming elastic collisions, a He - P collision can transfer up to 40% of the He atom's energy to the P atom. Using a displacement energy for bulk P of 8.7 eV, a He atom needs only 22 eV to displace a P atom. The majority of the atoms in the plasma have more energy than this, even after penetrating several monolayers (according to LSS calculations), so displacements of phosphorus atoms should be common, resulting in a phosphorus vacancy and a phosphorus interstitial. Displacement of P from the surface into the bulk could be even more common, because the surface atoms are less strongly bound, and are not screened by In atoms. The surface site will be quickly filled from the excess phosphorus flux, so only a phosphorus interstitial should result in this case.

The helium plasma has enough energy to produce both phosphorus vacancies and phosphorus interstitials, assuming elastic collisions. The vacancies will be produced only from bulk displacements, while the interstitials are created whenever a bulk or surface

phosphorus atom is displaced, so more interstitials will be produced. Some focussing collisions involving P interstitials can again be expected to occur, reducing the recombination rate of the defects.

5.2 Nomarski Microscope Results

Table 5.2: Surface defect density (/cm^2), determined by viewing with a Nomarski microscope.

Tg (°C)	No plasma	He plasma
500	42000	28000
465	560000	83000
440		32000
410		28000
400	Texture	56000
400	Texture	2800
350	Texture	1000
300	Texture	Texture

Table 5.2 gives the measured surface defect densities for the growths with He plasma, as well as the results without plasma for comparison. The growths from 500°C down to 400°C all have fairly similar surface defect densities. A transition in surface structure occurs at 400°C, as discussed in chapters 3 and 4. In this case, one of the growths nominally grown at 400°C has a much lower defect density than the other,

confirming that the transition is at almost exactly 400°C. The growth at 350°C also has a low defect density (two orders of magnitude lower than the value in the literature! [Rakennus *et. al.* (1992)]). The growth with He at 300°C is textured, as was the case for the growth without plasma. In contrast, the growths with H and D plasma (chapter 4) show no texture. This may be because the He plasma has a lower average ion current than the H plasma, so the temperature effects can eventually overcome the He plasma effect.

5.3 Thermal Desorption

Samples grown at 465°C, 400°C and 350°C with He plasma were subjected to thermal desorption measurements. In no case was helium present at measurable concentrations ($10^{16}/cm^3$). Even if He trapped as stable bubbles in InP, it should have been visible, since the films were heated well past destruction, as discussed in 2.9. Helium is light and inert, so it rapidly diffuses out of the films during growth. The observed effects of the plasma are clearly not due to He atoms present in the grown material, but rather to defects created by the plasma bombardment.

5.4 Xray Characterization

The samples grown in the 400-465°C range with He plasma bombardment have narrow Xray peaks, while the samples grown at lower and higher temperatures are significantly wider. Table 5.4 lists the measured FWHM of the growths. None of the peaks had enough structure to make modelling possible; even the direction of strain could not be determined. The average FWHM of the narrowest peaks is 15 arcsec, indicating

that there is some strain even in the best samples. This strain is probably due to the presence of phosphorus vacancies and interstitials, as predicted in section 5.1. The wider peaks at 300°C and 350°C are due to antisites resulting from the reduction in growth temperature. At 500°C, some annealing of the sample appears to occur as it is grown, but the result is more stress. This can be explained by the preferential annealing of one of the phosphorus defects. The interstitials will produce compressive strain while the vacancies produce tensile strain in the film, so they will tend to compensate for each other's effect. If one anneals out more quickly than the other during growth at 500°C, the result will be a sample with greater net strain, as is seen here.

Table 5.4: Results from study by Xray double crystal diffraction. Full width at half maximum of the peaks, in seconds of arc.

Tg (°C)	No plasma	He plasma	He plasma, annealed
500	12	23	12
465	13	15,15	14,11
440		15	14
410		15	16
400	11,13	16,14	13,12
350	16	21	13
300	21	22	15

If significant diffusion of the interstitials occurs, some phosphorus atoms could be lost through evaporation from the surface, while some combine with phosphorus vacancies

to re-form good crystal. The relative probabilities of these two events can be estimated by comparing the number of vacancies available to the number of surface sites, from which the atoms will presumably evaporate. The sample grown at 500°C was 1 μm thick, with a phosphorus vacancy concentration of ~$4x10^{18}/cm^3$ (next section), so there are a total of ~$4x10^{14}$ vacancies/cm^2. There are approximately $6x10^{14}/cm^2$ surface atomic sites, times two faces, for $1.2x10^{15}/cm^2$ evaporation sites. This gives a 3:1 value for the evaporation:recombination ratio, assuming similar cross-sections. Thus, a significant portion of the phosphorus interstitials will probably be removed by evaporation, if they are removed at all.

Annealing at 730°C reduced the net strain in the samples. The growths at 500°C, 350°C and 300°C all improved nearly to the ideal. The other (better) samples generally improved slightly, but didn't change significantly vs normal scatter of several arcseconds. The defects introduced by the He plasma appear to be largely removed by annealing.

5.5 Positron Annihilation

The positron annihilation profile data for the growths at 300°C and 500°C with He plasma bombardment are shown in figure 5.5, together with the results on the growths without plasma for comparison. Both the growths with He plasma are similar to the growth at 300°C without plasma, and are clearly different from the sample grown at 500°C without plasma. The plasma creates open-volume defects, of neutral or negative charge, in concentrations of approximately $4x10^{18}/cm^3$. From the earlier discussions, phosphorus vacancies are expected, so these are probably what was detected in the growth

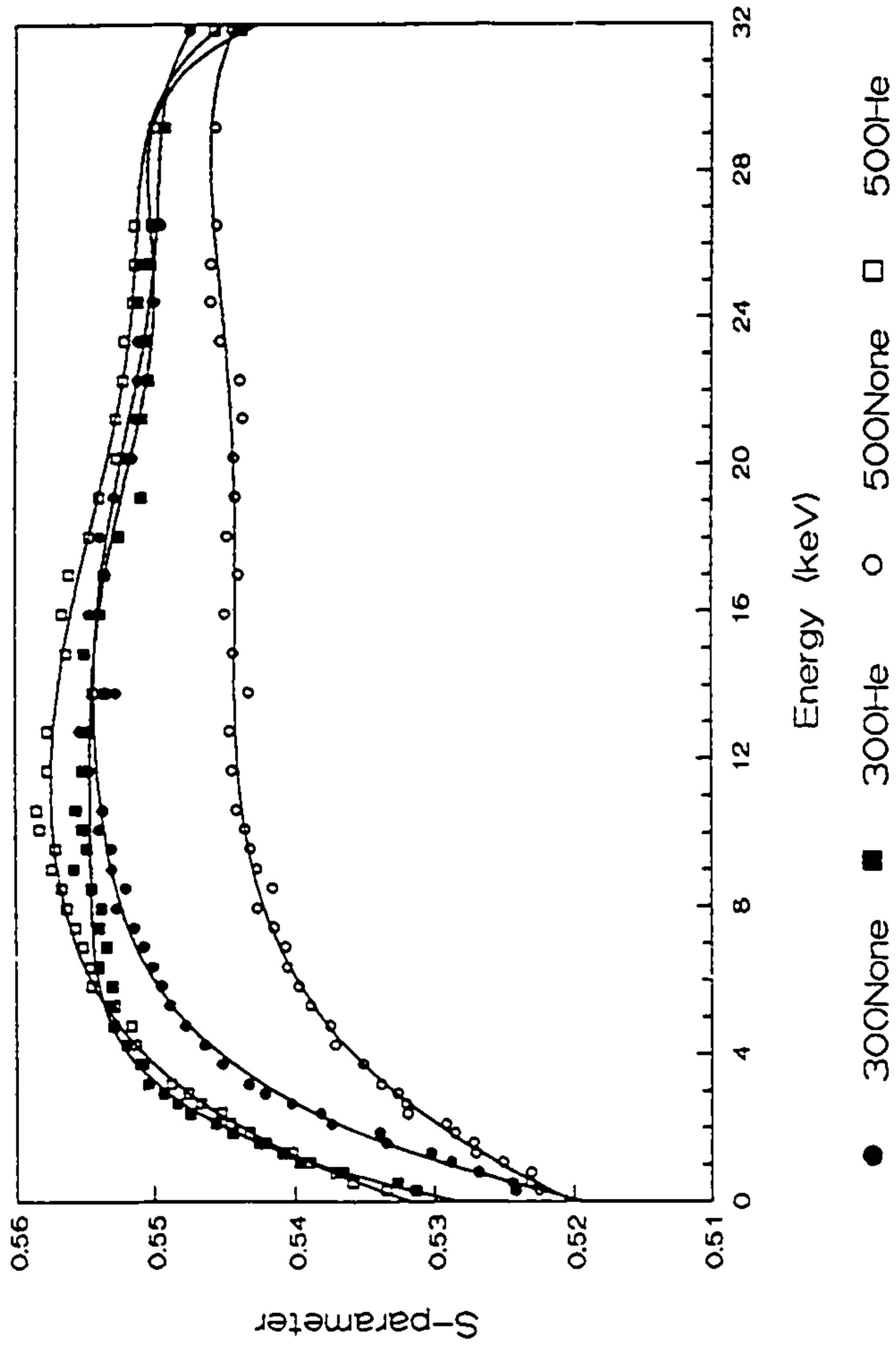

Figure 5.5: Positron annihilation profiles.

at 500°C. Phosphorus vacancies are commonly believed to act as donors, but to be detected by positron annihilation many must be uncharged. Hence, the Fermi level must be at or above the vacancy's donor level. The growth with plasma at 300°C is similar to the growth without plasma at 300°C, in spite of the additional vacancies produced by the plasma. This is because, for each P vacancy produced, a P interstitial is produced. The interstitials accept an electron from the phosphorus antisites, making them positively charged and thus not detectable by positron annihilation. The net result is an addition of one open volume defect (the P vacancy), with the removal of another (the P antisite) from the positron annihilation signal.

5.6 Hall Effect

The carrier concentrations of the films, as measured by Hall effect, are shown in figure 5.6a. They tend toward the $10^{18}/cm^3$ range, similar to the growths without plasma, as the growth temperature is reduced. Defects resulting from the low temperature clearly dominate the carrier concentration and mobility for growths at less than 400°C. For growth temperatures from 400°C to 465°C, the material is heavily compensated. Due to surface and interface depletion effects, any carrier concentrations below $1x10^{14}/cm^3$ are not accurately known.

The growth at 500°C has a carrier concentration of $1.2x10^{16}/cm^3$, almost an order of magnitude larger than the growth at the same temperature without plasma. The material is n-type, so the majority of defects are donor defects. From the positron results, a concentration of $\sim 4x10^{18}/cm^3$ of phosphorus vacancies is present in the sample grown at

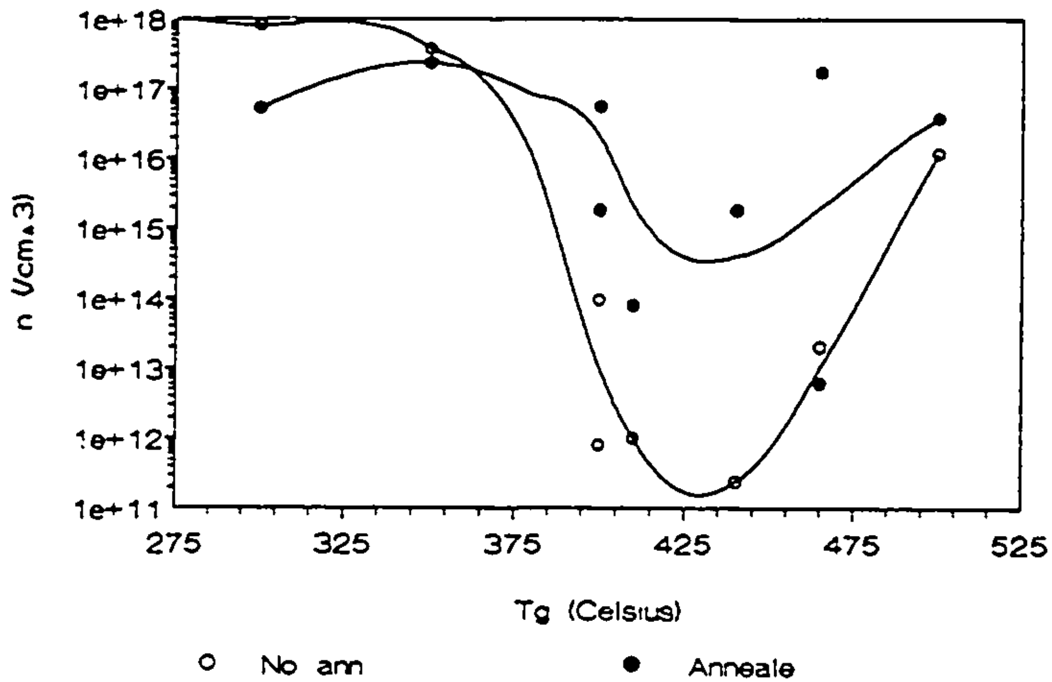

Figure 5.6a: Carrier concentration of InP grown with He plasma.

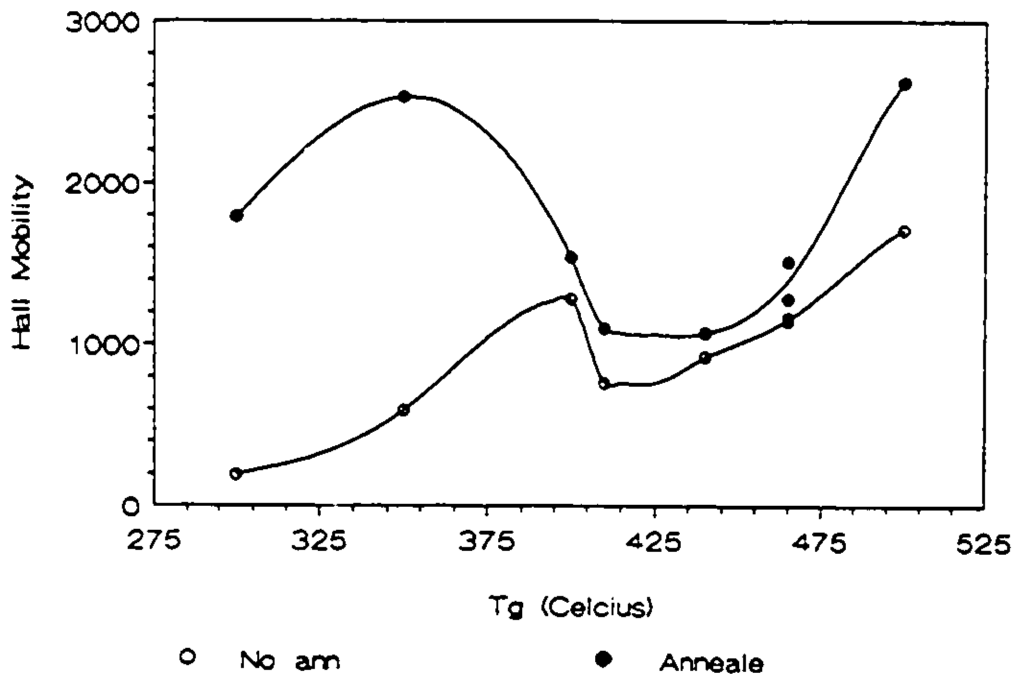

Figure 5.6b: Mobility of InP grown with He plasma.

500°C. They are acting as donors, as expected, but few of them are ionized, since the carrier concentration is only $1.2 \times 10^{16}/cm^3$. (From the Xray results, there are few phosphorus antisites present, so the low carrier concentration is not due to compensation. Also, they couldn't be detected by positron annihilation if they were just compensated.) The Fermi level must be pinned at the donor activation level of this vacancy. If the level was lower, the donors would have been positively charged, and therefore not visible to the positron annihilation measurements. If the Fermi level was higher, the donors would not be active at all. The carrier concentration corresponds to a Fermi level 0.1 eV below the conduction band.

Besides the donors, the plasma is creating acceptors which compensate the donor defects from 400°C to 465°C, but are ineffective at lower temperatures. Without plasma, the carrier concentration was $\sim 6 \times 10^{16}/cm^3$ at 400°C and $\sim 7 \times 10^{17}/cm^3$ at 350°C. The net concentration of compensating defects (#interstitials - #vacancies) must lie somewhere between, since the growth with He plasma at 400°C is fully compensated, while the growth at 350°C is not compensated significantly (fig. 5.6a). The acceptors are probably the phosphorus interstitials that the plasma is expected to create. They are expected to act as acceptors, because they are more electronegative than the indium atoms. Since the material never becomes p-type, it would appear that the acceptor level lies above the middle of the energy gap. At higher growth temperatures some of the interstitials appear to diffuse to the surface and evaporate, so that at 500°C the donor phosphorus vacancies are the dominant defect.

The concentration of phosphorus interstitials and vacancies created by the He ions

can be estimated assuming hard sphere elastic collisions, and a uniform energy distribution between 10 and 50 eV. At the surface, assuming a phosphorus displacement energy of 4.35 eV, 20.% of the incoming ions should displace a phosphorus atom. In the bulk, neglecting backscatterred ions, 12% of the initial flux of He ions should create a vacancy-interstitial pair. For an ion current of 3 μa, this corresponds to a creation rate for interstitials of $6x10^{12}/cm^2/s$, and for vacancies, $4x10^{12}/cm^2/s$. Since the growth rate was always near 0.75 μm/hr, these correspond to concentrations of $3x10^{20}/cm^3$ and $2x10^{20}/cm^3$, respectively. Inaccuracies due to the simple assumptions of the model can not account for such large deviations from the observed concentrations. High rates of defect recombination and diffusion must be occurring. These processes have both been found to occur in metals damaged by radiation [Thompson (1969)].

The effect of annealing on carrier concentration is also shown in figure 5.6a. At low temperature the concentration is reduced, just as for growths done without plasma bombardment. For growths at 400°C or higher, the carrier concentration generally increased, confirming that the interstitials (acceptors) are more easily removed by annealing than the vacancies (donors). In two of the six films that were highly compensated, enough interstitials remain to compensate the material, though there is some improvement in the Hall properties.

The measured Hall mobilities are shown in figure 5.6b. They are always much lower than growths at the same temperature without plasma, because the He plasma adds large concentrations of defects.

For all samples, annealing resulted in a higher mobility. All of the mobilities were

still lower than for the samples grown without plasma, showing that a significant concentration of the defects introduced by the helium plasma bombardment are still present after annealing. Since most of the films annealed are strongly n-type, phosphorus vacancies are the more common defect within, but the two films which remain compensated must still have a larger concentration of interstitials.

5.7 Photoluminescence

Most of the samples grown under a He plasma show no optical PL. This results as a consequence of the deep defect levels produced by the plasma. Only for the growth at 500°C, where some defect annealing has occured, is a weak signal observed (see figure 5.7a). Broad peaks are visible at about 1.33 and 1.16 eV. From the shape of the lower-energy peak, the usual plasma-induced signal appears to be present near 1.05 eV, but it is too weak to clearly label.

As mentioned in the Hall effect results, the carrier concentration corresponds to a donor level about 0.1 eV below the conduction band. The peak at 1.33 eV is about 0.09 eV below, which is close, given the noise in the scan. The Hall effect measurements were made at room temperature, while the photoluminescence measurements were made at about 11 Kelvin, so a small shift in relative donor level is also reasonable. This peak is probably due to the phosphorus vacancies introduced by the helium plasma bombardment.

No peak near 1.16eV is seen in the samples with any of the other plasmas. It is 0.26 eV below the conduction band. If this is the level of the compensating acceptor, large concentrations would pin the Fermi level to give a carrier concentration of

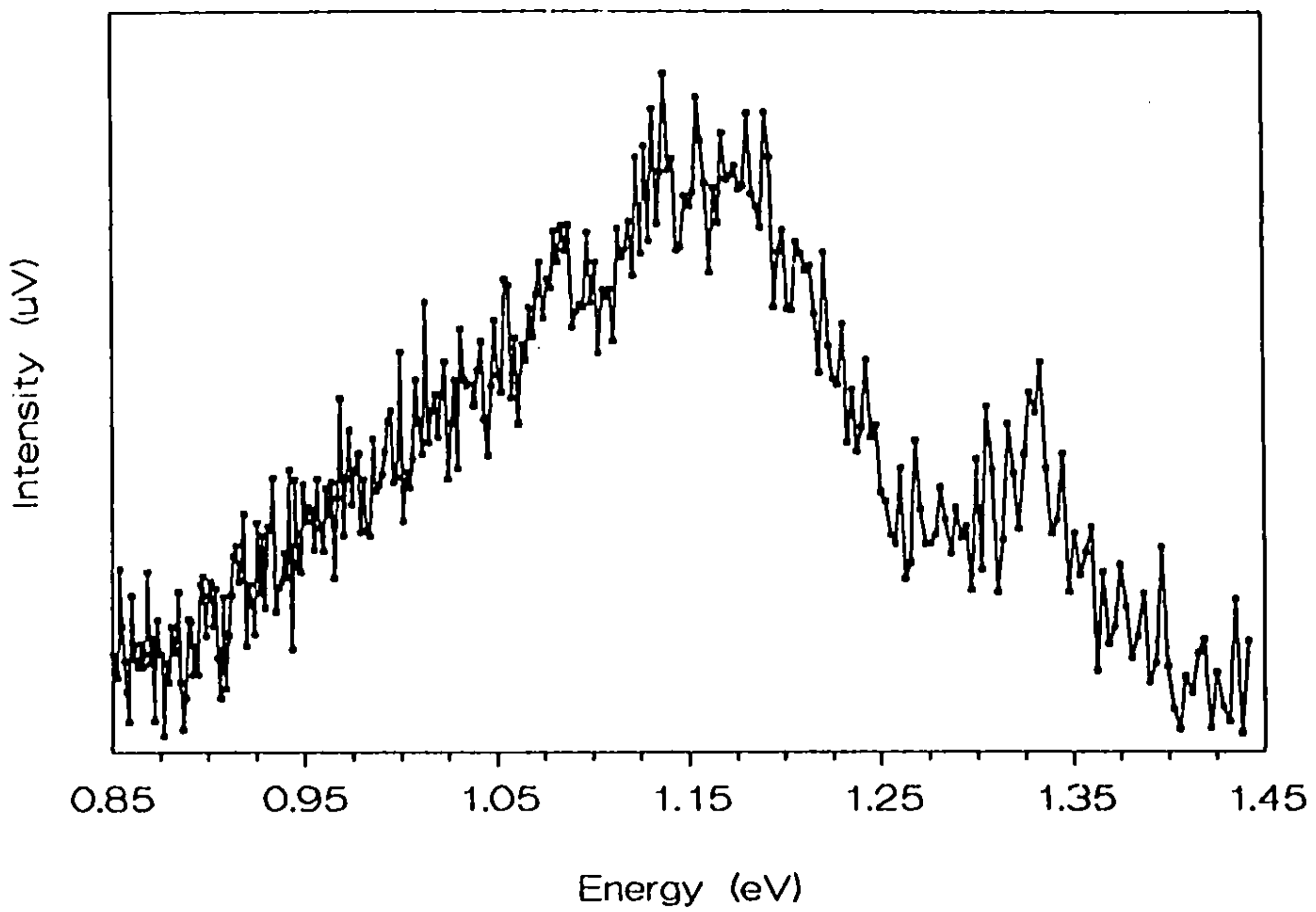

Figure 5.7a: PL spectrum of sample grown at 500C, with He plasma.

$2 \times 10^{13}/cm^3$. This is below the detection limit of the Hall equipment, so this could well be the level of the phosphorus interstitial acceptor producing the compensation in the 400-465°C growths.

The photoluminescence spectra of the samples also show improvement after annealing. Several of the growths with He plasma became luminescent (fig 5.7b). Peaks at 1.38, 1.34 and 1.16 eV are visible, in addition to the band edge. The other two peaks were seen in growths without plasma, but the 1.16 eV peak is particularly significant. It is present in all of the luminescent He-assisted growths, and is not unique to the growth at 500°C, so it is quite probably due to phosphorus interstitials.

5.8 Conclusions

Helium plasma bombardment produces phosphorus interstitials and phosphorus vacancies in the grown films. The interstitials are deep acceptors, with a photoluminescence level at 1.16 eV, for measurements at 11 K. The vacancies are donors, with a photoluminescence level at approximately 1.33 eV, also for measurements at 11 K. More interstitials than vacancies are produced, but the interstitials also diffuse out more readily, so growth at 500°C or annealing at 730°C can result in material with more vacancies than interstitials. The sample grown at 500°C was n-type, due to the excess of donors, with a carrier concentration of $1.2 \times 10^{16}/cm^3$, due to the pinning of the Fermi level at the defect level. Samples grown from 400°C to 465°C were compensated by the excess interstitials to less than $10^{14}/cm^3$, n-type. Below 400°C, the large concentrations of phosphorus antisites swamped the other defect concentrations, though the material was still much

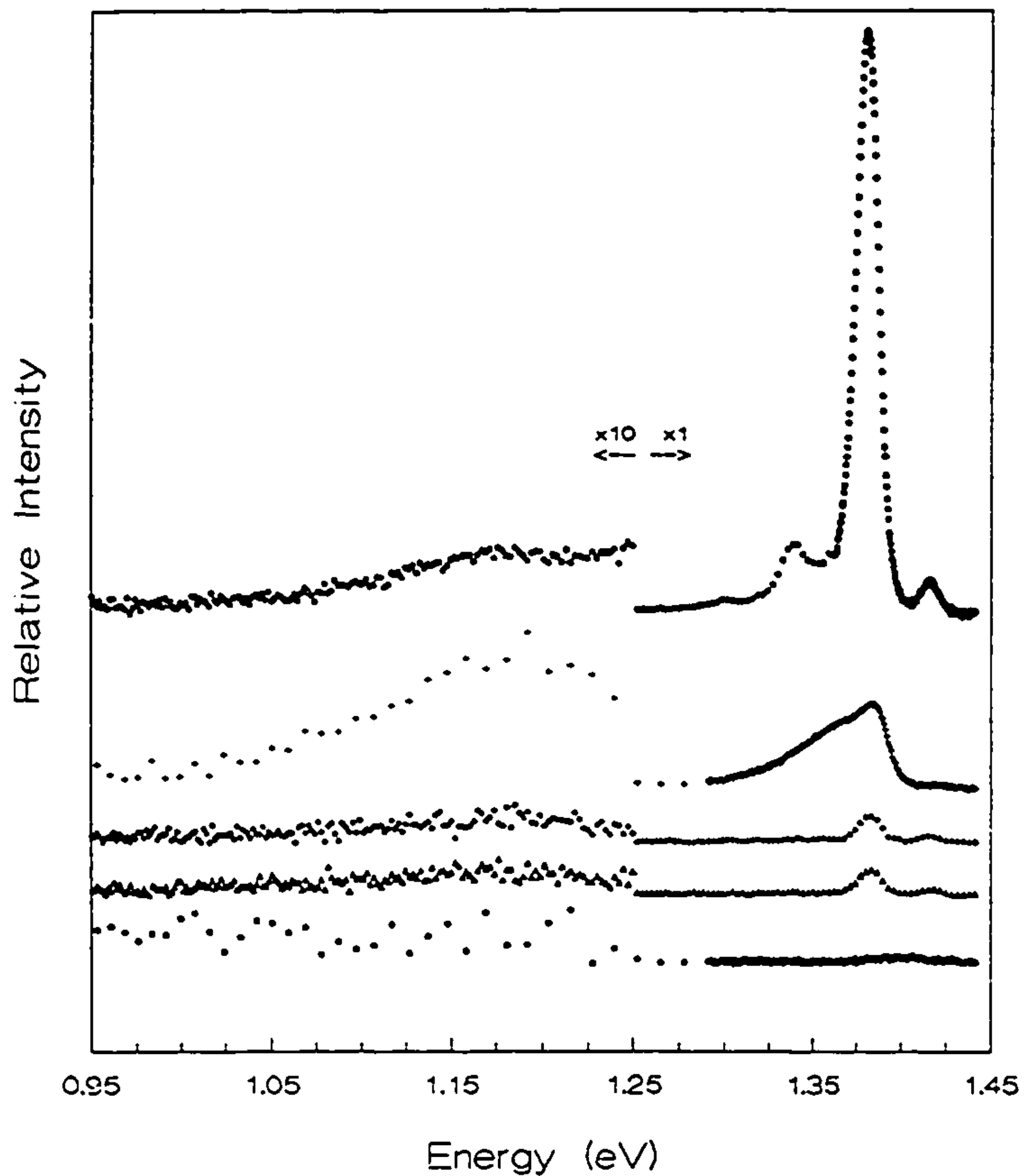

Figure 5.7b: PL results from InP grown with He, then annealed at 730C

1) 500C 2) 465C 3) 410C 4) 400C 5) 350C.

lower mobility than was found in growths without plasma. The plasma also smoothed the surface of the films grown at low temperatures to the lowest defect levels ever reported.

6. Growth of InP With Ar Plasma

6.0 Abstract

The argon plasma had no apparent effect on the films grown. The small changes that were seen (slightly increased carrier concentration, PL levels, etc.) appear to be produced by a weak hydrogen plasma resulting from backstreaming of the hydrogen produced by the gas cracker.

6.1 Growth Conditions

InP layers were grown over the temperature range 300°C to 500°C while the sample surface was exposed to an ECR Ar plasma. The argon gas directed into the ECR source was 99.9995% pure. Sample thicknesses were again chosen based on the expected carrier concentration, in order to minimize depletion effects. The ion current of the Ar plasma, as measured by a Langmuir probe, was approximately one fifth that of the hydrogen plasma. Some of this current would be due to hydrogen ions resulting from hydrogen produced in the cracking of PH_3, backstreaming into the ECR plasma chamber.

To penetrate the surface, Ar ions require an energy of 22 eV. An ion with 25 eV (ε 0.00022) will lose energy at such a rate that, while it will penetrate the surface, it won't pass through the In layer immediately underneath. Even with 50 eV, an Ar ion will typically travel only about 5 Angstroms. Any direct damage done by the plasma should

thus be confined to the immediate surface region. Focussing collisions, if they occur, could produce defects somewhat farther below the surface.

Argon is inert, so chemical reactions between it and the growing crystal do not occur. The larger mass of the Ar atoms will result in more energy transferred to the In and P atoms than was seen with the other plasmas. However, Ar atoms will not penetrate as deeply as the light plasma species, and the damage will occur closer to the surface. Consequently, more of the defects produced can be repaired by the growth fluxes. A head-on elastic Ar-P collision transfers about 98.4% of the energy of the Ar plasma species to the P atom. Hence, the surface P atoms should easily be displaced into the bulk, and replaced from the P growth flux. If the displaced atom doesn't interact with the crystal, a phosphorus interstitial will be formed. If the Ar penetrates into the bulk (very rare), displaced phosphorus atoms will leave phosphorus vacancies behind (donors), in addition to being phosphorus interstitials themselves.

If the Ar atoms penetrate past the surface phosphorus atoms, indium atoms can also be displaced. In addition, indium atoms might be displaced by collision with displaced phosphorus atoms. In a head-on elastic collision, 77% of the argon atom's energy is transferred to an indium atom. An indium vacancy (an acceptor) and an indium interstitial (a donor) will be created. In theory, an indium vacancy can also be created by a displaced phosphorus atom. Taking bond directions into account, an Ar-P-In chain collision can transfer up to 22% of the Ar atom's energy to the In atom, so the minimum Ar energy required is 33.5 eV. If the phosphorus atom takes the place of the indium atom, the result is an indium interstitial and a phosphorus antisite. Otherwise, an indium

interstitial, a phosphorus interstitial and an indium vacancy will be produced. This must happen near the surface, since the Ar atom won't penetrate far, if at all, so the phosphorus atom will probably be replaced from the growth flux. If it isn't, a phosphorus vacancy will also be produced.

6.2 Nomarski Microscope Results

Table 6.2 gives the measured surface defect densities for the growths, as well as the results without plasma for comparison. The defect densities are given per cm^2, and "texture" means that the surface is rough everywhere, with a similar pattern throughout. The growth at 350°C was smoothed by the plasma, but the growths at 300°C and 400°C were not significantly affected, possibly because the ion current was too small. The growth at 465°C was smoother than any other growth at this temperature, but it is not clear whether this is due to the plasma or because the growth system was doing particularly well at that time.

Table 6.2: Surface defect density ($/cm^2$), determined by viewing with a Nomarski microscope.

Tg (°C)	No plasma	Ar plasma
500	42000	83000
465	560000	11000
400	Texture	Texture
350	Texture	2800
300	Texture	Texture

6.3 Xray Charactrization

Table 6.3 lists the measured FWHM of the argon plasma-assisted growths. The direction of strain was not apparent in any of the samples.

None of the growths with Ar plasma produced very wide peaks. The films grown at 300°C and 350°C were both less strained than the growths without plasma, so the plasma introduced interstitials which compensated the strain introduced by the phsophorus antisites. At higher growth temperatures there are fewer antisites, so the strain from the interstitials results in some visible strain in the samples. Possible interstitials are phosphorus, indium and hydrogen (from the background). Vacancies may also be produced, but it appears that interstitials are primarily produced by the plasma, given the effect on the films grown at 300°C and 350°C.

Table 6.3: Results from study by Xray double crystal diffraction. Full width at half maximum of the peaks, in seconds of arc.

Tg (°C)	No plasma	Ar plasma	Ar plasma, annealed
500	12	14	17
465	13	15	11
400	11,13	14	12
350	16	11	11
300	21	16	15

The changes in FWHM of the annealed samples are all within scatter. The interstitials are apparently not removed by annealing at 730°C for 10 seconds. From the

results of the previous chapter, phosphorus interstitials are probably not present in significant concentrations, then. This leaves indium and hydrogen interstitials. If hydrogen interstitials are present it must be as donors, since it was shown in chapter 4 that hydrogen is otherwise removed by annealing.

6.4 Positron Annihilation

The positron annihilation profile results are approximately the same as for the growths without plasma. Fewer than $10^{17}/cm^3$ open-volume defects of neutral or negative charge are created by the argon plasma. A large concentration of open volume defects still occurs at low growth temperatures, which is not apparently affected by the plasma. It is noted that these results are very similar to those produced by the hydrogen plasma treatment.

6.5 Hall Effect

The carrier concentrations of the growths from 300°C to 400°C are very similar to the growths without plasma, so the primary defect is the phosphorus antisite due to the reduced growth temperature. At 465°C and 500°C the carrier concentration is roughly $3x10^{16}/cm^3$, significantly larger than for the growths without plasma ($1\text{-}3x10^{15}/cm^3$) but lower than the growths with H plasma (up to $10^{17}/cm^3$). At 465°C and 500°C, where the plasma effects dominate, the films had a much higher mobility than those grown with any other plasma, suggeting that fewer defects were produced.

The mobilities of the samples grown at 465°C and 500°C suggest that there are no

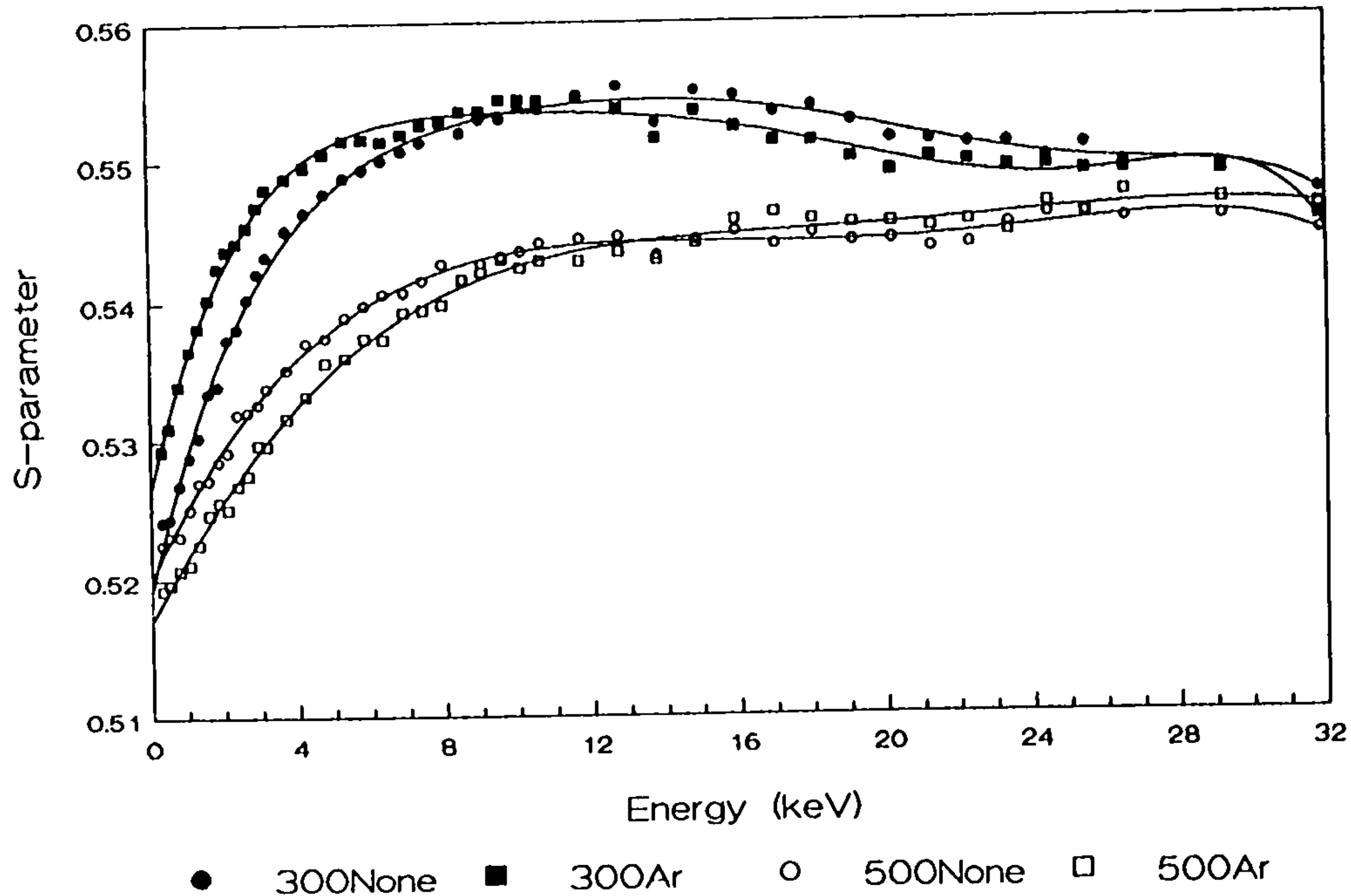

Figure 6.4: Positron annihilation profiles.

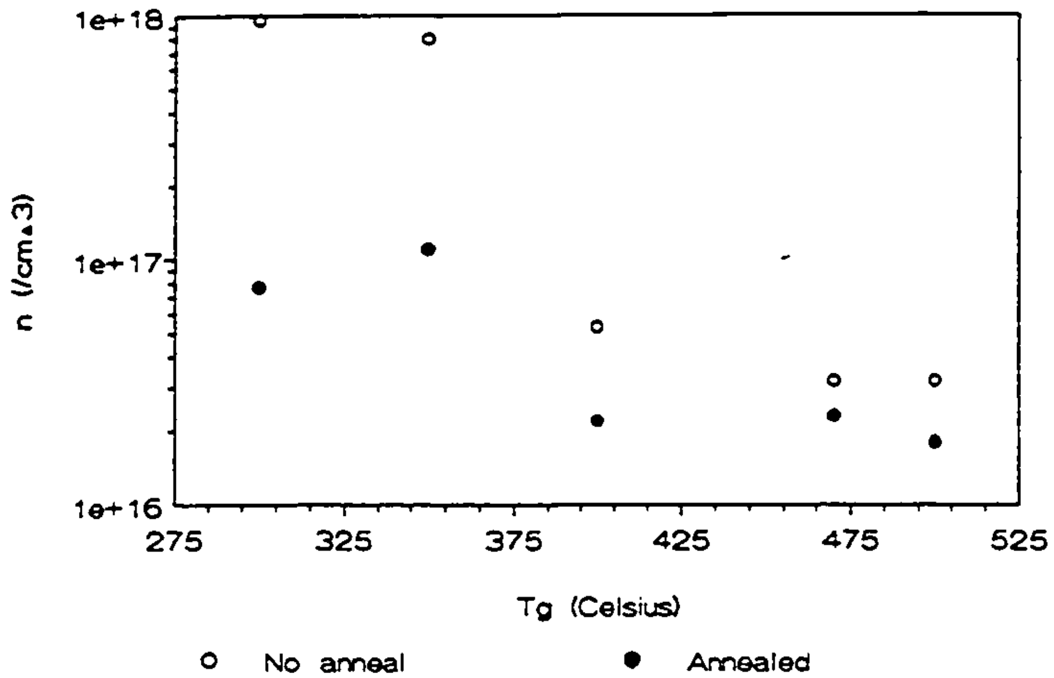

Figure 6.5a: Carrier concentration of InP grown with Ar plasma.

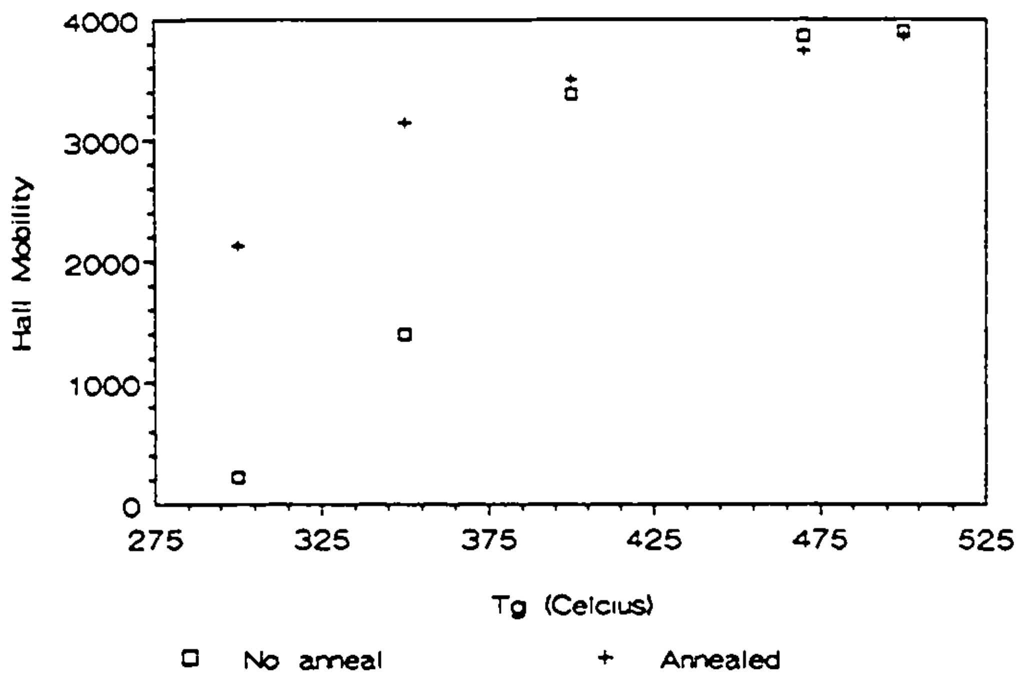

Figure 6.5b: Mobility of InP grown with Ar plasma.

compensating defects created by the argon plasma. The mobilities are higher than was predicted to be possible for these carrier concentrations, even without any compensation [Walukiewicz *et. al.* (1980)]. Thus, only donor defects are produced in significant quantities. Phosphorus interstitials and indium vacancies are rare or nonexistant. Phosphorus vacancies, phosphorus antisites and indium interstitials all act as donors. As discussed in section 6.1, these antisites, interstitials and possibly vacancies could be created in an Ar-P-In chain collision, but it seems improbable that this exact mechanism would occur in every case. If the displaced phosphorus atom doesn't occupy the site of the displaced indium atom, or doesn't displace the indium atom, a phosphorus interstitial will result. If phosphorus is being displaced, phosphorus interstitials should be produced in a significant proportion of the collisions. An alternative possibility is that the argon species in the plasma doesn't create any defects at all. The observations are consistent with a weak hydrogen plasma resulting from the backstreaming of the background hydrogen, as discussed earlier. This could produce the observed concentration of donors. As was shown in chapter 4, the hydrogen tends to chemically bond into the crystal, resulting in donor sites. The hydrogen plasma current in this case is much lower than in chapter 4, not more than 25% as large, so a smaller carrier concentration would result, as is seen. The lower concentration of H interstitials could also mean that fewer of the unbonded interstitials occur, so there is little effect on the mobility other than that due to the donor sites.

Annealing improved the electrical properties of the films grown at low temperatures, just as it did in all of the previous cases. The two films grown at higher

temperatures, where the plasma effects dominated, were hardly affected at all. The carrier concentrations and mobilities both were slightly reduced, so the changes are probably due to minor annealing damage rather than the removal of defects. The stability of the donors is like that seen with H and D plasmas.

6.6 Photoluminesence

The growths at 465°C and 500°C have strong band edge peaks, (fig. 6.6a) with additional peaks near 1.38, 1.35 and 1.08 eV. All of these were seen in growths with hydrogen plasma. The growths at 400°C and 300°C produced no signal. The growth at 350°C had a faint band-edge signal and a stronger and broader peak just above 1 eV.

The photoluminescence spectra of the samples also show improvement after annealing (fig. 6.6b). The samples grown with Ar varied in their response to the anneal, but the ~1 eV peak was removed in every case, just as with the hydrogen plasma. The growth at 400°C showed a broad, weak peak near 1.17 eV after annealing, just as two of the hydrogen-assisted samples did. In summary, annealing the growths with hydrogen plasma produced the same changes as were seen for these argon plasma-grown samples.

6.7 Conclusions

The Ar plasma has little or no effect on the growth of InP. Backstreaming of H into the ECR system results in a weak H plasma which creates donors and adds a PL peak near 1.08 eV. These effects are insignificant below 400°C, compared to the effects of the large concentrations of phosphorus antisites. The plasma also smoothed the surface

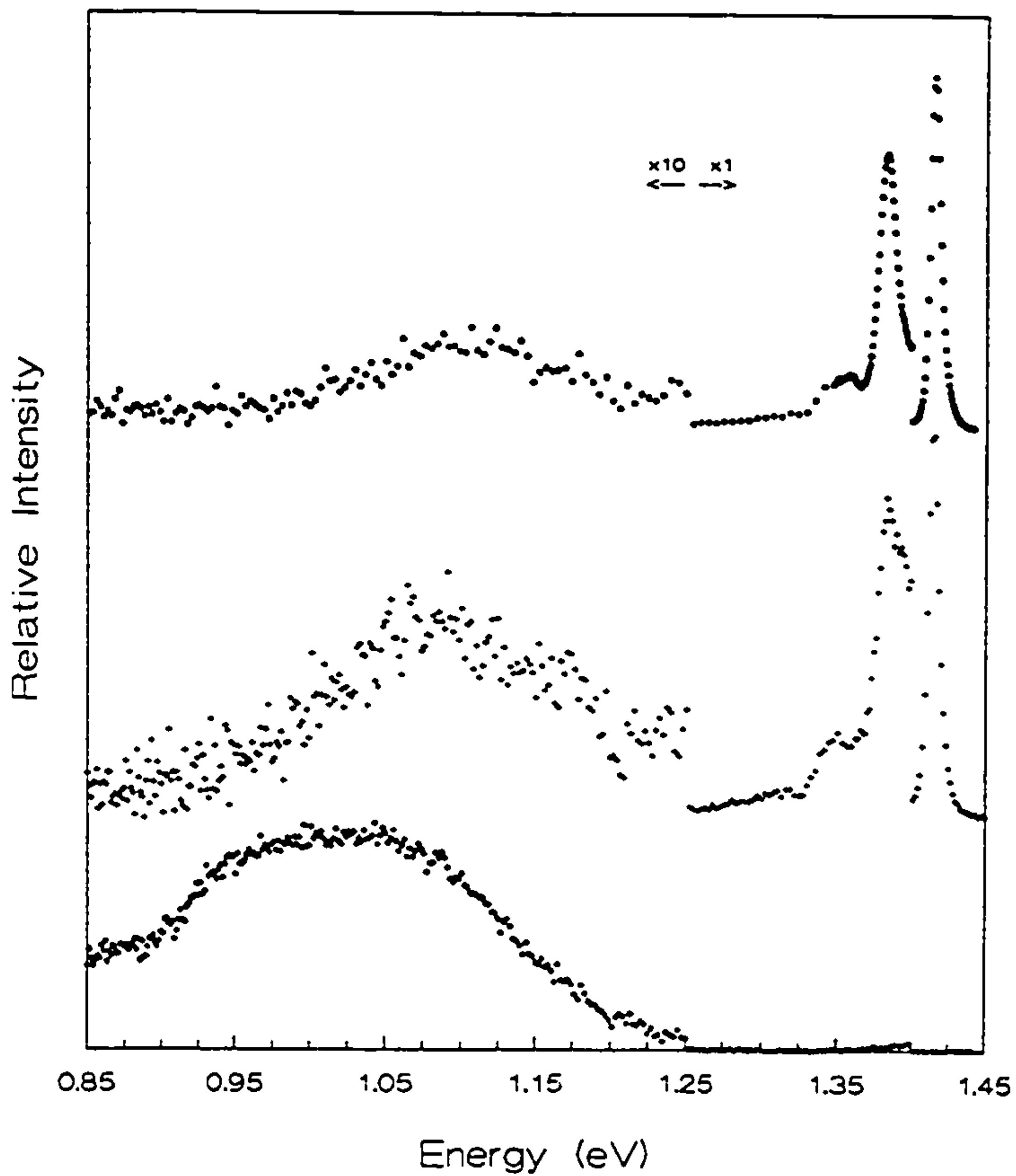

Figure 6.6a: PL results from InP grown with Ar at 1) 500C (top) 2) 465C 3) 350C. 0.85–1.25eV x100, 1.25–1.4eV x10.

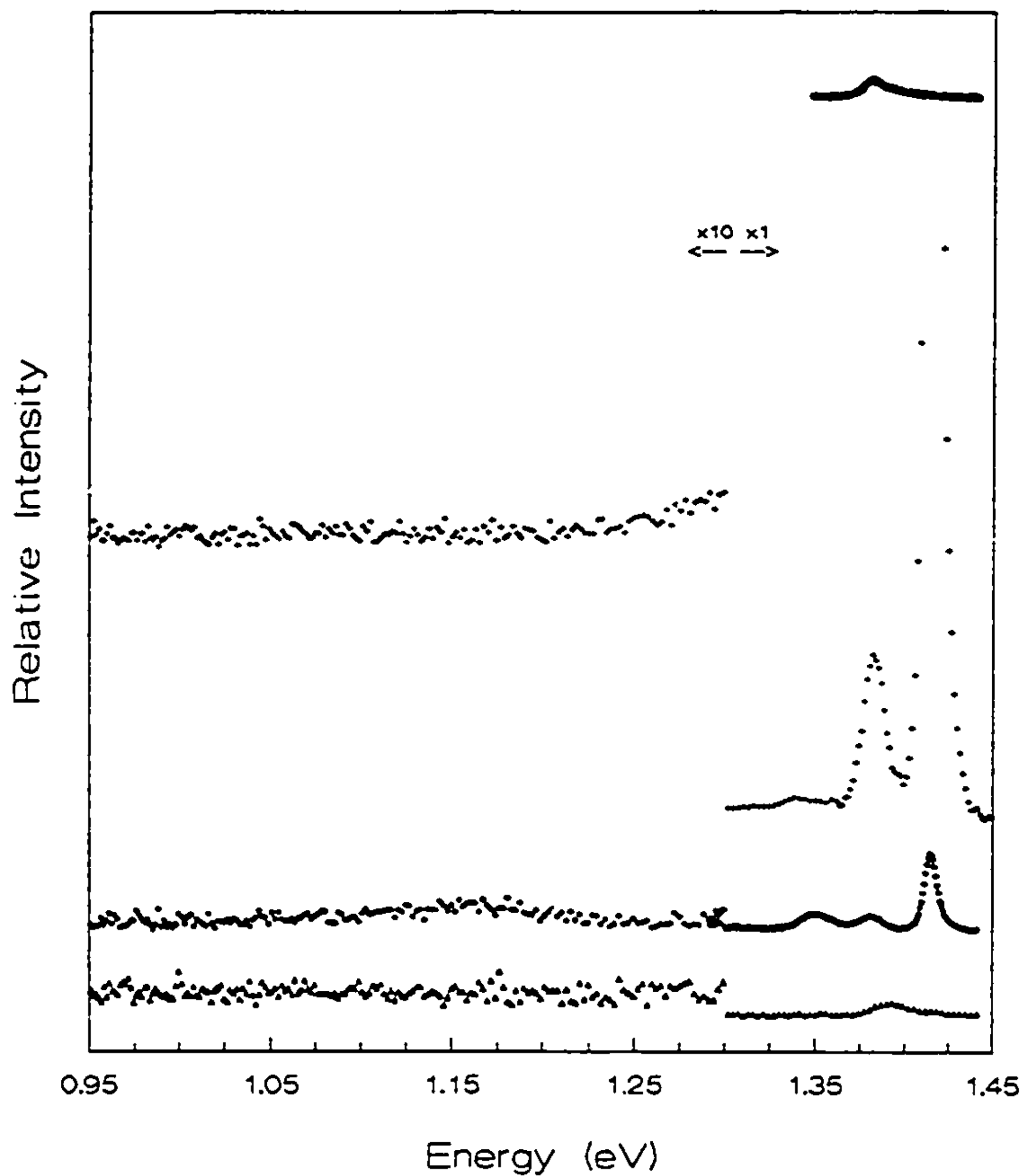

Figure 6.6b: PL results, after annealing, from InP grown with Ar at

1) 500C (top) 2) 465C 3) 400C 4) 350C.

of one film, but no others, probably because the current was too small. If the H contamination of the plasma could be avoided, Ar plasma might add energy to the growing film without adding defects.

7. Conclusions

As the growth temperature is reduced to 232°C, the quality of the InP films gradually decreases. The primary defect produced is the phosporus antisite. The antisites make the material n-type, with carrier concentrations reaching as high as $2.7 \times 10^{18}/cm^3$ at 232°C. The temperature dependence of the electrical properties is smoother than that reported by other groups, except for an unexpected increase in mobility at 232°C. Surface roughening also occurs at reduced growth temperatures. The changes in electrical properties due to reduced growth temperature are always dominant over the effects of the plasmas studied, for growths below 400°C.

Hydrogen, and its double mass isotope, deuterium, both seem to bond to phosphorus atoms, contributing an electron in the process. Growths with these plasmas are more n-type ($\sim 7 \times 10^{16}/cm^3$) than without plasma, until the temperature is reduced enough to swamp the effect. The deuterium plasma may also produce a small concentration of phosphorus interstitials ($\sim 3 \times 10^{16}/cm^3$).

Deuterium plasma-assisted growth passivates Be dopant atoms but doesn't significantly affect Si doping. The deuterium atoms bond at the Be site, and provide the electron that the Be lacks. Although hydrogen was already known to passivate p-type InP, this is the first time it has been accomplished in-situ, to my knowledge.

Helium plasma produces phosphorus interstitials and phosphorus vacancies, in concentrations well above $10^{16}/cm^3$, and possibly in excess of $10^{18}/cm^3$. More interstitials than vacancies are produced, but the interstitials are also more mobile. At 500°C, some of the interstitials diffuse out leaving vacancies in the majority. At lower growth temperatures the interstitials are more common than vacancies. The vacancies act as donors, at an energy level approximately 0.1 eV below the conduction band. The interstitials act as deep acceptors. From 400°C to 500°C, the interstitials compensate the InP to carrier concentrations of less than $1x10^{14}/cm^3$, without ever making the material p-type. Below 400°C, the concentration of phosphorus interstitials is too small to significantly affect the carrier concentration, though the mobility is still smaller than without plasma. From PL measurements, the acceptor level appears to be 0.26 eV below the conduction band at 11 K.

Argon plasma doesn't appear to directly produce a measurable concentration of defects. However, backstreaming hydrogen results in a weak hydrogen component in the argon plasma This plasma produced the smallest changes in the bulk properties of the films, and might not produce any, if the hydrogen backstreaming could be prevented.

For growth temperatures above 400°C, the plasmas had no effect on the surface smoothness or surface defect density. Below 400°C, the grown surfaces were always smoothed by the hydrogen and deuterium plasmas, and sometimes by the helium and argon plasmas. Plasma ion current may be the determinant of smoothing effectiveness. Without the plasmas, the surfaces of films grown below 400°C were very rough (textured). With the plasmas, the surfaces were smooth and the surface defect

concentrations were one to two orders of magnitude lower than the literature value of $10^5/cm^2$. The transition in the effectiveness of the plasmas occured at 400°C, which is where the transition to rough surfaces occurs for growths without plasma.

The original objective, to grow InP at reduced temperature while maintaining the quality of the films, has not been accomplished. While the surface smoothness is maintained and even enhanced by a plasma, the electrical and optical properties generally deteriorate. In two cases, however, the deterioration is pronounced enough to constitute potentially useful effects, in and of themselves. Helium plasma can be used to produce highly resistive InP. Deuterium (and hydrogen) plasma can be used to passivate p-type dopants during growth, again producing highly resistive films. Further study of these effects may yield new tools for semiconductor fabrication.

References

H.H. Anderson and J.F. Ziegler, *Hydrogen Stopping Powers and Ranges in All Elements*, (Pergamon, 1977).

J.W. Baranowski and J. Tatarkiewicz, *Acta Physica Polonica*, **A79**, p.263 (1991).

R.Z. Bachrach and B.S. Krusor, *Journal of Vacuum Science and Technology*, **18**, 756 (1981).

G. Carter and W.A. Grant, *Ion Implantation of Semiconductors*, (John Wiley and Sons, 1976) pp. 140-146.

Y.G. Chai, Y-C. Pao and T. Hierl, *Applied Physics Letters*, **47**, 1327 (1985).

N. Chand and S.N.G. Chu, *Journal of Crystal Growth*, **104**, 485 (1990).

A. Chandra, C.E.C. Wood, D.W. Woodard and L.F. Eastman, *Solid-State Electronics*, **22**, 645 (1979).

F.F. Chen, in *Plasma Diagnostic Techniques*, edited by R.H. Huddlestone and S.L. Leonard (Academic Press, 1965), p. 113-200.

H.Y. Cho, W.C. Choi and S-K. Min, *Applied Physics Letters*, **63**, 1558 (1993).

J.W. Corbett and J.C. Bourgoin, in *Point Defects in Solids*, edited by J.H. Crawford and L.M. Slifkin (Plenum, 1975), p. 96.

J.P. Donnelly and C.E. Hurwitz, *Solid-State Electronics*, **20**, 727 (1977).

P. Dreszer, W.M. Chen, K. Seendripu, J.A. Wolk, W. Walukiewicz, B.W. Liang, C.W. Tu and E.R. Weber, *Physical Review*, **B47**, 4111 (1993).

P. Dreszer, W.M. Chen, D. Wasik, R. Leon, W. Walukiewicz, B.W. Liang, C.W. Tu and E.R. Weber, *Journal of Electronic Materials*, **22**, 1487 (1993).

R.F.C. Farrow, *Journal of Physics*, **D7**, 2436 (1974).

L.C. Feldman and J.W. Mayer, *Fundamentals of Surface and Thin Film Analysis*, (Prentice-Hall, 1986), pp.95-96.

D.W. Fischer, M.O. Manasreh and G. Matous, *Semicond. Sci. Technol.*, **9**, 1 (1994).

K. Fujiwara, K. Kanamoto, Y.N. Ohta, Y. Tokuda and T. Nakayama, *Journal of Crystal*

Growth, **80**, 104 (1987).

J.Ch. Garcia, J.P. Hirtz, P. Maurel, H.J. Von Bardelben and J.C. Bourgoin, *Materials Research Society Symposium Procedings*, **241**, 277 (1992).

S.Hariu, K. Takenaka, S. Shibuya, Y. Komatsu and Y. Shibata, *Thin Solid Films*, **80**, 235 (1981).

J.M.E. Harper, J.J. Cuomo, R.J. Gambino and H.R. Kaufman, in *Ion Bombardment Modification of Surfaces*, edited by O. Auciello and R. Kelly (Elsevier, 1984), p. 127.

P. Hautojarvi, J. Makinen, S. Palko, K. Saarinen, C. Corbel and L. Liskay, *Materials Science and Engineering*, **B22**, 16 (1993).

K. Kondo, J. Saito, T. Igarashi, K. Nanbu and T. Ishikawa, *Journal of Crystal Growth*, **95**, 309 (1989).

L.R. Lepkowski, R.Y. DeLule, N.C. Tien, M.H. Kim and G.E. Stillman, *Journal of Applied Physics*, **61**, 4808 (1987).

B.W. Liang, Y. He and C.W. Tu, *Materials Research Society Symposium Procedings*, **241**, p. 283 (1992).

G.N. Maracas, K.T. Shiralagi, R.A. Puechner, F. Yu, K.T. Choi, J.S. Bow, R Ramamurti, M.J. Kim and R.W. Carpenter, *Materials Research Society Symposium Procedings*, **241**, 271 (1992).

G.N. Maracas, K.T. Shiralagi, R. Ramamurti and R.W. Carpenter, *Journal of Electronic Materials*, **22**, 1375 (1993).

S. Matsuo and M. Kiuchi, *Japanese Journal of Applied Physics*, **22**, L2 (1983).

T. Narusawa, S. Shimizu and S. Komiya, *Journal of Vacuum Science and Technology*, **16**, 366 (1979).

M.A. Omar, *Elementary Solid State Physics*, (Addison-Wesley), 332 (1975).

T. Ono, M. Oda, C. Takahashi and S. Matsuo, *Journal of Vacuum Science and Technology*, **B4**, 696 (1986).

M.B. Panish and J.R. Arthur, *J. Chem. Thermodynamics*, **2**, 299 (1970).

L.J. van der Pauw, *Philips Research Reports*, **13**, 1 (1958).

S.J. Pearton, W.S. Hobson and C.R. Abernathy, *Applied Physics Letters*, **61**, 1588 (1992).

S.J. Pearton, J.W. Corbett and T.S. Shi, *Applied Physics*, **A43**, 153 (1987).

O.A. Popov, *Surface and Coatings Technology*, **36**, 917 (1988).

O.A. Popov, *Journal of Vacuum Science and Technology*, **A7**, 894 (1989).

O.A. Popov and H. Waldron, *Journal of Vacuum Science and Technology*, **A7**, 914 (1989).

O.A. Popov and A.O. Westner, *Review of Scientific Instruments*, **61**, 303 (1990).

O.A. Popov, William Hale and A.O. Westner, *Review of Scientific Instruments*, **61**, 300 (1990).

K. Rakennus, T. Hakkarainen, K. Tappura, H. Asonen and M. Pessa, in: *Proceedings of the 4th International Conference on InP and Related Material*, Newport, April 1992, paper TUP24.

D.G. Schlom, W.S. Lee, T. Ma and J.S. Harris,Jr., *Journal of Vacuum Science and Technology*, **B7**, 296 (1989).

A.P. Seitsonen, R. Virkkunen, M.J. Puska and R.M. Nieminen, *Physical Review*, **B49**, 5253 (1994).

L.S. Sidhu, S. Zukotynski, R.V. Kruzelecky and D.A. Thompson, submitted to *Journal of Applied Physics*.

W.E. Spicer, I. Lindau, P. Sheath and C.Y. Su, *Journal of Vacuum Science and Technology*, vol. 17, p. 1019 (1980).

C.R. Stanley, R.F.C. Farrow and P.W. Sullivan, in *The Technology and Physics of Molecular Beam Epitaxy*, edited by E.H.C. Parker (Plenum Press, 1985), p. 279.

J.P. Suchet, *Chemical Physics of Semiconductors*, (D. Van Nostrand,1965), p. 100.

T. Sugino, H. Yamamoto and J. Shirafuji, *Applied Physics Letters*, **60**, 948 (1991).

G.E. Thomas, L.J. Beckers, J.J. Vrakking and B.R. de Koning, *Journal of Crystal Growth*, **56**, 557 (1982).

M.W. Thompson, *Defects and Radiation Damage in Metals*, (Cambridge University Press, 1969), p. 24.

J.Y. Tsao, E.Chason, K.M. Horn, D.K.Brice and S.T. Picraux, *Nuclear Instruments and Methods in Physics Research*, **B39**, 72 (1989).

J.A. Van Vechten, in *Handbook on Semiconductors*, edited by Seymour P. Keller (North-Holland, 1980), p. 102.

W. Walukiewicz, J. Lagowski, L. Jastrzebski, P. Rava, M. Lichtensteiger, C.H. Gatos and H.C. Gatos, *Journal of Applied Physics*, **51**, 2659 (1980).

K.B.Winterbon, *Ion Implantation Range and Energy Deposition Distribution (Volume 2)*, (Plenum, 1975).

K. Xie, C.R. Wie and G.W. Wicks, *Materials Research Society Symposium Procedings*, **241**, 265 (1992).

P.W. Yu, B.W. Liang and C.W. Tu, *Applied Physics Letters*, **61**, 2443 (1992).

P.W. Yu, D.N. Talwar, H.Q. Hou and C.W. Tu, *Physical Review*, **B49**, 10735 (1994).

P.C. Zalm and L.J. Beckers, *Applied Physics Letters*, **41**, 167 (1982).

J.F. Ziegler, *Helium Stopping Powers and Ranges in All Elemental Matter*, (Pergamon, 1977).